Abstract

Suspension System Optimisation to Reduce Whole Body Vibration Exposure on an Articulated Dump Truck

J.C. Kirstein

Department of Mechanical Engineering

Stellenbosch University

Private Bag X1, 7602 Matieland, South Africa

Thesis: MScEng (Mech)

September 2005

In this document the reduced order simulation and optimisation of the passive suspension systems of a locally produced forty ton articulated dump truck is discussed. The linearization of the suspension parameters were validated using two and three dimensional MATLAB models. A 24 degree-of-freedom, three dimensional ADAMS/VIEW model with linear parameters was developed and compared to measured data as well as with simulation results from a more complex 50 degree-of-freedom non-linear ADAMS/CAR model. The ADAMS/VIEW model correlated in some aspects better with the experimental data than an existing higher order ADAMS/CAR model and was used in the suspension system optimisation study. The road profile over which the vehicle was to prove its comfort was generated, from a spatial PSD (Power Spectral Density), to be representative of a typical haul road. The weighted RMS (Root Mean Squared) and VDV (Vibration Dose Value) values are used in the objective function for the optimisation study. The optimisation was performed by four different algorithms and an improvement of 30% in ride comfort for the worst axis was achieved on the haul road. The improvement was realised by softening the struts and tires and hardening the cab mounts. The results were verified by simulating the optimised truck on different road surfaces and comparing the relative improvements with the original truck's performance.

Uittreksel

Suspensie Stelsel Optimering om Heelliggaam Vibrasie in 'n ge-Artikuleerde Vragmotor te Verminder

("Suspension System Optimisation to Reduce Whole Body Vibration Exposure on an Articulated Dump Truck")

J.C. Kirstein

Departement Meganiese Ingenieurswese

Universiteit Stellenbosch

Privaatsak X1, 7602 Matieland, Suid Afrika

Tesis: MScIng (Meg)

September 2005

In hierdie dokument word die vereenvoudigde simulasie en optimering van die passiewe suspensie stelsels van 'n plaaslik vervaardigde veertig ton ge-artikuleerde vragmotor bespreek. Die linearisering van die suspensie parameters word deur twee- en drie-dimensionele MATLAB modelle gestaaf. 'n Drie-dimensionele, 24 vryheidsgraad ADAMS/VIEW model met lineêre parameters is ontwikkel en met gemete data sowel as simulasie uitslae van 'n bestaande, meer komplekse 50 vryheidsgraad nie-lineêre ADAMS/CAR model vergelyk. Die ADAMS/VIEW model het in sekere opsigte beter as die hoër vryheidsgraad ADAMS/CAR model met die gemete data ooreengestem, en is gebruik vir die optimeringstudie. Die padoppervlakte waaroor die voertuig se gemak geoptimeer moes word is van 'n ruimte-drywing-spektrale-digtheid verteenwoordiging van 'n tipiese ertsweg geskep. Die geweegde WGK (wortel gemiddeld kwadraat) en VDW (vibrasie dosis waarde) is gebruik om die doelfunksie vir die optimeringstudie op te stel. Die optimering is deur vier verskillende optimeringsalgoritmes uitgevoer en 'n verbetering van 30% in ritgemak in die ergste rigtingsas is behaal vir die gegewe ertsweg. Die verbetering is hoofsaaklik behaal deur die voorste gasdempers en bande sagter te stel en die kajuit montering te verhard. Die uitslae is gestaaf deur die geoptimeerde vragmotor oor verskillende padoppervlaktes te laat ry en die relatiewe verbeterings met die oorspronklike vragmotor te vergelyk.

Aknowledgements

This thesis I dedicate wholly to my Lord and Saviour Jesus Christ, that inspired, guided and enabled me throughout this entire project. Thank You for being my inspiration, my joy and my comforter every day since I met you.

My brother remarked that once you are finished with your master's degree, the rest of your life is easy. I don't know whether this is true, but thankfully I had incredible friends and family that supported me in the times that I needed it most.

Thank you SAB for allowing me to do a MSc full time; Theo Grovè and Danie du Plessis for your invaluable input into this thesis and Christian Jordaan and Erik Grovè for organising trucks for us to take measurements in.

Thank you professor van Niekerk for your guidance and sponsorship. You are an example to me in and out of the office and I am grateful for being able to learn so much from you. Thank you Giovanni, and the other people on the 6th floor who endured my excitability and made me feel welcome; my cell group that was always there with support, advice, guidance and food for the body, soul and spirit; Carl my dear brother and friend, for the example you are to me. And finally to my parents and Marno, my youngest brother, thank you for your prayer, support and patience throughout this thesis. I would certainly have failed had it not been for all of you.

Table of Contents:

List of Figures

List of Tables

Glossary

2D	Two Dimensional
3D	Three Dimensional
A(8)	Equivalent eight-hour RMS exposure
ADAMS[*]	Automatic Dynamic Analysis of Mechanical Systems
ADAMS/CAR[*]	Specialised environment in ADAMS for modelling vehicles
ADAMS/INSIGHT[*]	Specialised environment in ADAMS for design-of-experiments
ADAMS/VIEW[*]	Basic environment in ADAMS for simulating models
ADT	Articulated Dump Truck
BFGS	Broyden, Fletcher, Goldfarb and Shanno
CCD	Central Composite Design
DADS[*]	Dynamic Analysis Design Systems
DIRECT	Divided Rectangle
DOF	Degrees-of-Freedom
EAV	Exposure Action Value
ELV	Exposure Limit Value
EU	European Union
eVDV	Estimated Vibration Dose Value
FFT	Fast Fourier Transform
F-Tire	Flexible Ring Tire Model
GA	Genetic Algorithm
GENRIT	A general vehicle model for simulation of ride dynamics
GRG	General Reduced Gradient
HSE	Health and Safety Executive
ISO	International Organisation for Standardisation
MATLAB[*]	Matrix Laboratory
PAVD	Physical Agents Vibration Directive
PSD	Power Spectral Density
QP	Quadratic Programming
RMS	Root Mean Square
RSM	Response Surface Methodology

---

[*] Commercially available Software

SQP	Sequential Quadratic Programming
SWIFT	Short Wavelength Intermediate Frequency Tire
VDV	Vibration Dose Value
WBV	Whole-Body Vibration
W_d	ISO frequency weighting filter used for lateral and longitudinal vibrations of seated human
W_k	ISO frequency weighting filter used for vertical vibrations of seated human
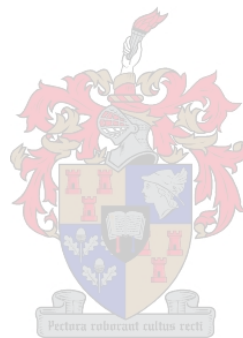
Chapter 1: Introduction

Drivers of Articulated Dump Trucks (ADTs) are exposed to vibration on a daily basis. In the past, the South African industry has paid little attention to the measurement and control of whole-body vibration, but new legislation introduced in Europe is encouraging that to change. The levels of vibration induced in the drivers have the potential to compromise occupational health and safety and are fast becoming a major concern in Europe; and in South Africa for exporting manufacturers. In this project the passive suspension systems of an ADT are optimised to reduce vibration exposure of the driver.

1.1 The Articulated Dump Truck

Articulated Dump Trucks are used in the mining and construction industries to efficiently transport material (usually earth) over irregular terrain. The "articulation" refers to the steering mechanism of the truck, which allows the front section to yaw independently of the rear by means of hydraulic rams. ADTs usually operate on a large variety of road surfaces ranging from very poor to well maintained dirt (or tar) roads. An ADT has various suspension systems that isolate the driver from the inputs at the wheel/road interface, the engine and other sources of noise and vibration. These include the tires, the primary suspension, the cabin suspension and the seat suspension.

The tires have a larger travel than any other suspension system and thus play an important role in isolating the driver from road irregularities. The primary suspension maintains contact of tires and road surface and improves the handling and carrying capacity of the truck. The cabin suspension (rubber mounts) and the seat suspension (air spring) isolates the driver from vibrations transmitted from the engine, drive-train or road.

The typical loading cycle of an ADT (in the mining and construction industries) comprises the following elements:

1. Moving across the quarry floor into the loading position (empty)
2. Loading (load dropped into the bin)
3. Moving across the quarry floor to the access road (fully laden)
4. Driving to the drop zone (fully laden)

5. Positioning in the drop zone

6. Tipping the load

7. Driving back to the quarry (empty)

The exposure levels vary from one cycle element to the next with the highest exposure levels being recorded while the truck is driving fastest (cycle elements 4 and 7) and the lowest exposure levels while loading or unloading (cycle elements 2 and 6). Drivers may be expected to work up to 12 hour shifts, depending on the environment and type of load (reviewed in appendix A).

1.2 Motivation

Until recently no legislation governing vibration exposure limits existed, but general legislation required designers to do what is reasonably possible to reduce the health risks associated with whole body vibration (WBV) exposure. The suspension systems were designed to what was considered to be "reasonable" vibration exposure levels, focusing more on handling and load carrying capacity. Studies have shown that in certain cases suspension systems amplified the vibrations between 0-20Hz by as much as 4 times and as many as 45% of seats used in industry increase rather than decrease the accelerations, mainly due to end-stop impacts (Deprez *et al*., 2004). Current research on the health risks of vibration exposure has led to a revision of legislation and the development of a Physical Agents Vibration Directive (PAVD) by the European Union (Directive 2002/44/EC). Included in this directive is an exposure action value (EAV) which determines what an acceptable level of exposure is and an exposure limit value (ELV), which may not be exceeded. The directive will be fully operational in Europe by 2010 (Brereton *et al*., 2004).

Manufacturers that export vehicles or other equipment to Europe will have to adhere to the new legislation requirements to remain competitive. A vehicle that produces a high vibration exposure on the driver may be required to stop before the end of a shift (when the ELV is reached), while a competing manufacturer's vehicle with lower vibration levels, may be allowed to continue. This not only decreases productivity, but also damages the image of the manufacturer whose vehicle had to stop. The European legislation may also be used in South African courts as the benchmark to "state-of-the-art" technology.

Research has shown that human response to whole body vibration can cause discomfort, interference with activities, impaired health, perception of low magnitude vibration and the occurrence of motion sickness (Griffin, 1990). The results of this in the short term are fatigue, loss of concentration and alertness (van Niekerk *et al.*, 1998) and can eventually lead to lower-back pain and musco-skeletal disorders. Drivers that are exposed to high levels of vibration are more likely to make mistakes and cause damage to themselves, the environment and the equipment they work with. A reduction in the exposure levels of the driver may well lead to a reduction in medical and maintenance costs for the employee.

Lower back pain is the leading cause of industrial disability in those younger than 45 years and accounts for 20% of all work injuries. The total cost a year in the US is estimated at $90 billion (Deprez *et al.*, 2004). These disorders are mainly caused by vibration between 0.5Hz and 80Hz, while motion at frequencies below 0.5Hz induces motion sickness (ISO 2631, 1997).

The manufacturer developed a complex 50 degree-of-freedom ADAMS/CAR model of the truck to be used in predictive modelling. The model took a long time to develop and was still not fully operational by the onset of the project. The suspension parameters (tested by and independent institution) were available and would not have to be determined experimentally. The tire stiffness and damping characteristics were obtainable from the tire manufacturer.

1.3 Objectives for the Project

A simplified, reduced order model of an ADT with a 40 ton carrying capacity that is suitable for use in a suspension system optimisation study to reduce the vibration exposure of the driver was developed. The model can:

- Accurately simulate the vibration exposure of the driver.
- Be used to investigate the sensitivity of the various suspension parameters on exposure levels.
- Simulate different loading conditions and road inputs.

In order to reduce the vibration level that a driver is exposed to, one needs to optimise the total transmissibility between the various inputs and the driver on the seat within some given constraints, such as the load the vehicle needs to carry, the vehicle dynamics, the

existing layout and available space. An objective of the project was to show that significant reduction in vibration exposure levels may be achieved without changing the operation, layout or physical dimensions of the current suspension systems or by reducing the load carrying capacity of the vehicle.

Another objective was to determine the parameters of the current passive suspension systems with the largest influence on the vibration exposure levels. These parameters were optimised to produce the lowest exposure levels for a typical haul road. The stiffness and damping characteristics of the various suspension systems were combined into a single parameter for the optimisation study.

1.4 Thesis Overview

The motivation and objectives of the project were presented in this chapter. Chapter 2 focuses on the literature review. Suspension systems, vehicle dynamic models, optimisation techniques and the legislation being introduced in Europe are discussed.

Chapter 3 deals with the modelling of the truck, the road inputs and general assumptions used to simplify the model. Chapter 4 discusses how whole-body vibration exposure on humans should be evaluated.
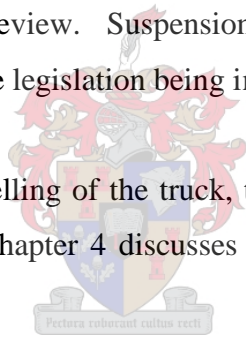
Chapter 5 focuses on objective functions and optimisation algorithms. Chapter 6 discusses the importance of the various parameters, the optimisation results and includes the verification of the results. The conclusions and recommendations are presented in Chapter 7.

Chapter 2: Literature Study

In the literature study the primary functions of the suspension systems and their contribution to comfort are discussed. Various methods and the associated assumptions to model the vehicle, road inputs and human dynamics are discussed. A dynamic simulation software package is reviewed in this chapter. Whole-body vibration and the incorporation of the newly developed legislation in Europe are presented. Finally optimisation techniques from literature are investigated and discussed.

2.1 Primary Function of Vehicle Suspension

According to Gillespie (1992), the primary functions of a vehicle suspension are to:

- Provide vertical compliance so the wheels can follow the uneven road, isolating the chassis from roughness in the road,
- Maintain the wheels in the proper steer and camber attitudes to the road surface,
- React to control forces produced by the tires,
- Resist roll of the chassis, and
- Keep the tires in contact with the road with minimal load variations.

A vehicle such as an ADT may have more than one suspension system. Each suspension system performs a different function. The tires of the ADT are softer (and have more travel) than the primary suspension and thus make a very large contribution to the isolation of the vehicle from the road irregularities. The primary suspension's (between wheels and chassis) main function is vehicle dynamics and load carrying capacity and not so much comfort. It serves to keep the wheels in contact with the ground and to prevent excessive body roll. The cabin suspension's (between chassis and cabin) and seat suspension's (between cabin floor and seat) main purpose is vibration isolation and thus contribute toward the comfort of the driver.

In general, an improvement of vehicle suspension (systems) could produce the following:

- Improvement of vehicle ride quality,
- Increased mobility, and
- Increased component life.

This study will focus on improving the vehicle ride comfort in order to reduce WBV exposure.

Cebon and Cole (1992) reported that, of all the types of suspensions generally used in heavy vehicles, the walking beam and pivoted spring tandem suspensions (such as is used in the ADT under investigation) generate the highest loads, leaf spring suspensions generate less, and air and torsion bar suspensions generate the smallest level of dynamic loads. Higher loads usually lead to the road surface being damaged quicker, which in turn leads to a more irregular road that will include higher vibrations. The maintenance of the road thus plays a vital role in reducing the vibration exposure levels on the driver.

2.2 Vehicle Dynamic Models

A reliable simulation model must include the vehicle (modelled as rigid or flexible bodies), the human on a seat and road profile input. Most of the problems associated with the safety, economy and overall quality of road transportation are affected by the characteristics of the roads and the dynamics of the vehicles and the manner in which they interact (Kulakowski, 1994).

Verheul (1994) suggested that a simplified truck model could be used as a prototype for a more complex model. The simplest vehicle ride model is the 2-DOF (degree-of-freedom) quarter car model. This model is useful to help understand basic concepts of suspension properties and vehicle vibrations (Jiang, Streit, El-Gindy, 2001), but Gillespie and Karamihas (2000) reported that because of the diverse properties of trucks, there is no sound basis for selecting a single model representative of the "average" truck. The attempts to generate a generic quarter-truck model were not very successful with results varying up to 20% with comprehensive, non-linear truck models.

Two- and/or three-dimensional models may be developed to model the ride of a truck. A number of models were investigated by El Madany and Dokainish (1980) and Cebon, (1999). Agreement between 2D (two-dimensional) and 3D (three-dimensional) models are usually good in the region of the sprung mass modes and where roll modes are not significantly excited. It was concluded that where pitch and single plane vibrations dominated, the two-dimensional model was adequate for ride studies. Fu and Cebon

(2002), in their analysis of truck suspension database, concluded that 2-DOF models are adequate to compare suspensions with one another.

Some of the 2D and 3D models that have been developed to model trucks were researched by Jiang, Streit and El-Gindy (2001). In their study they found that linear components could give reasonable results (Wang and Hu, 1998), tandem suspensions could be modelled as massless beams (Cole *et al*., 1992) and the road could be modelled from a power spectral density distribution (Zhou, 1998). These simplifications would be implemented in developing the optimisation model.

Ibrahim *et al.* (1994) developed a model to investigate the effect of a flexible frame on ride vibration in large trucks. He concluded that frame flexibility may contribute significantly to vibration measurements, especially on the trailer. In his article Donald Margolis (2001) stated that the rigid body modes of a truck are most important at frequencies below 5Hz, while beaming (transverse vibration of chassis) occurs close to the wheel-hop frequency at about 10Hz. Beaming is difficult to control from the suspension locations, as the shock absorbers do little to extract energy from the beaming mode. The primary suspension can, however, be used to control the rigid body modes. If beaming is excited, it could be dealt with through cab isolation techniques. A beaming investigation of the ADT (included in Appendix D) showed that it may be ignored for the purposes of this project.

Most tire models are better suited to either ride or handling simulations and few models can simulate both accurately. Two of the models that claim to be accurate enough to be used for either simulation are the SWIFT (Short Wavelength Intermediate Frequency Tire) and F-Tire (Flexible Ring Tire Model). Some of the models (in order of increasing complexity, showed in Figure 1) that can simulate the enveloping properties of tires on uneven roads, and are thus well suited to ride-models are (Zegelaar, 1998):

- single-point contact model (spring and damper in parallel),
- roller contact model (rigid wheel with one spring, one damper and a single contact point),
- fixed footprint model (linearly distributed stiffness and damping in the contact area),

- radial spring model (circumferentially distributed independent linear spring elements),
- flexible ring model
- finite elements models.
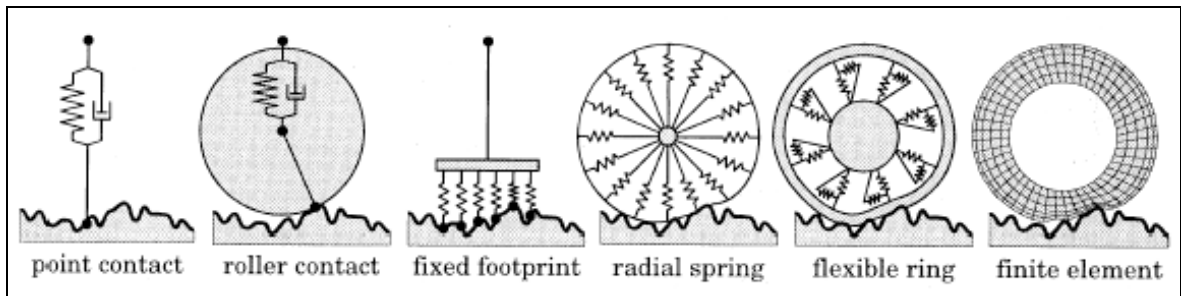
Figure 1: Tire models suitable for Ride Simulations (Zegelaar, 1998)

Prasad (1995) stated in his article that it is widely accepted that poor tire description is the main error in vibration prediction. Most researchers use Voigt-Kelvin (linear spring and viscous damper in parallel) to simulate the tire behaviour. Usually characteristics of the stationary tires are used although they may differ significantly from rolling tires. Kising and Gohlich (1988), and Lines and Murphy (1991) showed that the Voigt-Kelvin representation is a suitable representation of the radial characteristics of the tire. The Voigt-Kelvin, roller contact model as shown in Figure 1, was implemented.

In modelling the human, one may choose between many different models. Biodynamic models were obtained from the superposition of bio-dynamic responses from different individuals. Most current models are little more than convenient simple mechanical systems, the parameters of which have been adjusted to fit average transmissibility (vibration through body) or impedance (transmission of vibration to the body) data. Ideally, models should take into account the bending motions of the spine, the effects of body posture, the non-vertical motions of the head, the effect of non-vertical seat vibration, the effects of the backrest and the variation in motion at different points on the head. Models of the impedance of the body should allow for variations in the static mass of the body and the non-linearity evident with changing magnitudes of vibration (Griffin, 1990). These models, however, will have many degrees of freedom. The more degrees of freedom, the more accurate the model could be, but for optimisation studies a simplified model would be adequate. ISO 7962 of 1987 prescribes a four degree-of-freedom

transmissibility model. For the optimisation study an impedance model would be better suited. ISO 5982 of 1981 prescribes a three degree-of-freedom vertical-impedance model, but a simple lumped parameter model was developed by Fairly and Griffin in 1989 that gives satisfactory results up to 20Hz. It was decided to use the simple lumped parameter model since it has the least degrees of freedom yet still gives acceptable accuracy up to 20Hz. Prasad (1995) and Verma and Gouw (1990) also developed similar models to Fairly and Griffin (1989) with acceptable results, even incorporating non-linear effects such as end-stops.

2.3 ADAMS

ADAMS (Automatic Dynamic Analysis of Mechanical Systems) is commercially available multi-body system analysis software. It is the most widely used software package of its kind. Modelling elements are the basic building blocks of dynamics, i.e. forces, bodies, joints. By selecting and combining these elements, the user can build a dynamic model to the required level of detail.

Once the model is defined, the user can request static, quasi-static, linear, kinematic, dynamic or inverse-dynamic analysis of the system. ADAMS automatically formulates the equations of motion and solves them in the time domain. It can even handle non-linearities and impacts quite well.

ADAMS solves the equations of motion using a variable order and time step predictor-corrector integration technique. The user sets the upper limit for time steps, but ADAMS may use smaller time steps if it is necessary for achieving required accuracy or in the case of sudden change in equations. ADAMS predicts the solution one step forward in time and then corrects it with iteration. If the step is successful the next step is taken; otherwise, the step is rejected and a smaller time step is tried. For more information see the MSC.ADAMS Product Catalog (2002). It was decided to use ADAMS as the platform for the optimisation model.

2.4 Whole Body Vibration

Whole body vibration is the mechanical vibration (or shock) transmitted to the body as a whole. It is often due to the vibration of a surface supporting the body (Griffin, 1990). The effects of vibration could be subdivided into three main headings, namely (a) interference with comfort, (b) interference with activities and (c) interference with health. Each criterion has different considerations and limits associated with it. Not all vibrations, however, are bad and need to be avoided, for example shaking of hands or rocking in a chair. Vibrations may provide feedback to warn of impeding failures and is used for therapy or diagnostics in the medical field.

Vibration produces many different types of sensations as the frequency is increased and the acceptability of the motion varies, but does not fall as rapidly as the decrease in vibration displacement with increasing frequency (for a constant acceleration RMS magnitude). The magnitude of vibration displacement which is visible to the eye of an observer therefore gives a very poor indication of the severity of the vibration.

Frequencies below about 0.5Hz may eventually lead to symptoms of motion sickness (most sensitive between 0.1Hz and 0.125Hz.). Different parts of the body resonate at different frequencies. In the vertical direction resonance starts at about 2Hz, but the first major resonance occurs at about 5Hz. The transmissibility of vertical vibration to the head is sometimes a maximum at 4Hz and the driving force per unit acceleration (as well as the discomfort) is a maximum at about 5Hz. The voice may be caused to warble by vibrations between 10Hz and 20Hz. Vision may be affected at any frequency, but blurring occurs between 15Hz and 60Hz. The dominant vibration transmitted through the seats of vehicles is often at frequencies below 20Hz (Griffin, 1990). It was thus decided to limit the investigation to frequencies below 20Hz.

Comfort is a more difficult to determine since it is subjective and has a lot to do with the psyche. It is important to note that frequency and not only amplitude contribute to the perception of comfort. An experiment done by Fothergill and Griffin in 1977 showed that for a seated person excited by a 10Hz sinusoidal vibration for RMS values below 0.4m/s^2 it was noticeable, but not uncomfortable. A level of 1.1m/s^2 was considered to be mildly

uncomfortable, 1.8m/s^2 uncomfortable and RMS values above 2.7m/s^2 as very uncomfortable.

Most researchers agree that seated humans have a vertical vibration natural frequency at about 4 - 6Hz and a horizontal vibration natural frequency at about 1 – 2Hz. In these frequency ranges the seat motion is most easily transmitted to the upper parts of the body and is not just confined to the area of the body close to the source of vibration. Both Huang and Ji (2004) reported a decrease in natural frequency as the magnitude of the excitation frequency is increased. The resonance of humans decrease from 6 to 4Hz as the magnitude of vibration is increased from $0.25 – 2 \text{m/s}^2$ (Ji, 2004).

The human body's vibration characteristics are non-linear. In his article, Huang (2004) stated that some of the factors that cause non-linearity of apparent mass of a human are posture, muscle tone, dynamics of the buttocks tissue and body geometry. The muscle tone probably made the biggest contribution to non-linearity of the human body's apparent mass.

Research on the effect of posture of a person on natural frequency showed that when the feet of a seated human are not supported (i.e. the feet are hanging) two natural frequencies are witnessed (one between 1-2Hz and the other at around 5Hz), but when the feet of the person are supported only one natural frequency is witnessed (Nawayseh, 2004). Also, when holding a steering wheel, the resonance at 4Hz is more pronounced than when the hands are on the lap (Toward, 2004). A driver usually is excited more than the passenger because of this phenomenon.

Impedance measurements in the horizontal axes show resonances at around 1-2Hz when there is no backrest. A backrest has an effect on fore-aft axis, but little effect on the other axes (Griffin, 1990).

2.5 Legislation

The European Union Directive 2002/44/EC (known as the Physical Agents Vibration Directive or PAVD) set out the minimum standards to be achieved by Member States for

the protection of workers from vibration injury. The PAVD applies the principles of risk management to prevent risks presented by exposure to vibration.

The EU-Directive prohibits the exposure above the exposure limit value (ELV) of 1.15m/s^2 RMS for 8 hours (or $21 \text{m/s}^{1.75}$ VDV). If the exposure exceeds an exposure action value (EAV) of 0.5m/s^2 RMS (or $9.1 \text{m/s}^{1.75}$ VDV) a programme of continual improvement should be implemented by the employer. Whether RMS (root mean squared) or VDV (vibration dose value) should be used is at the choice of the Member State concerned (EU-Directive, 2002).

WBV exposures are to be determined separately for the three axes in accordance with ISO 2631-1:1997 and for health surveillance the axes with the highest level of vibration will be used. The EU-directive is to be implemented on the 6th July 2005 with a transitional period of 5 years for equipment issued before 6th July 2007. The EU-Directive is to be revised every 5 years (EU-Directive, 2002).

In managing the risk of exposure to vibration, exposure should be reduced, but only so far as is reasonably practical. It would be fair to assume that most operators of machinery used off-road are exposed above the EAV. A few processes will cause exposures above the ELV and these should become well known over the next few months as guidance is published. In short, employers should ask themselves: What is good practice? And is good practice being followed? (Brereton, 2004).

At present the EU-Directive and ISO 2631-1:1997 stipulates what the requirements and standards of WBV exposure and measurement are. These documents don't account for all possible situations and consequently a couple of questions (such as what equipment should be used to measure accelerations) were raised about the measurement and evaluation of WBV on humans. A study done by Darlington (2004) on different measuring instruments showed that certain instruments claiming to conform to international standards, that were correctly calibrated and used within their intended operating envelope returned results differing by as much as 30%.

Gallais (2004) found that comfort is time dependent and suggested that time dependency filters should be incorporated in the evaluation of WBV. ISO 2631 of 1997 does not

compensate for time dependency of comfort. It was noted that such dependency curves were included in the ISO of 1974, but was since removed.

Up to date there has been much debate about whether the energy equivalent acceleration A(8) or the VDV measurements should be used to evaluate WBV on seated humans. The arguments for and against the VDV measurements are usually that it is better at indicating the presence of peaks (which tend to be more harmful to humans), but is also more sensitive to human induced motions such as shuffling. Research done by Newell (2004) showed that an operator could exceed the vibration dose action value of the Physical Agents Vibration Directive ($9.1m/s^{1.75}$) by artefacts such as ingress and egress alone with no "authentic" WBV exposure. If it were important that ingress and egress should form part of the daily WBV measurements, then office workers should also be included in the Directive. Tests done on a wheel loader showed that getting in and out of the loader 6 times per day would be enough to exceed the EAV.

2.6 Suspension Optimisation

From Naudè (2001) we see that: Suspension optimisation is the process through which decisions are made on the specific choices of characteristics for the suspension components such that certain prescribed design objectives or evaluation criteria are fulfilled. These criteria may be the attainment of a certain level of ride-comfort over specified terrain and vehicle speed.

Basic approximation vehicle models are used to test the assumptions that simplify the modelling of the specific vehicle. The initial basic approximation models usually assume linear characteristics for suspension components such as the springs and dampers. The second step is to perform a more extensive and detailed analysis of the vehicle concerned. This can be done by performing vehicle simulations using vehicle dynamic simulation programs such as, for example, DADS (Dynamic Analyses Design Systems) or ADAMS. In these more advanced programs the suspension components could have linear or non-linear characteristics. Once the model is validated, the vehicle dynamics may be evaluated over different specified routes and speeds. By changing the suspension characteristics, their influence on the vehicle dynamics may be assessed.

There are many examples of optimisation studies from literature. Heyns (1992) optimised the suspension of a container carrier for ride comfort using GENRIT software. Heui-bon Lee *et al.* (1997) optimised the suspension of a medium truck for ride comfort using road inputs from PSD (Power Spectral Density) plots and DADS software. Motoyama (2000) used a genetic algorithm to optimise the 18 design variables to minimise suspension toe angle. The optimal solution was obtained from a response surface. Lee *et al.* (2000) optimised a train's bogie suspension using fuzzy logic and Vampire software. The 26 design variables were optimised with the help of a response surface. The procedures used in the above examples would also be applied to the current optimisation study.

As can be seen from the abovementioned examples, as well as other investigations reported in literature, optimisation and analysis of a vehicle suspension can be complex, expensive and time consuming. These factors force the design engineer to take a more pragmatic approach summarised by the statement of Esat (1996): "The important goal of optimisation is improvement and attainment of the optimum is much less important for complex systems".

Due to the fact that the suspension characteristics in semi-active or active suspensions can be changed according to the terrain requirements, these types of suspension systems can improve ride quality over a wide spectrum of terrain. These improvements come at the penalty of increased complexity and higher cost. A large amount of research has been done on control algorithms for such suspension systems.

Due to the associated higher cost and increased complexity, semi-active and active suspension systems are still relatively rare. This study will be limited to the optimisation of passive suspension systems.

2.7 Optimisation Algorithm

Engineers use *models* to predict a response or a dependent variable, given the values of other characteristics, called independent variables (regressors or predictors). Engineers require data to estimate these *models*. The method of least squares estimates the parameters of the *model* by minimizing the errors between predicted and observed data. SS_{total}, the variability in the data, can be partitioned into two components: SS_{reg}, which represents the

variability explained by the regression model, and SS_{res}, which measures the variability left unexplained and usually attributed to error. The coefficient of determination, R^2, uses the relative sizes of the variability explained by the regression model and the total variability to measure the overall adequacy of the *model* (Vining, 1998). It is defined by:

$$R^2 = 1 - \frac{SS_{res}}{SS_{total}},$$ (**1**)

this guarantees that $0 \leq R^2 \leq 1$. R^2 may be interpreted as the proportion of the total variability explained by the regression *model*. For the purposes of optimisation, an R^2 value of 0.9 (that is, 90% of the variability is described by the regression model) is acceptable (ADAMS/INSIGHT help file, 2004).

The response surface methodology (RSM) is a method to generate a regression *model* and uses a sequential philosophy of experimentation. To estimate a second-order *model* the design must have at least as many distinct treatment combinations as terms to estimate in the model and each factor must have at least three levels. The most common used design to estimate the second order model is the *Central Composite Design* (CCD). There are different CCD's that uses different values for α. Typical choices for α are:

- 1, creating a *face-centred cube* CCD,
- $k^{0.5}$, creating a *spherical* CCD
- $n_f^{0.25}$, creating a *rotatable* CCD, where n_f is the number of factorial runs used in the design.
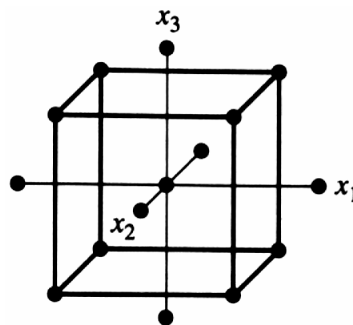
Figure 2: Three-Factor Central Composite Design (Vining, 1998)

For *k* factors, the full factorial design consists of every possible combination of the three levels (upper, lower and centre) for the k factors, giving 3^k combinations. The regression *model* may then serve as the objective function for an optimisation study (Vining, 1998).

Several classes of optimisation algorithms have been developed. The most important classes are (Naudè, 2001):

- Mathematical programming methods (including gradient based methods such as, for example, Sequential Quadratic Programming)
- Lipschitzian and deterministic optimisation and
- Genetic algorithms (GAs)

For the purposes of this project a single Lipschitzian based algorithm (DIRECT) is implemented. The DIRECT algorithm is more robust in determining the approximate coordinates of the global minimum than the gradient based methods. The gradient based algorithms are more efficient in determining the coordinates of local minima (which may or may not include the global minimum). Three gradient based algorithms are used to determine the optimal solution. The solution is then correlated with the DIRECT algorithm's solution to ensure that it is indeed a global minimum. The algorithms are discussed in Chapter 6.
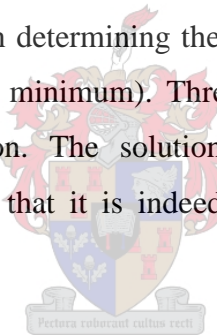
In this chapter it was shown that the suspension could be optimised to improve the ride quality. The assumptions that could reduce the complexity of the truck model were presented. It was seen that only frequencies below 20Hz are important for this study and that VDV or RMS measures may be used to judge the severity of a vibration exposure level. Examples from literature showed that the response surface methodology is a feasible optimisation technique for a study such as this. The regression model and procedure required to generate a response surface was presented. Finally the optimisation strategy was presented.

Chapter 3: Modelling

In this chapter simplified, reduced order models of an ADT with a 40 ton carrying capacity are developed. The models are suitable for use in a suspension system optimisation study to reduce the vibration exposure of the driver. Models that simulate the vibration exposure on the driver at different loading conditions and road inputs are first developed in MATLAB and then refined in ADAMS/VIEW. The ADAMS/VIEW model is then used to investigate the sensitivity of the various suspension parameters on exposure levels and, eventually, to find the optimal parameters.

In this chapter the modelling objectives are stipulated. The suspension layout of the truck is discussed, as well as the assumptions that are made to simplify the modelling of it. The procedure to generate the road profile, as input into the model, is explained. The linearization of the suspension parameters as well as the validation of the assumptions by modelling in MATLAB is presented. Finally, the reduced-order ADAMS/VIEW model used for the optimisation study is reviewed.

3.1 Objective

In order to obtain a realistic computer model of the truck, one would have to represent the real truck as comprehensively as possible in mathematical terms. This can, however, be extremely difficult, time consuming and costly. Instead of modelling the truck exactly as it is, a number of assumptions are made to simplify the model, reduce the number of calculations required and speed up the modelling process. The correct assumptions, that will enable a much simplified model to give solutions within reasonable accuracy of the real truck, need to be determined.

A model that may be used for optimisation of the passive suspension components of the truck for vibration comfort is to be developed. In order to complete an optimisation study the truck has to be modelled accurately enough so that when changes are made to the model it would accurately predict how the real truck would respond with similar changes. The optimal solution found using the model should then also be the optimal solution for the real truck.

A 50 degree-of-freedom ADAMS/CAR model of the 40 ton ADT was developed by the manufacturer. For this optimisation study, a simplified model with fewer degrees-of-freedom than the one that already exists is to be developed. The model should also be simulated under different loading conditions and on different road surfaces. The influence of the various suspension parameters on the vibration exposure should be suitably simulated by the model.

3.2 Vehicle Characteristics

It is important to understand how each suspension component functions before it may be simplified. The different suspension components will be discussed next according to Grovè (2003):

The front suspension consists of the A-frame structure (also called banjo housing), the front suspension struts and the cross-link (pan-hard). The A-frame is connected to the front chassis via a flexible pivot mount. The suspension struts are connected to the A-frame and the front chassis via flexible spherical mounts (sphericals). The cross link is connected to the A-frame structure and the front chassis with the same sphericals as for the suspension struts. The front suspension struts are filled with a combination oil and nitrogen under high pressure. The nitrogen provides the required "spring" characteristics while the hydraulic oil provides the required "damping" characteristics. On both ends of the strut, sphericals are used to connect the struts to the front chassis at the top and the A-Frame structure at the bottom. Figure 3 shows the front suspension without the front chassis:
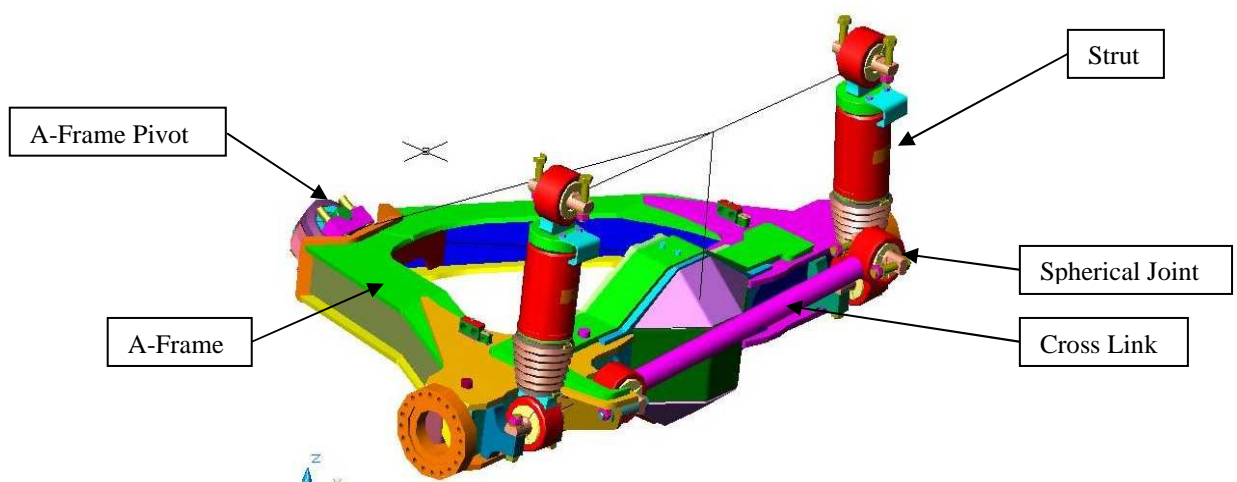
Figure 3: Front Suspension (Grovè, 2003)

18

The rear suspension is more complex than the front suspension. The mid and rear axle housings are connected to the walking beam via sandwich blocks. The walking beams are connected to the rear chassis via flexible pivot mounts. All of the links (top drag, bottom drag & cross) are connected to the axle housings and to the rear chassis via the same flexible spherical mounts as on the front suspension. Figure 4 below shows the rear suspension without the rear chassis:
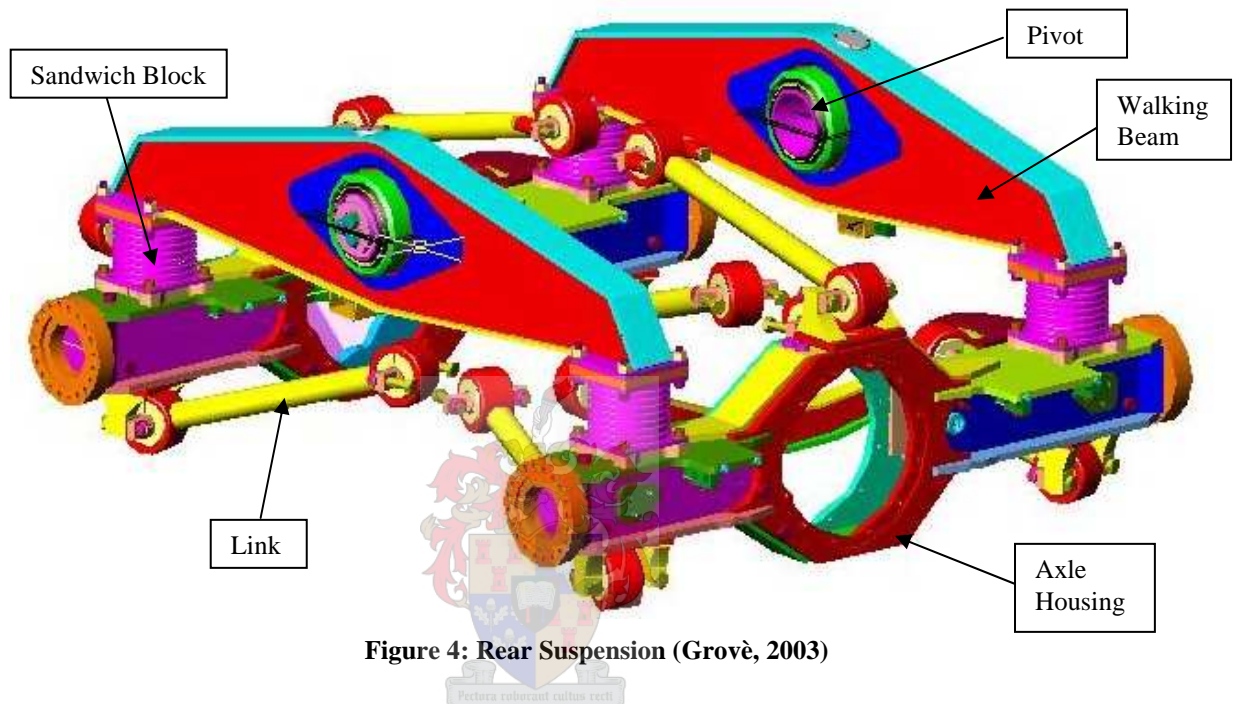
Figure 4: Rear Suspension (Grovè, 2003)

The sandwich blocks are used as flexible elements between the walking beams and the mid and rear axles. In Figure 4 and Figure 5 c) the sandwich blocks are seen in their attached position in the rear suspension.
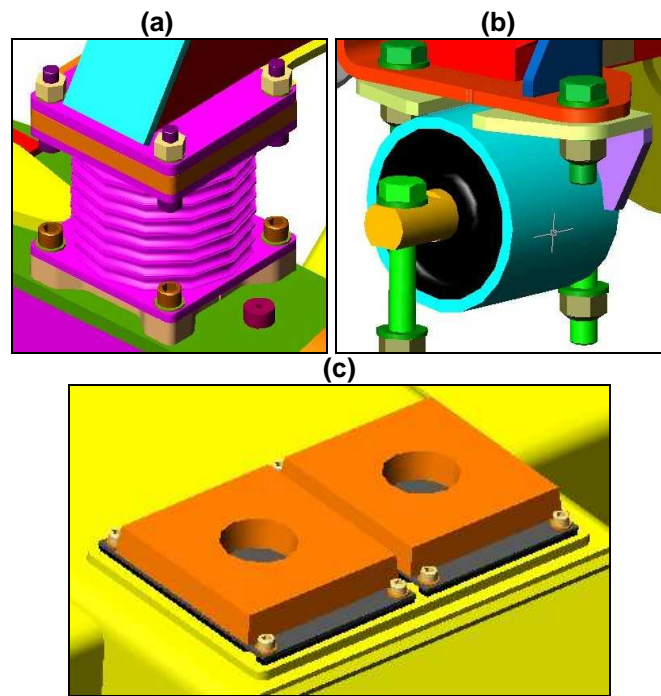
Figure 5: a) Sandwich block, b) Cab mount, c) Bin shock mats (Grovè, 2003)

Four cab mounts as shown in Figure 5 are used to mount the cab to the front chassis of the vehicle. The bushings that form the cab suspension only isolate the cabin from high frequency vibration caused by the engine and ancillary equipment.

The bin shock mats are used to provide a cushioned support for the bin on the rear chassis. There are two sets (2 x 2) mats in the mid position and one set (1 x 2) at the front position. The mats are in essence bump stops. The bin mats are shown in Figure 5 c).

The force versus displacement (static) and force versus velocity (dynamic) characteristics for various components were experimentally determined. The components that were measured are: A-Frame pivot, spherical, strut and link spherical, suspension stops, walking beam pivot, sandwich blocks, cab mountings, bin shock mats, engine mountings, drop box mountings and suspension strut. There was variability in the dynamic and static characteristics of the components of up to 18% (van Tonder, 2003). The mass and inertia of the structural components of the truck were supplied by the manufacturer.

To reduce the complexity of the model the following assumptions were made:

- All components that are to be optimised are modelled with linear characteristics.
- Only parts or assemblies with a mass of 200kg (about 0.7% of the empty truck) or more is considered (except for the human and seat).
- Steering and drive-train are not included (except for mass and inertia properties).
- Tires are modelled as Voigt-Kelvin (spring damper) systems.
- Front suspension is modelled as a single (constrained) axle with struts.
- The human on the seat is modelled as a simple 2-DOF lumped parameter model.
- All structural components are considered to be rigid.

3.3 Road Profile

Road profiles fit the general category of "broad band random signals" and, hence, can be described either by the profile itself or its statistical properties. One of the more useful representations is the PSD function (Gillespie, 1992).

As any random signal, the elevation profile measured over a length of road can be decomposed by a Fourier transformation into a series of sine waves varying in their amplitudes and phase relationships. A plot of the amplitudes versus spatial frequency can be represented as a PSD. Spatial frequency is expressed as the "wave-number" with units of cycles/meter and is the inverse of the wavelength of the sine wave on which it is based. The displacement spectral densities of different road classes (smooth highway, gravel road, ploughed field) are recorded in literature (Wong, 1978, Gillespie, 1992 and Cebon, 1999).

It has been found that the relationship between spectral density and spatial frequency can be approximated by (Cebon, 1999):

$$S_u(\kappa) = S_u(\kappa_0)(\frac{\kappa}{\kappa_0})^{-n} \qquad (2)$$

where

κ = wavenumber

κ_0 = datum wavenumber, $1/(2\pi)$ cycles/m

$S_u(\kappa)$ = displacement spectral density, m^3/cycle

$S_u(\kappa_o)$ = spectral density at κ_o, m^3/cycle

Table 1: Values of $S_u(\kappa_o)$ for Spectral Density Functions for Various Surfaces (Wong, 1987)

Description	n	$S_u(\kappa_o)$ in m^3/cycle
Smooth runway	3.8	4.3×10^{-11}
Rough runway	2.1	8.1×10^{-6}
Smooth highway	2.1	4.8×10^{-7}
Highway with gravel	2.1	4.4×10^{-6}
Pasture	1.6	3.0×10^{-4}
Ploughed field	1.6	6.5×10^{-4}

Typical spectral densities of road elevation profiles simply reflect the fact that deviations in the road surface are larger when the wave-number is large, but decreases as the wave-number is decreased.

Road roughness is the deviation in elevation as seen by the vehicle as it drives over the road. The most meaningful measure of ride vibration is the acceleration produced. The roughness should thus be viewed as an acceleration to understand the dynamics of the ride. Two steps are involved. Firstly a speed must be assumed such that the elevation profile is transformed to displacement as a function of time. Differentiating once gives velocity and twice gives acceleration. The conversion from spatial frequency (cycles/meter) to temporal frequency (cycles/second or Hz) is obtained by multiplying the wave-number by the vehicle speed in meter/second.

Viewed as an acceleration input (Figure 6 c)), road roughness presents its largest inputs at high frequency, and thus has the greatest potential to excite high-frequency ride vibrations unless attenuated accordingly by the dynamic properties of the vehicle. At any given temporal frequency the amplitude of the acceleration input will increase with the square of the speed.
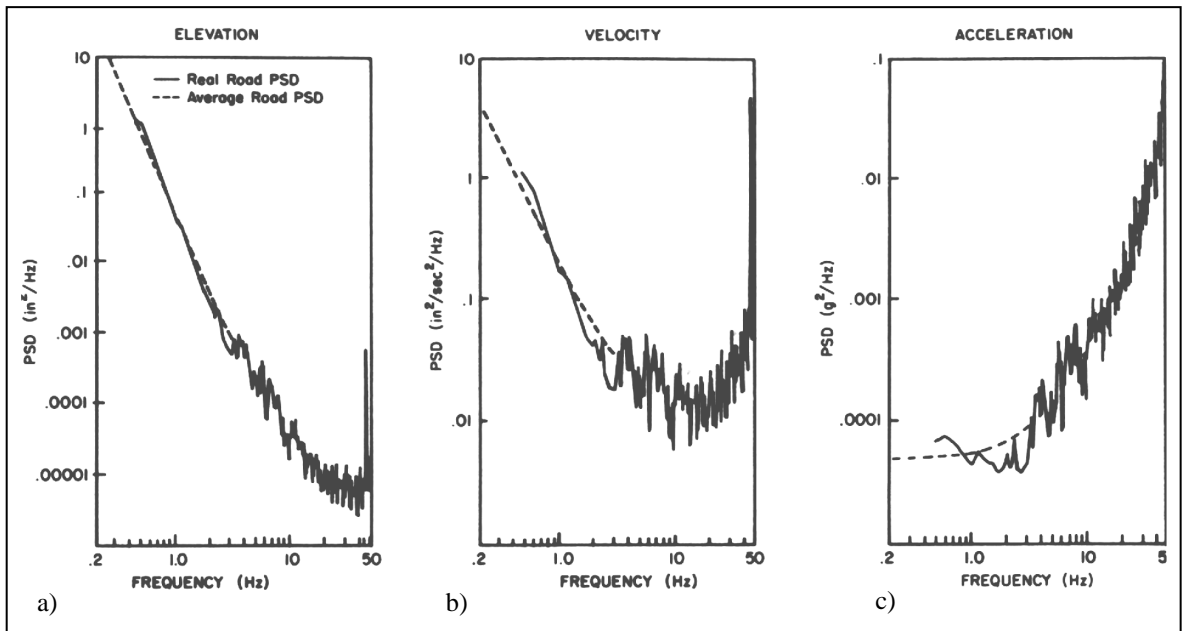
Figure 6: a) Elevation, b) velocity and c) acceleration PSDs of road roughness input (Gillespie, 1992)

The normalised roll input (roll/vertical) PSD (Figure 7) show that at low wave-numbers (long wavelengths) the roll input is much less than the vertical input, but as wavelengths become shorter the correspondence between left and right diminishes and the roll input magnitude grows. The roll resonance is thus excited a lot more at low velocities than at high velocities. This may explain why the lateral vibration exposure may exceed the vertical vibration exposure at low speeds.
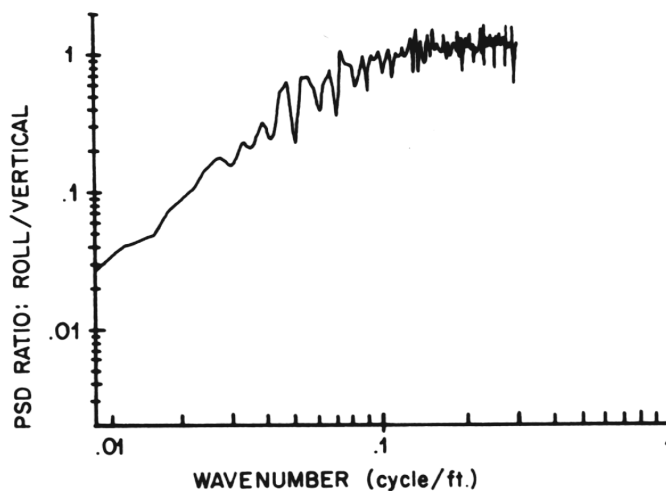
Figure 7: Spectral density of normalised roll input for typical road (Gillespie, 1992)

A rigid tread band model from Ahmed and Goupillon (1997) was used to take into account the spatial filtering of the ground profile by the tires. This model assumes a point contact between the tire and the ground and, to determine the excitation path due to the unevenness of the ground, the road profile $p(x)$ was replaced by the path $u(x)$ of the centre of the tire tread band, which was assumed to be rigid. $u(x)$ is expressed in terms of $p(x)$ by the following equation:

$$u(x) = p(x + x') + \sqrt{R^2 - x'^2} \qquad\qquad (3)$$
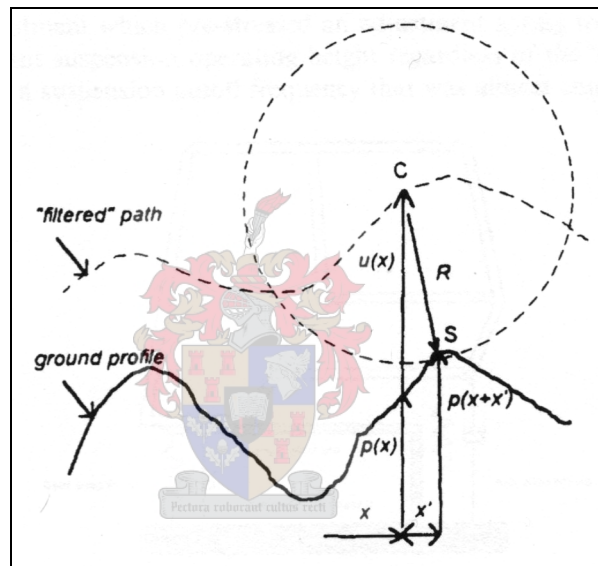
Figure 8: Rigid tread band model (Ahmed and Goupillon, 1997)

where R is the radius of the tire (undeformed) and x' is such that the contact point S is at $x+x'$ (with $|x'|<R$). x' is determined by assuming the angle between the normal force (which is parallel to the line SC joining the point of contact with the centre of the tire) and the vertical is equal to the slope of the ground profile at the point of contact S.

3.4 Linearization

All the suspension components are usually non-linear. The object of linearization is to derive a linear model whose response will agree closely with that of the non-linear model. Although the responses of the linear and non-linear models will not agree exactly and may

differ significantly under some conditions, there will generally be a set of inputs and initial conditions for which the agreement will be satisfactory. (Close *et al.*, 2002)

Linearization is carried out about an operating point and there are different ways to determine the linear curve that suits the problem. If the range about the operating point is small, the gradient of the non-linear curve at the operating point is taken as the linearized equivalent. This may be done by replacing all non-linear terms by the first two terms of their Taylor series expansion and ignoring the higher order terms. If the range about the operating point is larger it may be necessary to perform a curve fit using an optimisation technique such as least squared, alternatively more than one operating point may be considered.

In real life the truck's suspension often collides with the top and bottom end-stops indicating that the full range is used. For the unloaded truck the extension-stops are hit more often, while for the loaded trucks the bump-stops are hit more often. The parameters were linearized (using the least squares curve fitting technique) over the entire range between bump/extension stops. Figure 9 shows the measured stiffness of two struts, a non-linear approximation to the measured results as well as the linearized stiffness of the strut over its operating range. The displacement is negative when the strut is elongated and positive when compressed (as tested). The gradient of the curve is the stiffness of the strut, while the y-axis intercept describes the preload (as tested). The procedure was repeated for all the suspension components and the results are included in Table 2. The stiffness and damping of the seat is taken from the lumped model developed by Fairly and Griffin (1989).
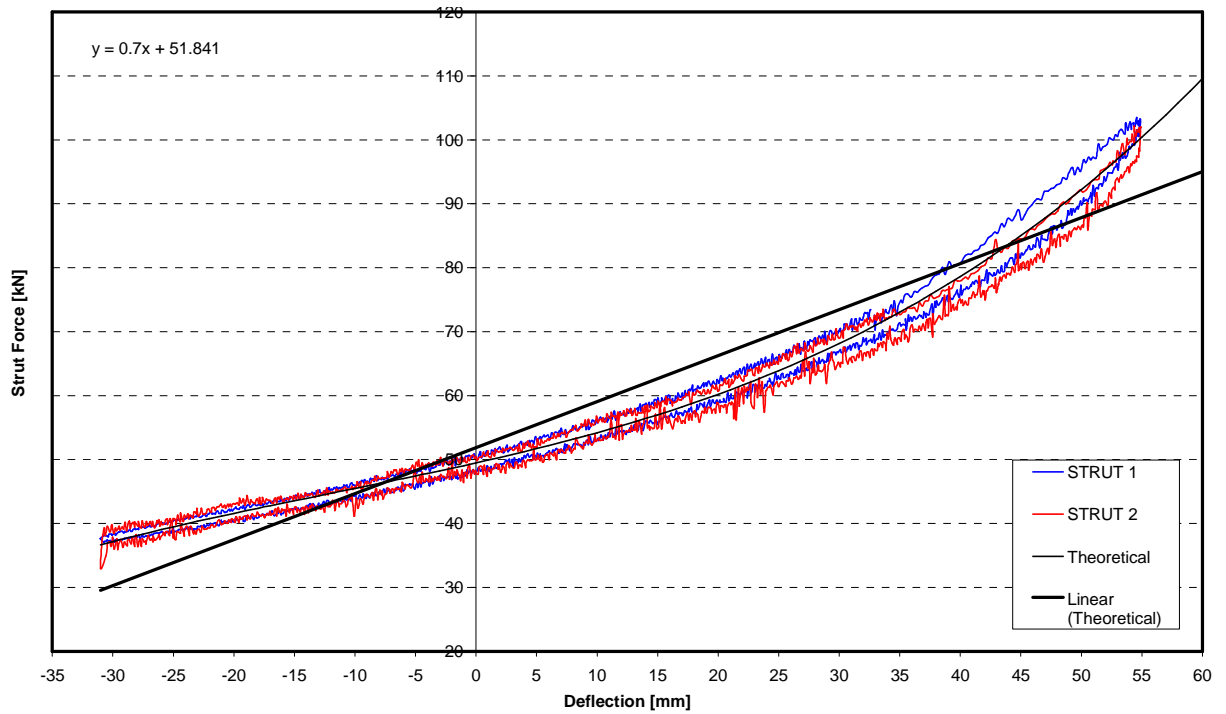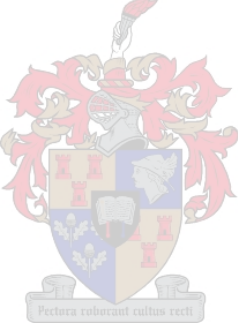
Figure 9: Linearization of Strut Stiffness

Table 2: Linearized Parameters of Suspension Components

Suspension Component	Linearized Parameters (N/mm), (Ns/mm), (kNm/deg)	Unloaded Preload kN	Loaded Preload kN
Strut Stiffness	700	58.2	98.7
Strut Damping	17.1	-	-
Front Tires Stiffness	1130	71.7	75
Front Tires Damping	15	-	-
Rear Tires Stiffness	1250	34.9	100
Rear Tires Damping	19	-	-
Cab mounts Stiffness	1157	2	2
Cab mounts Damping	1.22	-	
Bin Shock Mats Stiffness	15000	99	157.5
Bin Shock Mats Damping	25.1	-	-
Torsion Spring Stiffness	840.6	-	-
Torsion Spring Damping	5.1	-	-
Sandwich Blocks Stiffness	8000	31.2	84.8
Sandwich Blocks Damping	20	-	-
Seat Stiffness	120	0	0
Seat Damping	3.23	-	-

To check the validity of the assumptions and linearization of the suspension parameters, three models of the ADT, each with increasing complexity, were developed and modelled in MATLAB (see Table 3).

Table 3: Degrees-of-freedom of MATLAB models

2 Dimensional 4 degree-of-freedom model	2 Dimensional 7 degree-of-freedom model	3 Dimensional 15 degree-of-freedom model
Vertical displacement: • Chassis • Walking beam Angular displacement about y-axis (pitch): • Chassis • Walking beam	Vertical displacement: • Chassis • Walking beam • Cabin • Bin Angular displacement about y-axis (pitch): • Chassis • Walking beam • Cabin	Vertical displacement: • Chassis • Two walking beams • Cabin • Bin • Seat Angular displacement about y-axis (pitch): • Chassis • Two walking beams • Cabin • Bin Angular displacement about x-axis (roll): • Front chassis • Rear chassis • Cabin • Bin

To assess their performance a spectral analysis was performed on the vibration signal from each model and the signals were converted from the time domain to the frequency domain. The idea being that if there is energy present at any frequency it will appear in the spectral plot. The most useful technique for analysing the frequency content of the signals is the PSD. It generates a measure of the energy contained within a frequency band and is calculated from the FFT of the signal (Mansfield, 2005).

Each model was simulated as driving over a rough road and the results (indicated as normalised PSDs in Figure 10) were compared to the measurements taken in a real truck. The PSDs are normalised, because the exact road surface on which the truck measurements were made is not known and the relative amplitudes at specific frequencies are more important than the absolute amplitudes.

Initially a 2-dimensional, 4-DOF model of the truck was developed and simulated. The model managed to capture the 2Hz peak on the floor in the z-direction (correlating with the rigid body mode of the ADT). The 2-dimensional model was then extended to a 7-DOF model and was again simulated in MATLAB. The 7-DOF model managed to capture the second peak near 20Hz (correlating with the rear-suspension wheel-hop frequency) which the 4-DOF model could not. Finally a 3-dimensional, 15-DOF model was developed and simulated in MATLAB. The model had reasonable accuracy as may be seen in Figure 10. Most of the peaks were obtained fairly accurately except for the lateral (Y) direction on the seat. The MATLAB models are further discussed in Appendix C.

The exact profile of the road is not known. Modelling an incorrect road surface will contribute to the discrepancy between measured and simulated results. Simulating the cross correlation between left and right wheel inputs incorrectly would influence the lateral direction the most. The MATLAB models did not simulate the non-linear end-stops and is expected to produce lower vibration dose values than the real truck. The simulations also assumed a constant speed, which is not possible in a real truck travelling over irregular terrain. The longitudinal direction would be influenced most by this assumption. The VDV and RMS values for the MATLAB models and measured results are recorded in Table 4.

Table 4: RMS and VDV values for MATLAB models

		Seat X	Seat Y	Seat Z	Floor Z
Measured	**RMS (m/s^2)**	0.34	0.86	0.58	0.55
3-dimensional 15-DOF model		0.23	0.81	0.51	0.55
2-dimensional 7-DOF model		-	-	-	0.39
2-dimensional 4-DOF model		-	-	-	0.31
Measured	**VDV $(m/s^{1.75})$**	0.96	2.37	1.67	1.54
3-dimensional 15-DOF model		0.26	1.87	1.31	1.34
2-dimensional 7-DOF model		-	-	-	1.5
2-dimensional 4-DOF model		-	-	-	0.76
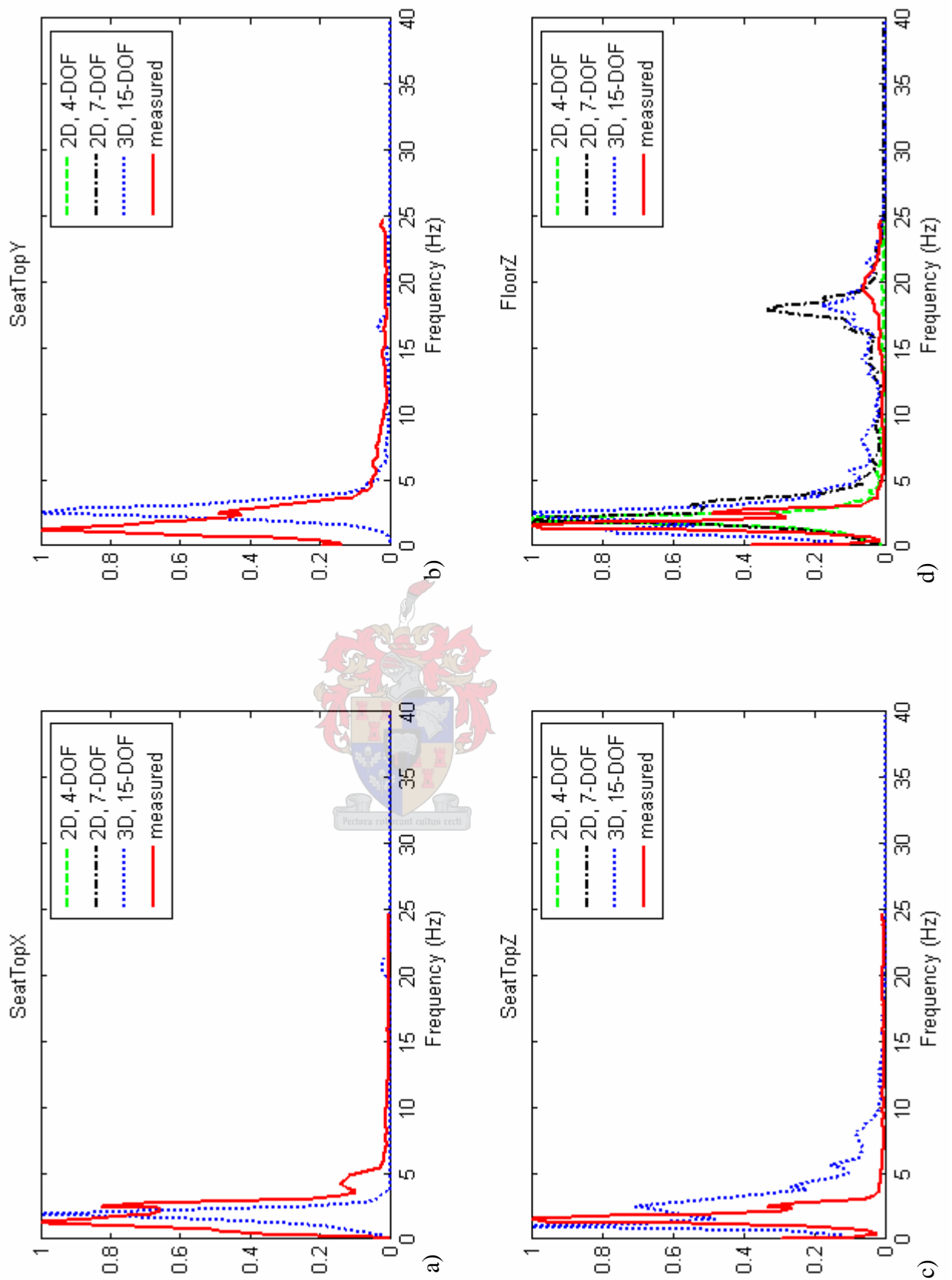
Figure 10: Validation of MATLAB models

3.5 ADAMS/VIEW Model

In the previous section it was shown that the linearization of the suspension parameters and the assumptions that were made gave reasonably good results. The end-stops were not included in the MATLAB models, and the travel of certain suspension subsystems was consequently exceeded. In order to optimise the parameters, the non-linear effects of the end-stops had to be incorporated, especially when simulating very rough terrain as the input. To simulate the truck even more accurately, a model was developed using ADAMS/VIEW. The 24-DOF ride model that was developed in ADAMS/VIEW is shown in Figure 11.
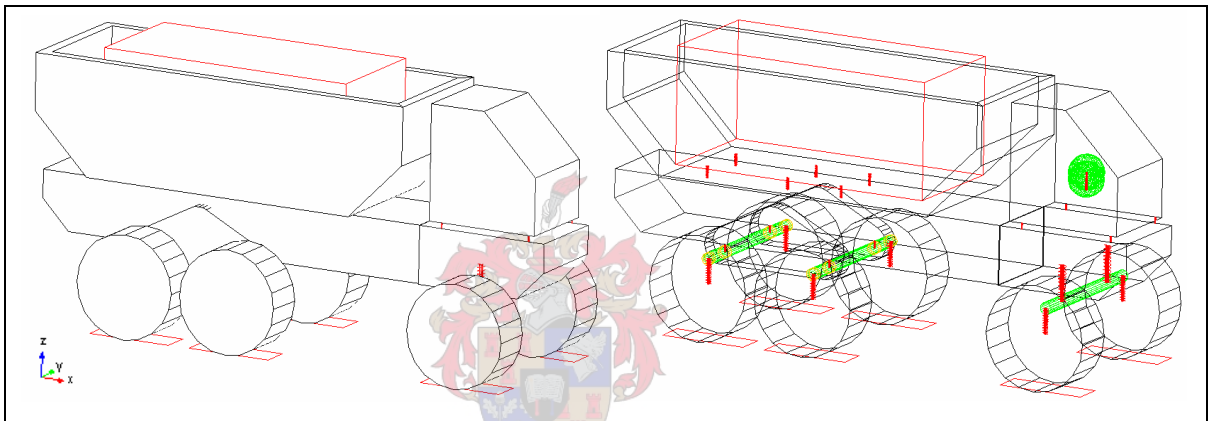
Figure 11: ADAMS/VIEW model of loaded truck

Since the truck does not have a drive-train or steering mechanism the truck was modelled with each wheel positioned on top of a vertical actuator. The actuators move up and down representing the surface of the road. The wheels are free to lift off the actuator when the acceleration becomes too large. The human and seat was modelled as a lumped parameter system. The bump and rebound stops were modelled as contact forces. If a certain displacement is exceeded, spring and damper forces would increase exponentially, forcing the body back into the operating range. The load is fixed to the bin and the bin can only move vertically relatively to the rear chassis. None of the components are allowed to rotate about the vertical (Z) axis. The degrees of freedom may be summarised as:

- vertical displacement of each wheel (6),
- angular displacement of the axles about the x-axis (3),
- vertical displacement of the axles (3),
- angular displacement of the walking beams about the y-axis (2),

30

- vertical displacement of the chassis (1),

- angular displacement of front and rear chassis about the x-axis (2),

- angular displacement of the chassis about the y-axis (1),

- vertical displacement of the cab (1)

- angular displacement of the cab about the x- and y-axis (2),

- vertical displacement of the load-bin (1),

- vertical displacement of the seat and the human (2).

3.6 Validation

A comprehensive ADAMS/CAR model of the ADT was developed by the manufacturer to simulate the truck as accurately as possible. The ADAMS/CAR model is fairly complex, having 50 degrees-of-freedom and non-linear suspension parameters. The tires were not modelled as point contact Voigt-Kelvin (see Figure 1) as was the case with the ADAMS/VIEW model, but instead the F-Tire developed by Michael Gipser (1999) was used. The results obtained by the simplified model created in ADAMS/VIEW were compared with results obtained by the ADAMS/CAR model as well as with measured results from real trucks.

In order to validate the model it is important that the inputs into the model are the same as the inputs experienced by the truck. It is very difficult to accurately describe a road's surface, thus it was decided to use an obstacle of known shape and size for verification purposes. A cosine-shaped bump was constructed with a wavelength of 1.8m and a height of 0.3m. The truck attempted to drive over the bump at approximately 8km/h, but the speed of the truck did not remain at exactly 8km/h as it crossed the bump.

A comparison between the complex ADAMS/CAR model and a real truck had already been done. These results served as the basis for validation of the newly developed, ADAMS/VIEW model. To reproduce the inputs a spline of the displacement as a function of time was generated. The displacements were then reproduced by the actuators at the base of the wheels of the model.

Unfortunately no data was available for the cabin or seat, thus the comparisons had to be based on strut and chassis data.

In Figure 12 the acceleration on the front chassis was recorded. In both graphs the dash-dotted line represents the ADAMS/VIEW model while the solid lines represent the data from the more complex model (top figure) and the measured data (bottom figure). In the measured data a small bump is seen just after 2s, the ADAMS/VIEW model simulated the bump, while the more complex model did not. Due to the linearization of the parameters over the entire range (see Figure 9 on pg 26), one would expect the frequencies to correspond well when large displacements are present (such as when crossing the bump), but slightly inaccurate (over or under, depending on load condition) when displacements are small. This explains why the results of the ADAMS/VIEW model oscillate slightly faster than the other results when the amplitude decreases.

In Figure 13 the normalised PSDs of the acceleration data from Figure 12 is shown. It is clear from the graphs that the frequency content of both ADAMS models are the same, but their relative importance are not quite the same. The frequency of the main peak corresponds well with what was measured in the real truck, but the other frequencies were slightly too high, mainly due to the linearization and load condition of the truck (the frequencies would shift slightly to the left for the loaded truck.)
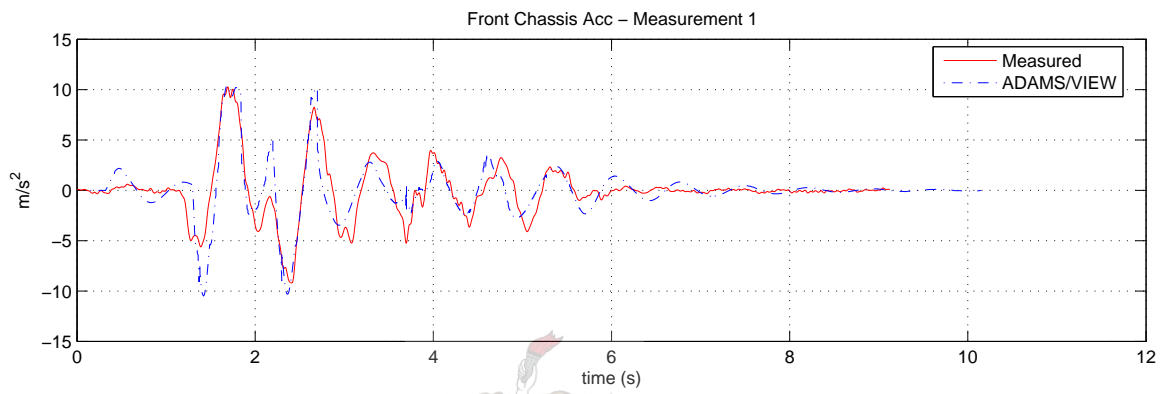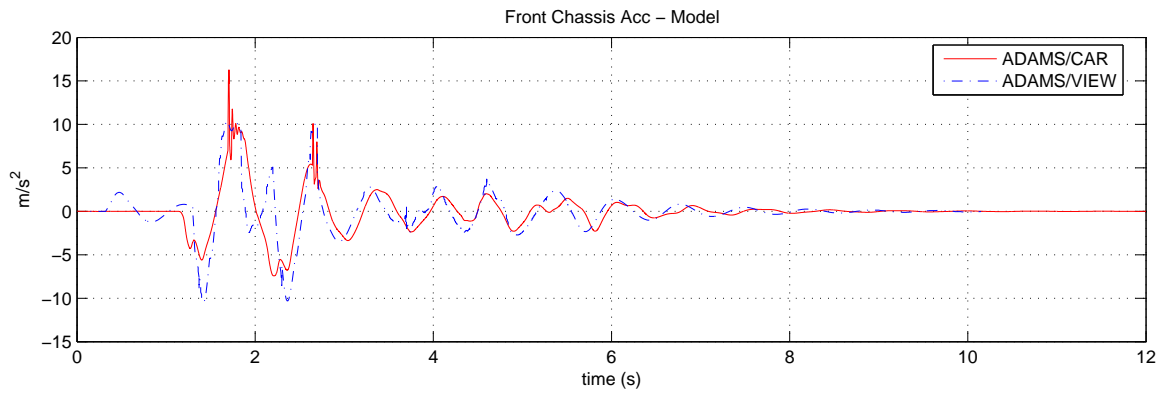
Figure 12: Validation - Front Chassis acceleration time history
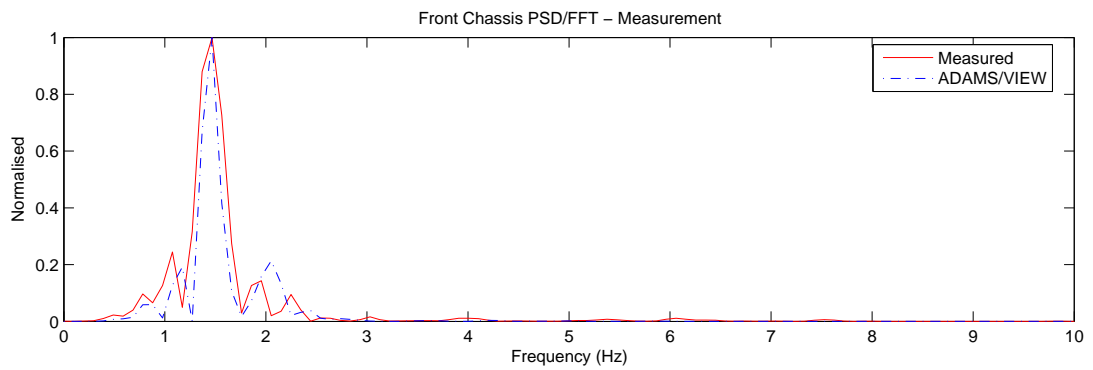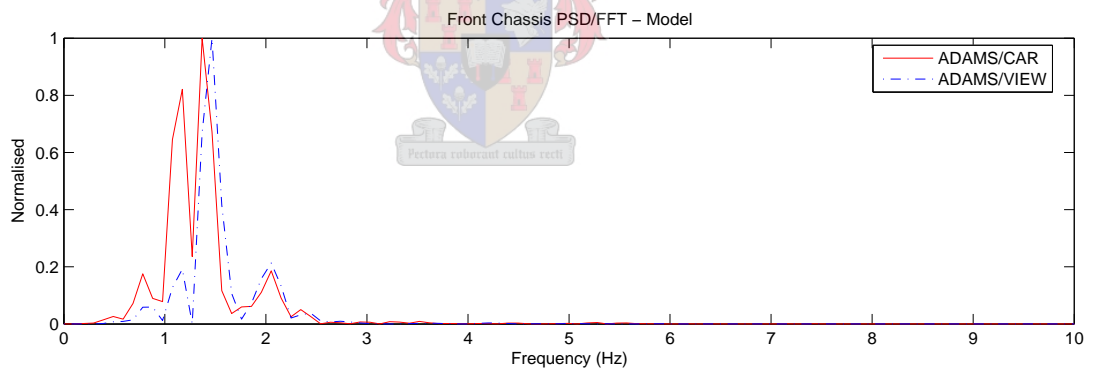
Figure 13: Validation - Front Chassis PSD

33

In Figure 14 the displacement of the strut is recorded as the truck traverses the bump. The flat peaks are due to end-stop impacts. It is again clear that the ADAMS/VIEW model follows the measured results more closely than the ADAMS/CAR model. Again the spike at about 2s is missed by the ADAMS/CAR model, but simulated by the ADAMS/VIEW model. The frequencies correspond fairly well over most of the data range, but become slightly too high as the displacements decrease. The damping in the real truck also seems to be higher than in either model.
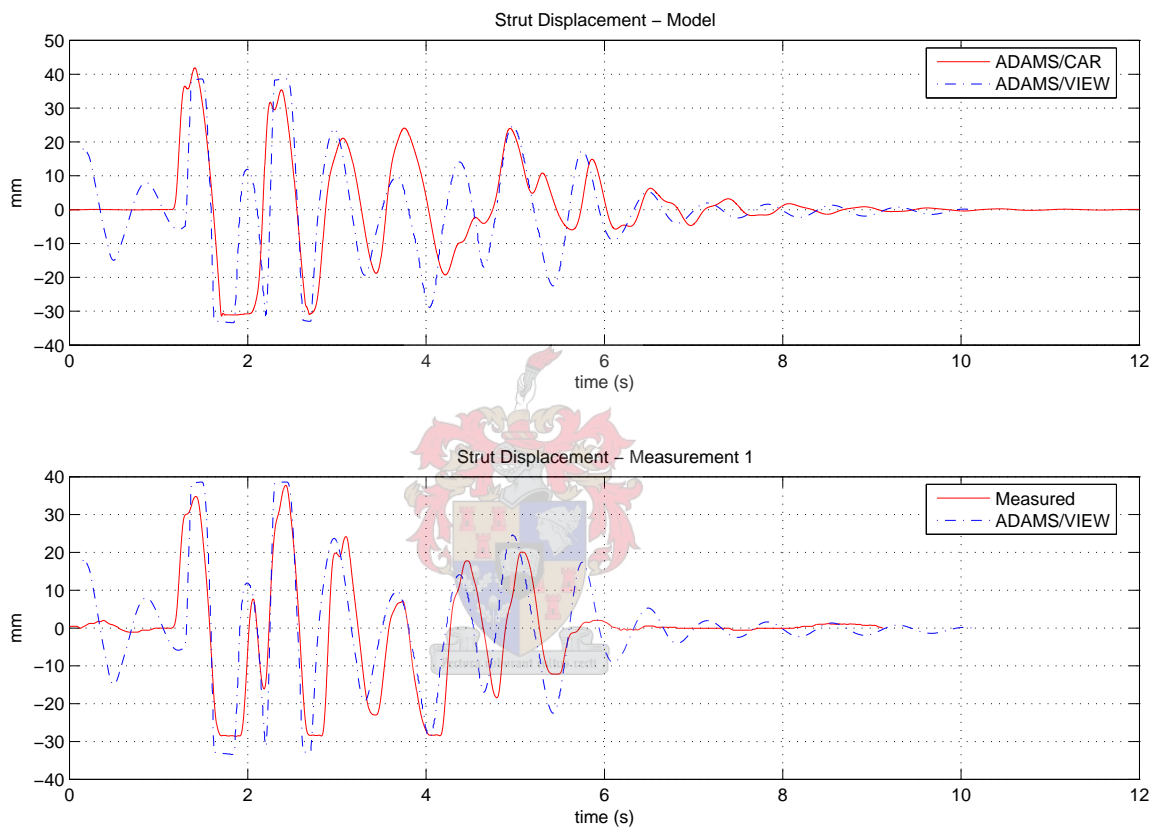
Figure 14: Validation - Strut displacement time history

In Figure 15 the normalised PSDs of the strut displacement data is shown. The ADAMS/VIEW model seems to be a little closer to the real truck than the ADAMS/CAR model. The minor peaks are slightly over-estimated as before.
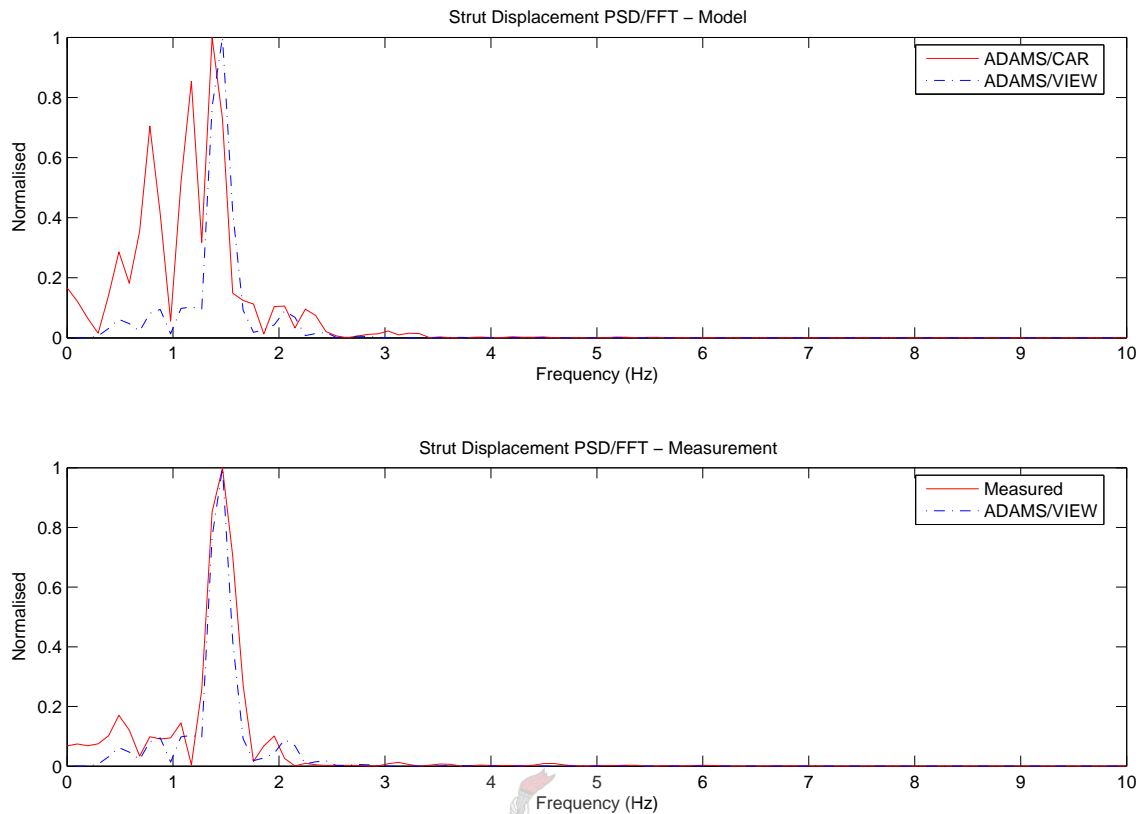
Figure 15: Validation - Strut Displacement PSD

A comparison between the newly developed ADAMS/VIEW model and the manufacturer's ADAMS/CAR model, on the randomly generated road surface that was used for the optimisation study, is shown in Figure 16. The FFTs are calculated from acceleration measurements taken on the cabin floor underneath the seat.

In the top graph of Figure 16 the FFTs of the longitudinal vibrations are recorded. The first peak (corresponding to the rigid body pitching mode) compares well with the more complex model. The two peaks that are generated by the ADAMS/CAR model close to 4Hz are not generated by the ADAMS/VIEW model. It is believed that these peaks are due to input from the drive-train as the drive-train would have the largest influence on the longitudinal vibration exposure. The drive-train was not simulated in the ADAMS/VIEW model. It is, however, also possible that these peaks are overestimated by the ADAMS/CAR model as was the case in Figure 13 and Figure 15 above.

In the middle and bottom graphs of Figure 16 the FFTs of the lateral and vertical vibrations are recorded respectively. The ADAMS/VIEW model correlated well with the more

complex ADAMS/CAR model for both vibration axes even though it had less than half the number of degrees-of-freedom.
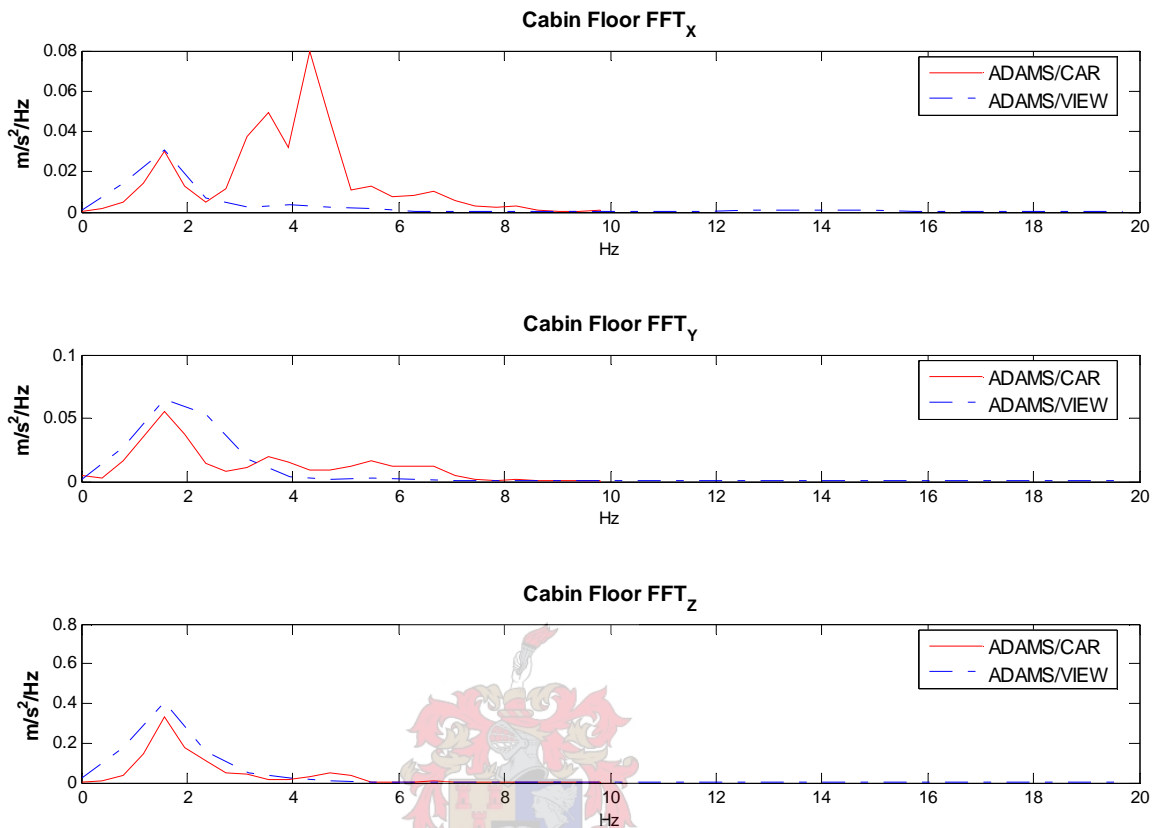
Figure 16: Validation - Cabin Floor FFTs

In this chapter the assumptions that were used to simplify the modelling of the truck were stipulated and verified with simplified MATLAB models. A 24-DOF model was developed in ADAMS/VIEW that accurately simulates the vibration exposure on the driver. This model may be used to investigate the sensitivity of the various suspension parameters on exposure levels and can be simulated with different loading conditions and road inputs. The model was verified by comparing the simulated results to a more complex model (with 50 degrees-of-freedom) and measurements from a real truck. It was discovered that the newly developed model was more accurate in simulating the response of the real truck than the more complex model despite the reduced complexity.

Chapter 4: Evaluating Whole Body Vibration

The EU-Directive established two limits (EAV and ELV) for the whole body vibration exposure of a person during an 8 hour working day (measured as a RMS or VDV) as explained in section 2.5 of the literature review. In this chapter the method by which the whole body vibration is to be evaluated is discussed.

The perception and influence of whole body vibration on humans is strongly dependent on the direction, magnitude and frequency of the vibration exposure. To enable measurements of vibration exposure from one direction, frequency and magnitude to be compared to a vibration exposure of another direction, frequency and magnitude, a frequency rating system was developed by the International Organization of Standardisation (ISO 2631, 1997). A frequency rating provides a model of the response of a person to the vibration direction and frequency weightings are used to simulate the frequency dependence of a person.

From the literature review it was seen that seated humans have a vertical resonance at about 4-6Hz and a horizontal resonance at about 1-2Hz (Griffin, 1990). At these frequencies the motion of the seat is transferred most easily to the upper parts of the body. Frequency weightings are applied to the acceleration data measured at the human/seat interface. The frequency weightings are designed to not affect those frequencies where the body is most sensitive and to attenuate at those frequencies where the response of the body is less sensitive. In principle, weightings do not amplify at any frequency. There are, however, a couple of limitations to human vibration frequency weightings. The first is that they are derived from meta-analysis studies of equal sensation curves and are thus representative of the population rather than an individual. A second limitation is that the weightings assume linearity, i.e., there is only one rating for both low- and high magnitude environments. A third limitation is that the weightings assume that perception techniques may be used to predict injury. Although there are problems with the use of the frequency weightings, there are currently no alternative methods of assessment (Mansfield, 2005).

A couple of weighting curves (filters) are specified by ISO 2631 (1997) depending on the orientation of the person and the direction of vibration. For a seated person the W_k filter is

used to weigh the frequency contribution for vertical vibrations and the W_d filter is used to weigh the frequency contribution for lateral vibrations (ISO 2631, 1997, EU-Directive, 2002). The frequency weighting curves are shown in Figure 17.
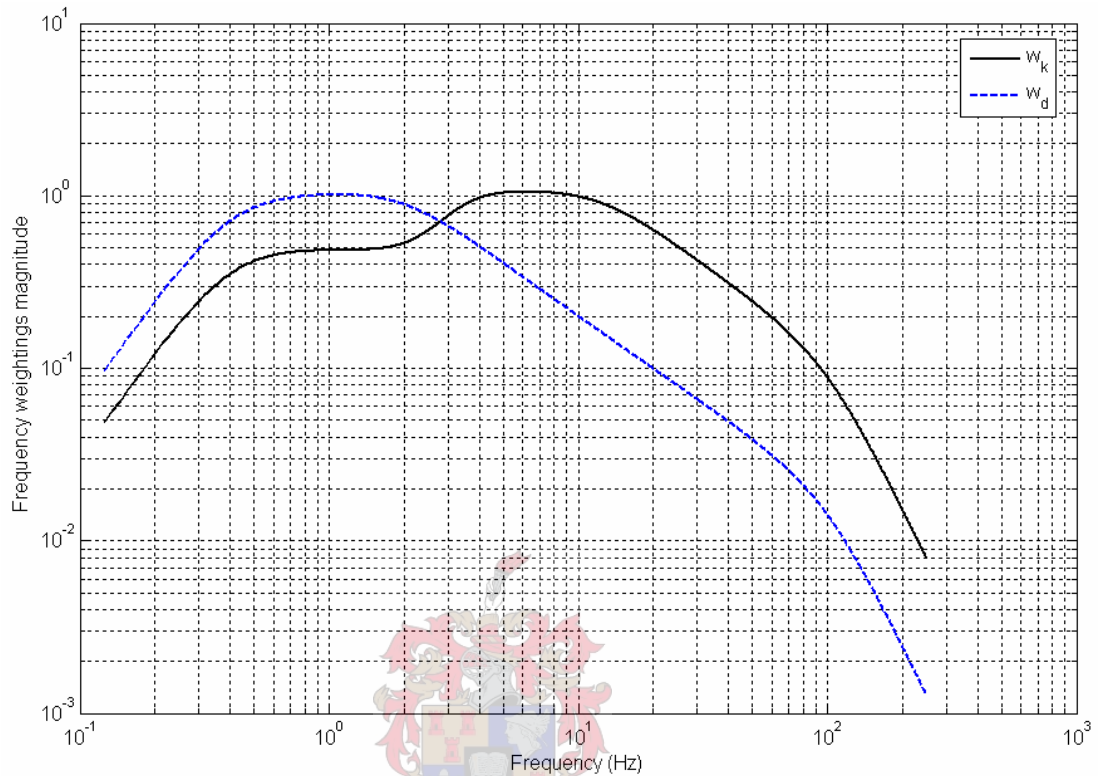
Figure 17: Frequency weighting curves for principle weightings (ISO 2631, 1997)

Evaluation of the effects of vibration on the health, according to ISO 2631 (1997), is determined using the frequency weighted RMS for each axis of translational motion on the supporting surface if the crest factor (ratio of peak acceleration to the RMS) is less than 9. Assessments are made independently in each direction, and horizontal vibration is multiplied by a scaling factor of 1.4. The overall assessment is usually carried out according to the worst axis of frequency weighted RMS acceleration (including multiplying factors). If crest factors exceed 9, then an alternative method of assessment is suggested, the VDV (Mansfield, 2005). This is because shocks have been shown to cause more discomfort than other stimulus types of the same frequency-weighted RMS vibration magnitude (Mansfield et al 2000). The EU-Directive (2002) accepts either the RMS or VDV measurements as indicative of the exposure level of the driver. Figure 18 shows which weighting filter and which scaling multiplier should be applied to which axis.
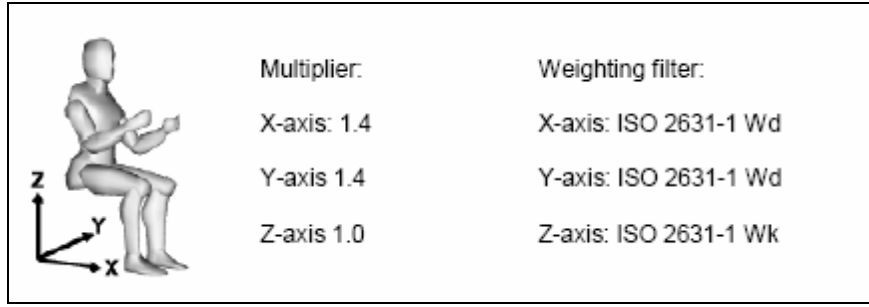
Figure 18: Axes, multipliers and weighting filters (Rimell, 2004)

The limits imposed by the EU-Directive are applicable to an 8-hour working day, thus the 8-hour equivalent RMS and VDV values are to be calculated to see whether the limits have been exceeded. The 8-hour VDV equivalent (VDV$_8$) may be determined by using equation (8) (from Mansfield, 2005). Alternatively an estimated VDV (eVDV) may be calculated from the 8-hour RMS equivalent. Values for the RMS, VDV and eVDV may be calculated using equations (4 – 6) (Griffin, 1990), the 8-hour RMS equivalent, A(8), may be calculated using equation (7).

$$RMS = \sqrt{\frac{1}{N}\sum_{i=0}^{N-1} a_w^2(i)} \qquad (4)$$

$$VDV = \sqrt[4]{\frac{1}{f_s}\sum_{i=0}^{N-1} a_w^4(i)} \qquad (5)$$

$$eVDV = \sqrt[4]{(1.4 a_{RMS})^4 T_s} \qquad (6)$$

$$A(8) = \sqrt{\frac{1}{f_s T_8}\sum_{i=0}^{N-1} a_w^2(i)} \qquad (7)$$

$$VDV_8 = \sqrt[4]{\frac{T_8}{T_s}\times VDV_s^4} \qquad (8)$$

Where $a_w(i) = i^{th}$ sample of the weighted acceleration, N = total number of samples, f_s = sample rate, a_{RMS} = RMS value of weighted acceleration over time T_s, T_8 = eight hours in seconds (28800) and VDV_s is the VDV measured over time T_s. Only the axis with the largest contribution is considered when calculating total exposure (EU, 2002).

The Health and Safety Executive (HSE) in the United Kingdom has developed a whole-body vibration exposure calculator. This calculator allows daily exposures to WBV to be compared with the EAV and ELV. Once the frequency weighted vibration exposures multiplied by the correct scaling factors and the exposure times are defined, the calculator uses equations (7) and (8) to calculate the 8-hour equivalent exposures. The calculator also calculates the time required to reach the EAV and ELV with the measured RMS and VDV. The calculator was used for the measurements recorded in Appendix A.

In this chapter the procedure for evaluating whole body vibration exposure was explained. The raw data is weighed and scaled according to ISO standards and is then converted to an RMS or VDV value so that the severity of the exposure may be assessed.
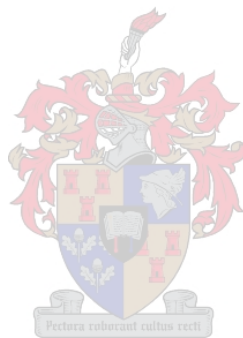
Chapter 5: Optimisation

During the hauling periods, the truck is driven as fast as possible and the driver cannot do much to reduce the exposure levels (measured as RMS or VDV). At the loading and dumping sites, the road is usually very rough, and the truck is driven much slower. The level of exposure is highly dependent on the driving style (line and speed) of the driver. It was decided to focus the optimisation study on the hauling periods, as an improvement in the suspension during the other periods could lead to more aggressive driving (the driver would not slow down as much when the road gets rough) and similar exposure levels. This is discussed further in Appendix A. The haul road used for the optimisation resembled a "very rough dirt road" as described by Cebon (1999), see Chapter 3.3.

From basic calculus we know that for a point in a function to be a minimum, the partial derivatives (gradient) of the function with respect to its design variables must be zero and the function needs to be upwards concave at that point. In the general *n*-dimensional case this translates into the requirement that the Hessian matrix (the matrix of second partial derivatives of the function with respect to the design variables) be positive definite. If the variables are restricted to values within a specific range, the optimal (minimum) point is a little harder to find. Numerical methods are usually used to find the minimum of such functions. The non-linear constrained optimisation problem is written mathematically as:

Minimise: F(X)   objective function   (**9**)

Subject to:

$g_j(X) \leq 0$ $j = 1, m$ inequality constraints   (**10**)

$h_k(X) = 0$ $k = 1, l$ equality constraints   (**11**)

$X_i^l \leq X_i \leq X_i^u$ $i = 1, n$ side constraints   (**12**)

where *X* is the vector of design variables.

To reduce computational time, it is desirable to limit the number of design variables. By coupling the stiffness and damping of the suspension components (i.e. adjusting them together such that a 10% increase in the stiffness is accompanied by a 10% increase in

damping and vice versa), the number of design variables could be halved. Six design variables (X_i) were identified for optimisation, they were:

- The struts' stiffness and damping,
- The cab mounts' stiffness and damping,
- The tires' stiffness and damping,
- The sandwich blocks' stiffness and damping,
- The seat's stiffness and damping,
- The walking beams' torsion springs' stiffness and damping.

Since the influence of the optimised suspension parameters on the handling of the vehicle was not investigated, it was decided to limit the search for an optimal solution to ±20% of the current linearized values. The struts and seat, however, were allowed to be even softer (-40%) as research from literature showed that the rolling stiffness of the steering axle usually is much higher than required (Fu *et al*., 2002, and Cebon, 1999) and the seat does not contribute to the handling of the vehicle. The roll stiffness could also be increased later by adding a torsion bar to the front suspension. These limits were introduced as side constraints (equation (12)). No inequality or equality constraints (equations (10) and (11)) were necessary.
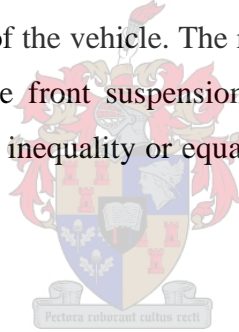
5.1 Objective Function

The objective function is the function that is to be minimised by the optimisation algorithm. The comfort of the truck is represented by the RMS or VDV values. The lower these values are, the more comfortable the truck will be. The objective of the optimisation is thus to minimise the RMS or VDV measured at the seat/human interface. For the purpose of this optimisation study the RMS and VDV values of the weighted vibration data of all three axes were calculated at the seat/human interface for different suspension setups as defined by the face centred cube central composite design methodology (see Chapter 2.7 and Figure 2) and were recorded. Separate quadratic response surfaces were fitted to the recorded results of the RMS and VDV values for each axis.

For three variables (X_1, X_2, X_3), the equation of a quadratic response surface is of the form:

$$F(X) = b_0 + b_1 X_1 + b_2 X_2 + b_3 X_3 + ... \qquad \text{(linear terms)}$$

$$+ b_{12}X_1X_2 + b_{13}X_1X_3 + b_{23}X_2X_3 + ... \text{(interaction terms)}$$

$$+ b_{11}X_1^2 + b_{22}X_2^2 + b_{33}X_3^2 \qquad \text{(quadratic terms)} \qquad \textbf{(13)}$$

where the coefficients (b_{ij}) are determined by the regression calculation (explained in Chapter 2.7 and equation (1)). For six variables (as for this optimisation study) the equation of a quadratic response would contain more terms, but still have the same form.

The response surfaces of all the axes were superimposed and the response surface of the axis with the highest exposure at the point of investigation was used as the objective function. The optimisation algorithms will thus be required to jump from the response surface of one axis to the response surface of another axis if the other axis becomes the worst axis at the point of investigation. In Figure 19 a hypothetical example of how the objective function would switch between the axes, to always represent the worst axis as a parameter is varied, is shown. For the optimisation study two objective functions are defined, one for the RMS and one for the VDV respectively, and optimised independently.
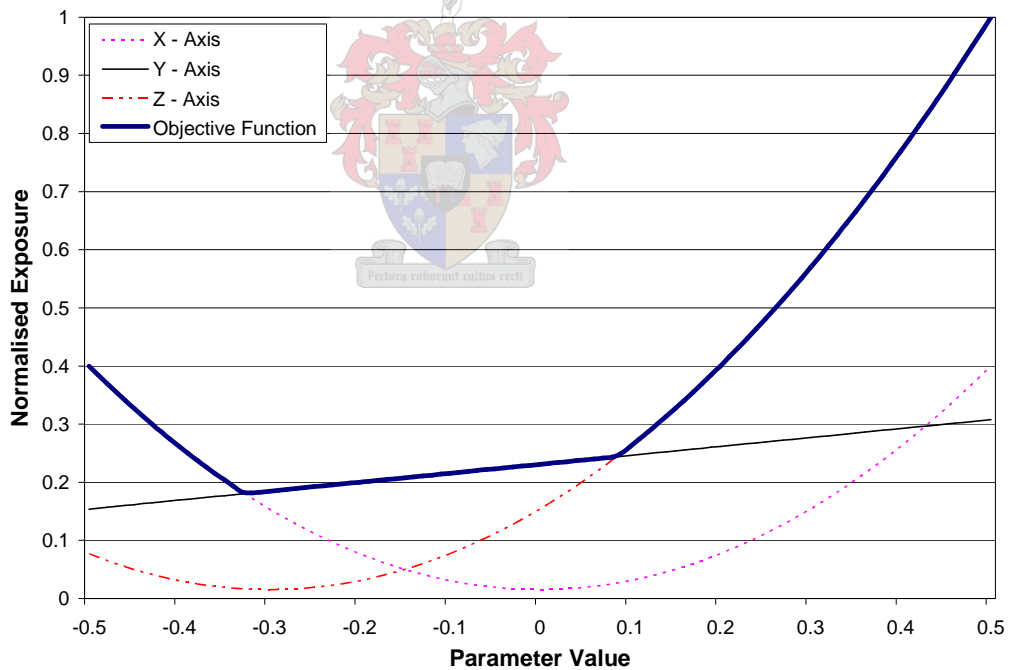
Figure 19: Objective function representing switching of the worst-axis

5.2 Algorithms

Four optimisation algorithms were used to minimise the objective functions for RMS and VDV respectively. The DIRECT algorithm developed by Dan Finkel (2003) was used. From MATLAB's optimisation toolbox the *fmincon* function was used. Finally the General

Reduced Gradient (GRG) and Sequential Quadratic Programming (SQP) algorithms from ADAMS/INSIGHT were used.

The DIRECT (Divided Rectangles) algorithm is a global optimization scheme which can be tuned for both local and global properties. It begins at the centre of the design space (the starting point) and divides the design space into smaller rectangles. The algorithm iteratively continues this process of electing and subdividing those rectangles that have the highest likelihood of producing an objective function lower than the current lowest value. It is this process of subdividing the rectangles that the algorithm achieves both global and local properties. Unlike the genetic algorithm which is a global scheme, DIRECT is a deterministic process and needs to be run only once. A disadvantage of this scheme is that it only terminates after a certain number of iterations have been achieved. For more information on how this algorithm operates, see E.S. Siah, P. Papalambros and J.L. Volakis (2002).

Unlike DIRECT, the other three algorithms are gradient based methods. In gradient based algorithms, information about the first (or second) derivative of the objective function is used to determine the optimal solution. With such methods it is difficult to know whether the solution has converged to a global or a local minimum. The DIRECT algorithm (although slightly more coarse than the other algorithms implemented) could be used to check whether a global minimum was obtained by the other algorithms.

The GRG method implemented in ADAMS/INSIGHT is an extension of an earlier reduced gradient method which solved equality-constrained problems only. This is accomplished by adding slack variables to each inequality constraint (or side constraint in our case) to make them equality constraints. The method uses first order (gradient) information only to determine the search direction. The algorithm is well suited to this optimisation problem since the objective function is not highly non-linear (which could lead the one-dimensional search to become ill-conditioned) and there were not many inequality constraints (side constraints only). The number of independent variables would thus not become too large, requiring lots of memory and making the algorithm inefficient. A detailed description of this algorithm is given in Vanderplaats (2001) Chapter 6.7 and Rao (1996) Chapter 7.9.

The *fmincon* function in MATLAB's optimisation toolbox uses a SQP method. Unlike the GRG method, the SQP method also uses second order (curvature) information to determine the search direction. The method is also more robust as it ensures that the positive definiteness of the Hessian is maintained, can cope with inequality and equality constraints and deals internally with infeasible designs. The SQP method is perhaps one of the best methods of optimisation as it incorporates the best features of several concepts (Vanderplaats, 2001). The algorithm is well suited to this optimisation problem as the objective function is quadratic and the constraints linear. The SQP method implemented in *fmincon* differs slightly from the SQP method used in ADAMS/INSIGHT. Although the general strategy is the same, the sub-problems are solved differently. The *fmincon* function in MATLAB could thus be used to verify the solutions of the ADAMS/INSIGHT algorithms (and vice versa). For more information on how this function operates, see MATLAB Optimisation toolbox User's Guide (2004). A detailed description of how the SQP method from ADAMS/INSIGHT operates is given in Vanderplaats (2001) Chapter 6.9 and Rao (1996) Chapter 7.10.

In this chapter the design variables, constraints, objective functions and algorithms that are used in the optimisation study is discussed. The optimisation will focus on reducing the vibration exposure in the worst-axis (as defined by the objective function and Figure 19) only.
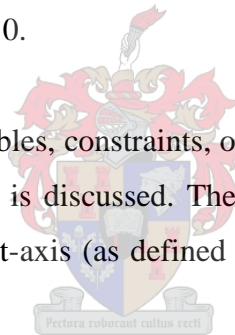
Chapter 6: Results

The optimisation procedure followed is summarised in three consecutive tasks. The first task (discussed in the first section of this chapter) was to investigate the influence of the design variables on the results. This was done by varying the design variables (suspension parameters) over the allowed range and determining the influence they have on the response. The second task (discussed in the second section of this chapter) was to apply the optimisation algorithms discussed in the previous chapter to the objective functions (response surfaces) to obtain the suspension parameters that will provide the lowest vibration exposure on the driver. The third task (discussed in the third section of this chapter) was to verify the optimal solution by exposing the truck to different road inputs under different loading conditions using the optimised suspension characteristics.

The results from each task are divided into three subsections. The first subsection focuses on the truck whilst unloaded. The second subsection focuses on the truck whilst loaded. The third subsection focuses on a combined cycle, i.e. first unloaded, then loaded travelling the same section of road; as normally occurs in practice. The parameters were optimised within the prescribed limits for RMS and VDV values, evaluated according to ISO 2631 (1997), for each of the subsections discussed above.

6.1 Influence of Design Variables

To determine the influence of a design variable on the response, all the variables are kept constant while the variable being investigated is varied over its entire allowed range. The *Effect %* is defined as the ratio of the change in response to the neutral (unchanged truck) response expressed as a percentage (see equation (14)). It will be negative for a variable that causes a decrease in the response with an increase in stiffness.

$$Effect\_\% = \frac{Exposure(stiff) - Exposure(soft)}{Exposure(neutral)} \times 100\% \qquad (\,14\,)$$

A summary of the *Effect %* of the various design variables on the various responses is recorded in Table 5. The Effect % is also included in Figures 19 - 24 for clarity.

Table 5: Effect% of design variables on response

VERTICAL VIBRATION	RMS (m/s^2)			VDV (m/s$^{1.75}$)		
	Unloaded	Loaded	Combined	Unloaded	Loaded	Combined
Parameter						
Strut	25.0	28.2	26.8	25.1	25.6	24.6
Cab Mount	-31.7	-2.49	-12.9	-31.1	-1.72	-19.9
Tires	24.0	9.15	14.2	4.25	5.60	4.83
Sandwich Block	2.40	-0.74	0.35	0.52	-0.72	0
Seat	5.05	-5.14	-1.50	8.26	-4.33	3.47
Torsion Spring	-0.03	-0.3	-0.20	0.09	0.28	0.18

LATERAL VIBRATION	RMS (m/s^2)			VDV (m/s$^{1.75}$)		
	Unloaded	Loaded	Combined	Unloaded	Loaded	Combined
Parameter						
Strut	5.59	23.2	14.6	15.7	24.6	19.6
Cab Mount	-5.05	2.64	-1.07	-4.88	-1.05	-3.16
Tires	9.30	10.7	10.1	14.1	8.04	11.3
Sandwich Block	-3.16	3.77	0.37	1.79	2.60	2.12
Seat	0.56	0.41	0.51	0.60	0.43	0.53
Torsion Spring	0.22	-0.07	0.07	0.21	-0.26	-0.01

LONGITUDINAL VIBRATION	RMS (m/s^2)			VDV (m/s$^{1.75}$)		
	Unloaded	Loaded	Combined	Unloaded	Loaded	Combined
Parameter						
Strut	-3.25	2.21	-2.55	2.48	30.9	3.43
Cab Mount	-139	3.99	-112	-166	-0.77	-162
Tires	22.0	26.4	24.1	12.2	19.1	12.4
Sandwich Block	2.66	3.14	2.74	0.96	0.2	0.92
Seat	1.44	-0.03	1.17	2.52	0.33	2.47
Torsion Spring	1.55	-0.14	1.26	0.01	-0.09	-0.01

6.1.1 Unloaded:

Simulation results of the unloaded truck for different suspension setups as defined by the CCD methodology (discussed in Chapter 2.7) were recorded and a quadratic response surface fitted to the results. The RMS quadratic response surface for the unloaded truck had a coefficient of determination of $R^2 \approx 0.97$, that is, the regression model (response surface) that was fitted to the trial values accounted for 97% of the variability in the simulated data. The VDV response surface for the unloaded truck had a coefficient of determination of $R^2 \approx 0.99$. The sensitivity of the design variables to the response could be

determined from the response surfaces. The response surface also described the variability well enough to be used as the objective function in the optimisation of the RMS and VDV exposure levels (see equation (1)) as the R^2 values for both exceeded 0.9.

In Figure 20 and Figure 21 the influence of the variables on the RMS and VDV in the direction of the main axes is recorded. The light-coloured bars represent a negative *Effect %*, indicating that increasing the stiffness will reduce the exposure level. From Table 5, Figure 20 and Figure 21 it may be seen that for the unloaded truck the cab mounts, struts and tires have the largest influence on the responses. It is seen that improving one response may lead to a deterioration of another (reducing the stiffness of the sandwich blocks leads to a reduction in vertical and longitudinal RMS, but an increase in the lateral RMS) and that each response is not equally influenced (cab mounts influence the vibrations in the longitudinal direction by up to 139%, the vertical by 31% and the lateral by 5% when varied over the same range).

RMS Vertical Vibration	
Factor	**Effect %**
Cab Mount	-31.7
Strut	25
Tires	24
Seat	5.05
Sandwich Block	2.4
Torsion Spring	-0.03

RMS Lateral Vibration	
Factor	**Effect %**
Tires	9.3
Strut	5.59
Cab Mount	-5.05
Sandwich Block	-3.16
Seat	0.56
Torsion Spring	0.22

RMS Longitudinal Vibration	
Factor	**Effect %**
Cab Mount	-139
Tires	22
Strut	-3.25
Sandwich Block	2.66
Torsion Spring	1.55
Seat	1.44
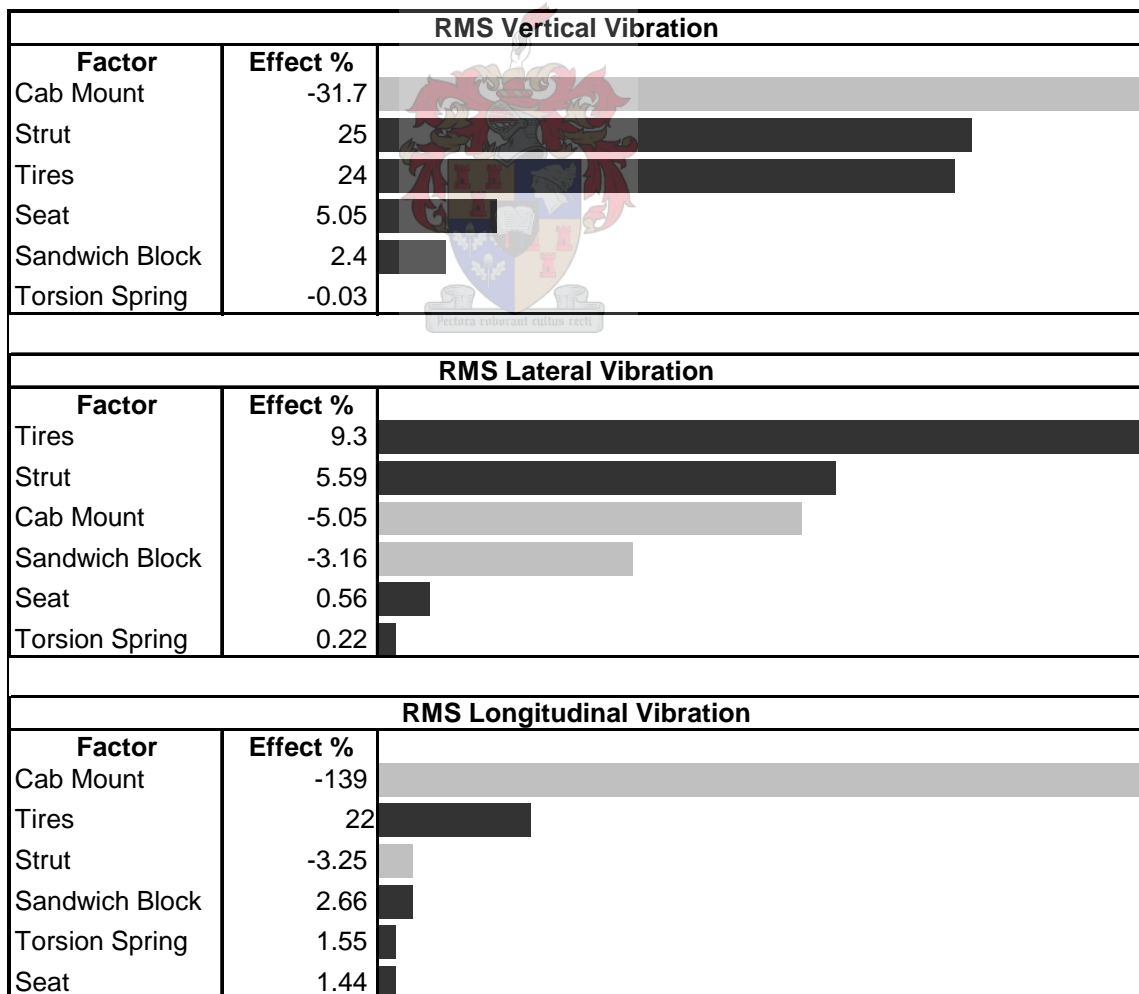
Figure 20: Influence of variables of unloaded truck on RMS

VDV Vertical Vibration	
Factor	**Effect %**
Cab Mount	-31.1
Strut	25.1
Seat	8.26
Tires	4.25
Sandwich Block	0.52
Torsion Spring	0.09

VDV Lateral Vibration	
Factor	**Effect %**
Strut	15.7
Tires	14.1
Cab Mount	-4.88
Sandwich Block	1.79
Seat	0.6
Torsion Spring	0.21

VDV Longitudinal Vibration	
Factor	**Effect %**
Cab Mount	-166
Tires	12.2
Seat	2.52
Strut	2.48
Sandwich Block	0.96
Torsion Spring	0.01

Figure 21: Influence of variables of unloaded truck on VDV

6.1.2 Loaded:

Simulation results of the loaded truck for different suspension setups as defined by the CCD methodology were recorded and a quadratic response surface fitted to the results. The RMS quadratic response surface for the loaded truck had a coefficient of determination of $R^2 \approx 0.93$, that is, the regression model (response surface) accounts for 96% of the variability in the simulated data. The VDV response surface for the loaded truck had a coefficient of determination of $R^2 \approx 0.99$. The sensitivity of the design variables to the response could be determined from the response surfaces. The response surfaces could also be used as the objective function in the optimisation of the RMS and VDV exposure levels (see equation (1)) as the R^2 values for both exceeded 0.9.

In Figure 22 and Figure 23 the influence of the variables on the RMS and VDV in the direction of the main axes is recorded. The light-coloured bars represent a negative *Effect*

%, indicating that increasing the stiffness will reduce the exposure level. From Table 5, Figure 22 and Figure 23 it may be seen that for the loaded truck the struts and tires have the largest influence on the responses. The cab mounts do not influence the responses as much as for the unloaded truck. It is again seen that improving one response may lead to a deterioration of another (reducing the stiffness of the sandwich blocks, cab mounts and seat leads to a reduction in vertical RMS, but an increase in the lateral and longitudinal RMS) and that each response is not equally influenced (struts influence the vibrations in the vertical and longitudinal directions by approximately 25%, but the longitudinal direction by only 2% when varied over the same range.)

Studying Table 5, or Figures 19 to 22, it is interesting to note that all the variables (except the tires) have had a change in sign for the *Effect %* in at least one of their responses. This will cause the optimal solution to change as the loading condition is changed from unloaded to loaded.

RMS Vertical Vibration	
Factor	**Effect %**
Strut	28.2
Tires	9.15
Seat	-5.14
Cab Mount	-2.49
Sandwich Block	-0.74
Torsion Spring	-0.3

RMS Lateral Vibration	
Factor	**Effect %**
Strut	23.2
Tires	10.7
Sandwich Block	3.77
Cab Mount	2.64
Seat	0.41
Torsion Spring	-0.07

RMS Longitudinal Vibration	
Factor	**Effect %**
Tires	26.4
Cab Mount	3.99
Sandwich Block	3.14
Strut	2.21
Torsion Spring	-0.14
Seat	-0.03
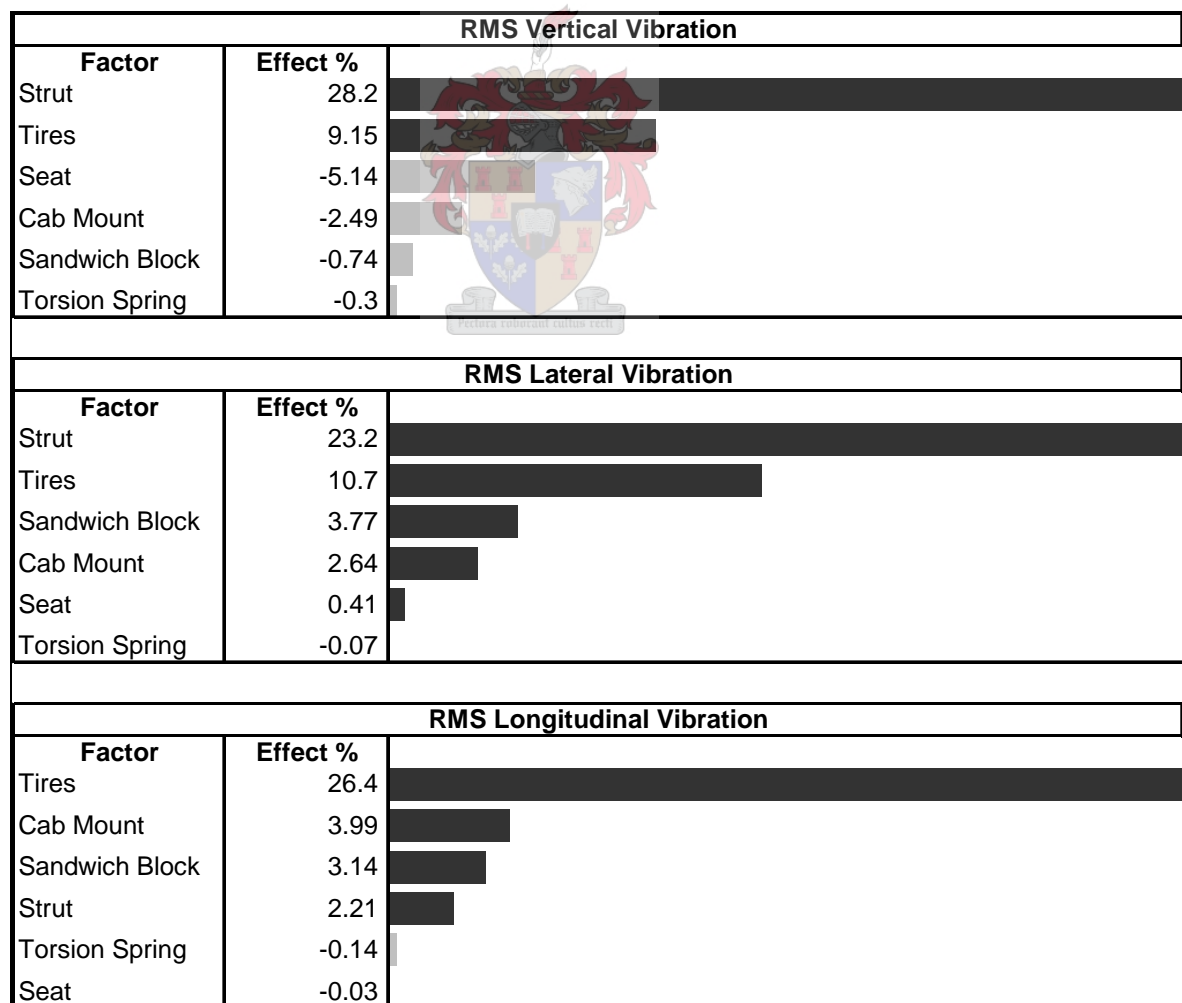
Figure 22: Influence of variables of loaded truck on RMS

VDV Vertical Vibration		
Factor	**Effect %**	
Strut	25.6	
Tires	5.6	
Seat	-4.33	
Cab Mount	-1.72	
Sandwich Block	-0.72	
Torsion Spring	0.28	

VDV Lateral Vibration		
Factor	**Effect %**	
Strut	24.6	
Tires	8.04	
Sandwich Block	2.6	
Cab Mount	-1.05	
Seat	0.43	
Torsion Spring	-0.26	

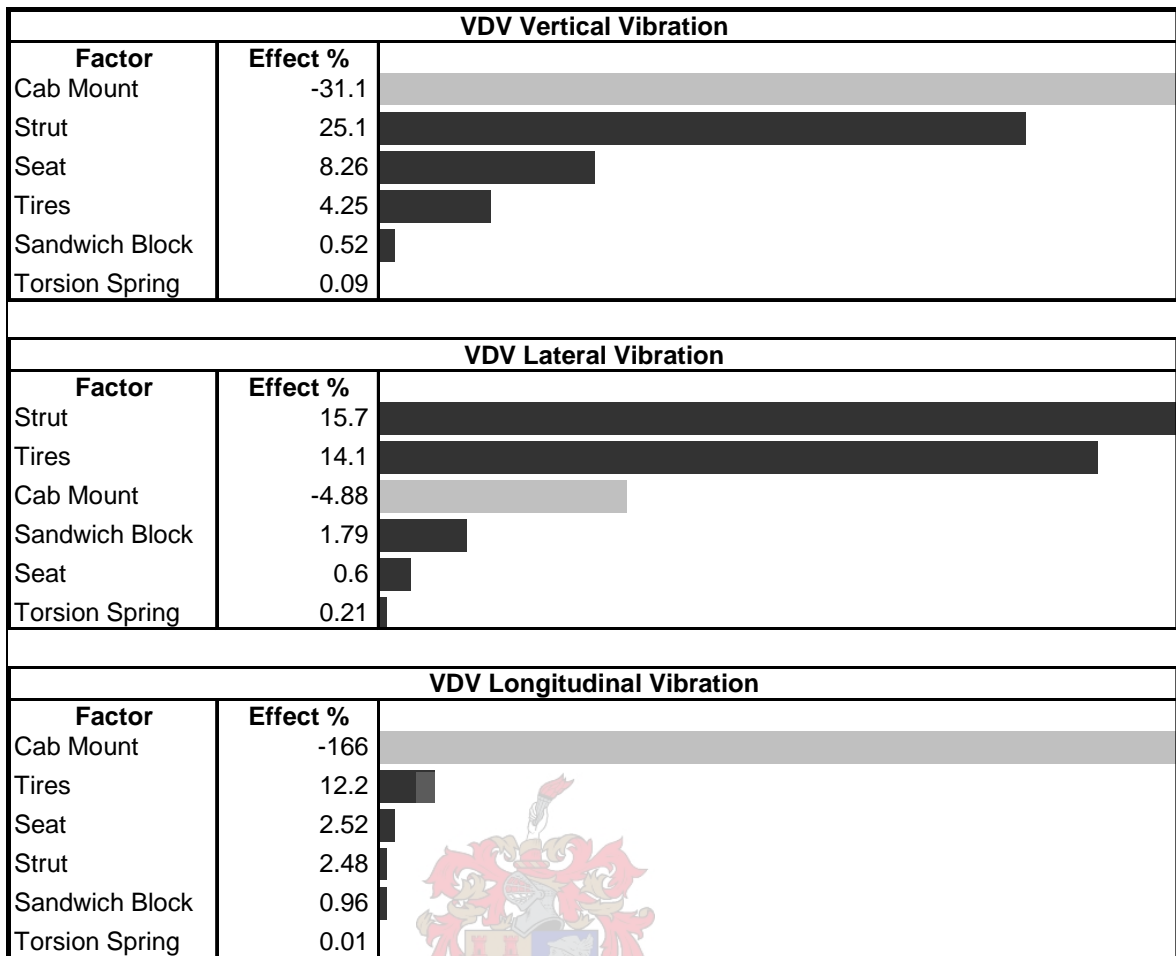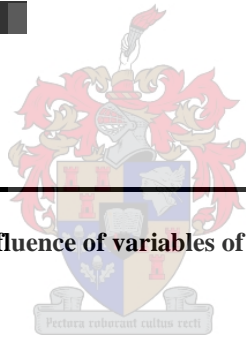| VDV Longitudinal Vibration		
Factor	**Effect %**	
Strut	30.9	
Tires	19.1	
Cab Mount	-0.77	
Seat	0.33	
Sandwich Block	0.2	
Torsion Spring	-0.09	
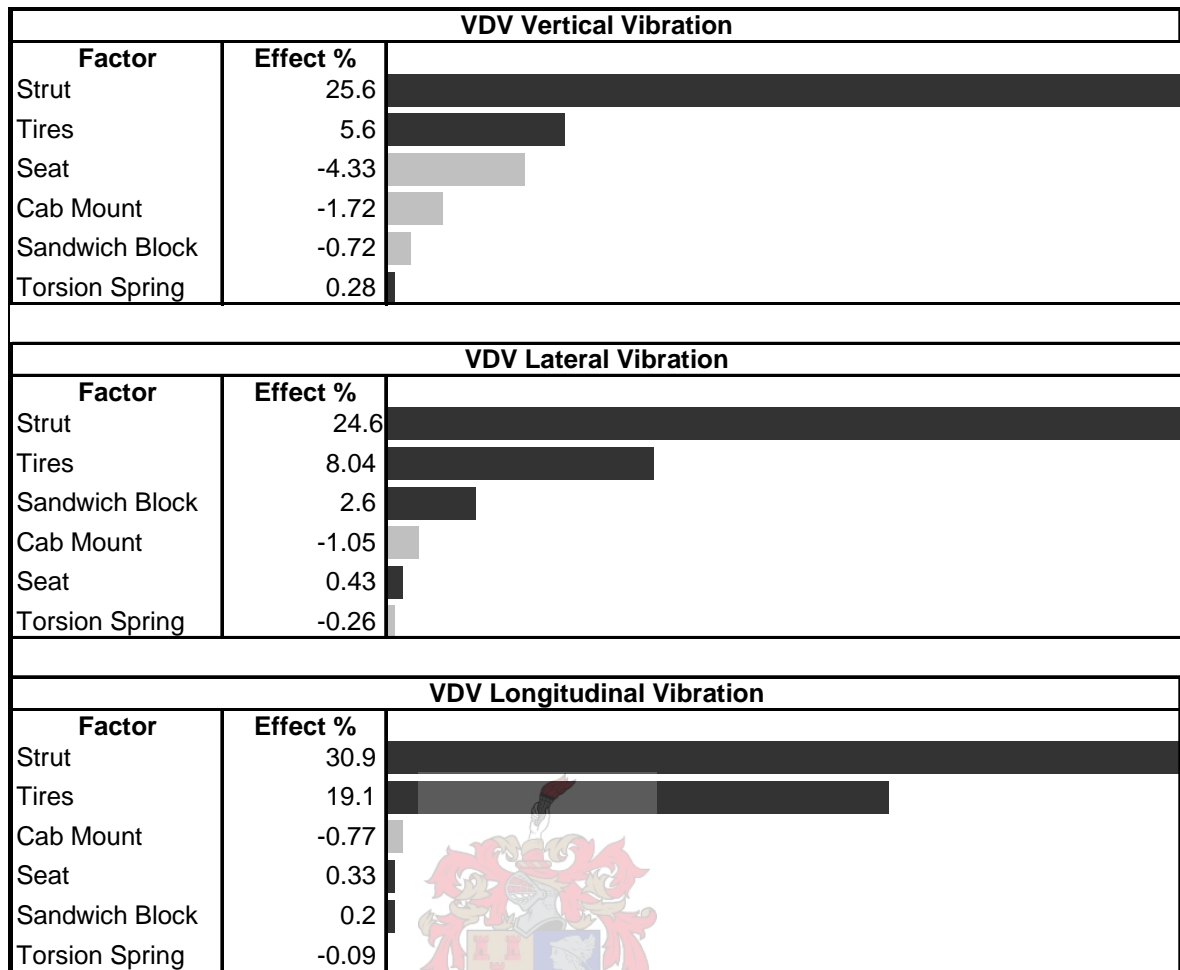
Figure 23: Influence of variables of loaded truck on VDV

6.1.3 Combined:

The simulation results obtained for different suspension setups as defined by the CCD methodology of the loaded and unloaded truck were combined, recorded and a quadratic response surface fitted to the results. The RMS response surface of the combined cycle had a coefficient of determination of $R^2 \approx 0.96$, that is, the regression model (response surface) accounts for 96% of the variability in the simulated data. The VDV response surface for the combined cycle had $R^2 \approx 0.99$. The sensitivity of the design variables to the response could be determined from the response surface. It also meant that the response surface described the variability well enough to be used as the objective function in the optimisation of the RMS and VDV exposure levels (see equation (1)) as the R^2 value for both exceeded 0.9.

In Figure 24 and Figure 25 the influence of the variables on the RMS and VDV in the direction of the main axes is recorded. The light-coloured bars represent a negative *Effect %*, indicating that increasing the stiffness will reduce the exposure level. From Table 5, Figure 24 and Figure 25 it may be seen that for the combined cycle the struts, cab mounts and tires have the largest influence on the responses. The combined cycle's responses are a weighted combination of the results obtained from the loaded and unloaded truck. Optimising the combined results should give improvements for the loaded and unloaded truck, but will not necessarily be the optimal solution for either response.

RMS Vertical Vibration

Factor	Effect %
Strut	26.8
Tires	14.2
Cab Mount	-12.9
Seat	-1.5
Sandwich Block	0.35
Torsion Spring	-0.2

RMS Lateral Vibration

Factor	Effect %
Strut	14.6
Tires	10.1
Cab Mount	-1.17
Seat	0.51
Sandwich Block	0.37
Torsion Spring	0.07

RMS Longitudinal Vibration

Factor	Effect %
Cab Mount	-112
Tires	24.1
Sandwich Block	2.74
Strut	-2.55
Torsion Spring	1.26
Seat	1.17
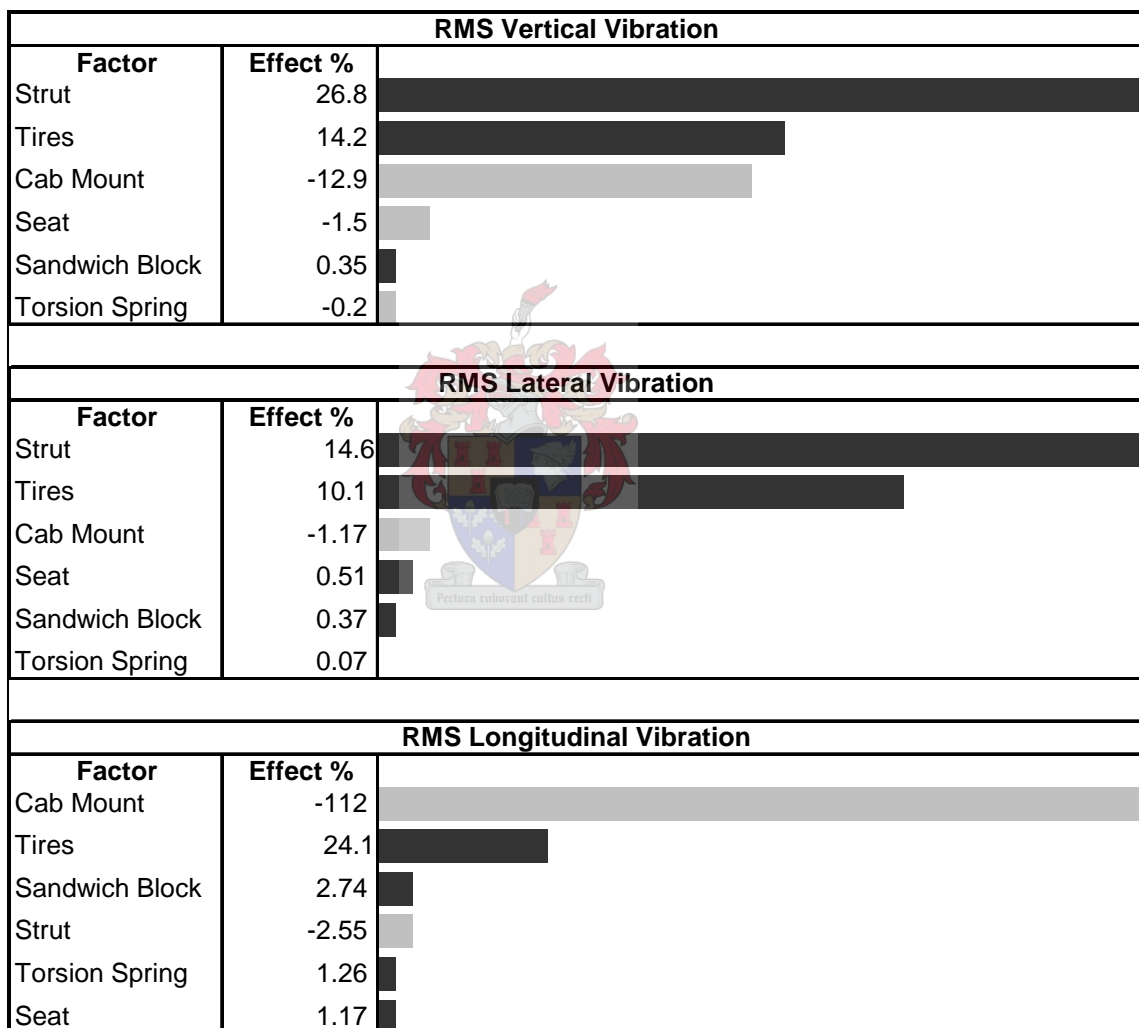
Figure 24: Influence of variables of combined cycle on RMS

VDV Vertical Vibration		
Factor	**Effect %**	
Strut	24.6	
Cab Mount	-19.9	
Tires	4.83	
Seat	3.47	
Torsion Spring	0.18	
Sandwich Block	0	

VDV Lateral Vibration		
Factor	**Effect %**	
Strut	19.9	
Tires	11.3	
Cab Mount	-3.16	
Sandwich Block	2.12	
Seat	0.53	
Torsion Spring	-0.01	

VDV Longitudinal Vibration		
Factor	**Effect %**	
Cab Mount	-162	
Tires	12.4	
Strut	3.43	
Seat	2.47	
Sandwich Block	0.92	
Torsion Spring	-0.01	
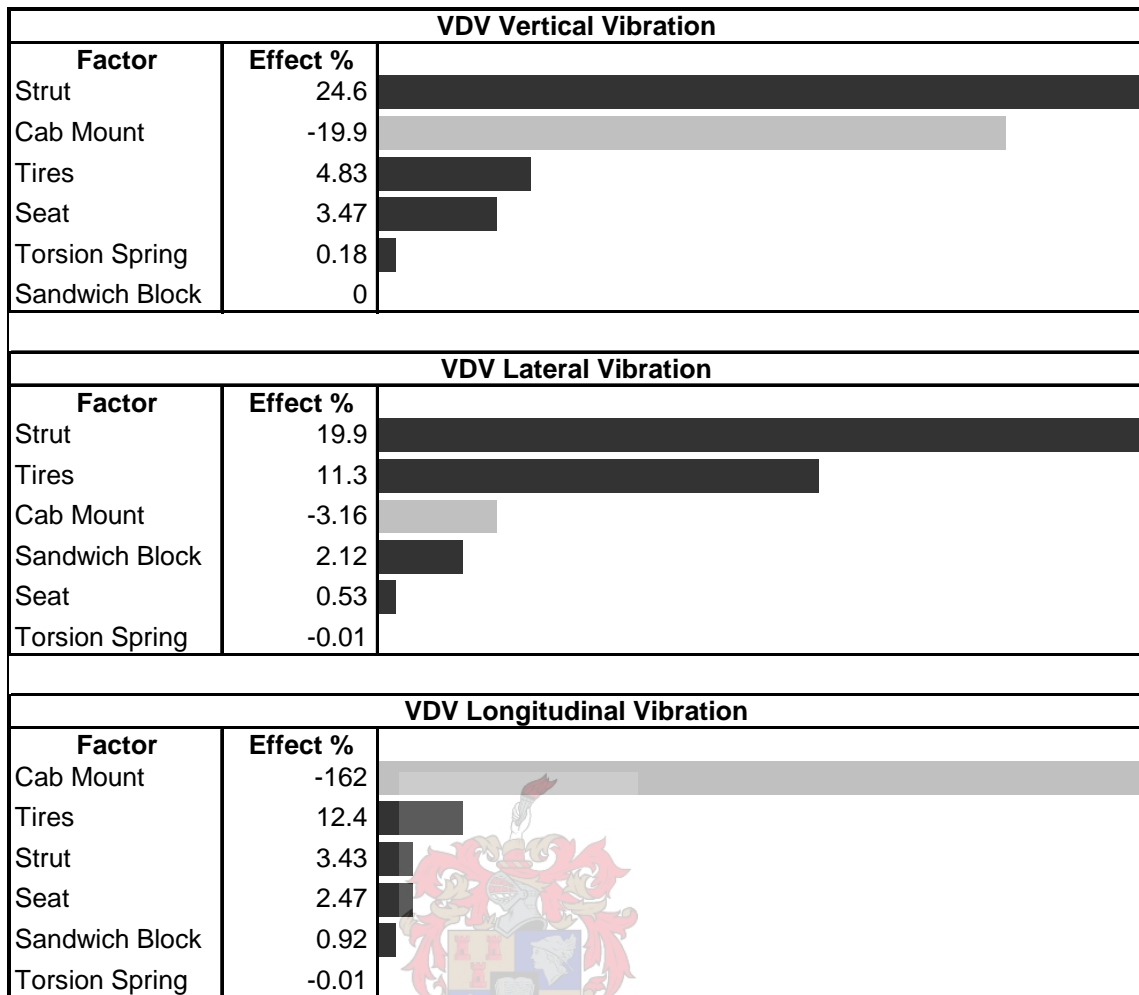
Figure 25: Influence of variables of combined cycle on VDV

6.2 Optimal Parameters

It is important to note that the EU-Directive currently requires **the axis with highest vibration** to not exceed the exposure levels. The suspension is thus optimised for the worst axis only, which may cause the response of another axis to improve or deteriorate. Should the response of another axis deteriorate to such an extent that it becomes the worst axis; the objective function is adapted to continue optimising that axis' response (see Figure 19).

6.2.1 Unloaded:

The objective function for the unloaded truck was optimised by using the different optimisation algorithms explained previously. The solutions (recorded in Table 6 and Table 7) indicate the relative stiffness of the optimal parameter to the current linearized parameter. A value of, for example, 1.2 indicates that the optimal parameter is 20% stiffer

than the current linearized parameter, while a value of 0.8 indicates that the optimal parameter is 20% less stiff than the current linearized parameter.

The worst axis for this test condition was the lateral axis. Improvements for all the axes were, however, achieved. The optimal solutions for the RMS and VDV exposures were confirmed by more than one algorithm. Only the greatest improvement is converted into a percentage. The grey blocks show for which algorithm the greatest improvement was achieved. It was discovered that an *18.5%* reduction in RMS and *31%* reduction in VDV is attainable within the given constraints (albeit not at the exact same suspension setting).

Table 6: Unloaded optimal suspension parameters for RMS exposure

Optimisation Algorithm		MATLAB		ADAMS		
	Nominal	DIRECT	fmincon	SQP	GRG	
Strut	1	0.61	0.6	0.6	0.6	
Cab Mount	1	1.18	1.2	1.2	1.2	
Tires	1	0.8	0.8	0.8	0.8	
Sandwich Block	1	0.99	1	1	1	
Seat	1	0.9	0.6	0.6	0.6	
Torsion Spring	1	1	1.1	1.1	1.1	
		RMS (m/s^2)				% Improvement
Vertical	0.114	0.062	0.060	0.060	0.060	47.2
Lateral	0.226	0.190	0.184	0.184	0.184	18.5
Longitudinal	0.140	0.080	0.083	0.083	0.083	42.9

Table 7: Unloaded optimal suspension parameters for VDV exposure

Optimisation Algorithm		MATLAB		ADAMS		
	Nominal	DIRECT	fmincon	SQP	GRG	
Strut	1	0.61	0.6	0.6	0.6	
Cab Mount	1	1.1	1.1	1.1	1.1	
Tires	1	0.8	0.8	0.8	0.8	
Sandwich Block	1	0.8	0.8	1	1	
Seat	1	0.9	0.8	0.6	0.6	
Torsion Spring	1	1	1.1	1.1	1.1	
		VDV (m/s$^{1.75}$)				% Improvement
Vertical	0.373	0.232	0.229	0.220	0.220	40.8
Lateral	0.685	0.477	0.474	0.473	0.473	31.0
Longitudinal	0.496	0.240	0.245	0.245	0.245	51.7

6.2.2 Loaded:

The objective function for the loaded truck was optimised by using the different optimisation algorithms explained previously. The solutions (recorded in Table 8 and Table 9) indicate the relative stiffness of the optimal parameter to the current linearized parameter. It is again seen that while optimising the worst axis (the lateral axis for this load condition), improvements for all the axes were achieved. All the algorithms produced similar improvements. Only the greatest improvement is converted into a percentage. The grey blocks show for which algorithm the greatest improvement was achieved. It was discovered that a *38.6%* reduction in the RMS and *33.8%* reduction in VDV is attainable within the given constraints (albeit not at the exact same suspension settings, as VDV is lower when cab mounts are hard and seat soft, while RMS is just the opposite).

Table 8: Loaded optimal suspension parameters for RMS exposure

Optimisation Algorithm		MATLAB		ADAMS		
	Nominal	DIRECT	fmincon	SQP	GRG	
Strut	1	0.62	0.61	0.61	0.61	
Cab Mount	1	0.82	0.8	0.8	0.8	
Tires	1	0.8	0.8	0.8	0.8	
Sandwich Block	1	0.8	0.8	0.8	0.8	
Seat	1	0.9	0.98	1	1	
Torsion Spring	1	1	1.1	1.1	1.1	
		RMS (m/s^2)				% Improvement
Vertical	0.147	0.101	0.100	0.100	0.099	32.4
Lateral	0.312	0.194	0.191	0.191	0.191	38.6
Longitudinal	0.079	0.052	0.052	0.051	0.051	34.9

Table 9: Loaded optimal suspension parameters for VDV exposure

Optimisation Algorithm		MATLAB		ADAMS		
	Nominal	DIRECT	fmincon	SQP	GRG	
Strut	1	0.68	0.67	0.67	0.67	
Cab Mount	1	1.19	1.2	1.2	1.2	
Tires	1	0.83	0.85	0.85	0.85	
Sandwich Block	1	0.8	0.8	0.8	0.8	
Seat	1	0.9	0.6	0.6	0.6	
Torsion Spring	1	1	1.1	1.1	1.1	
		VDV ($m/s^{1.75}$)				% Improvement
Vertical	0.337	0.255	0.262	0.262	0.262	24.5
Lateral	0.736	0.490	0.487	0.487	0.487	33.8
Longitudinal	0.209	0.137	0.139	0.139	0.139	34.4

6.2.3 Combined:

The objective function for the combined loaded/unloaded cycle was optimised by using the different optimisation algorithms explained previously. The solutions (recorded in Table 10 and Table 11) indicate the relative stiffness of the optimal parameter to the current linearized parameter. Improvements for all the axes were achieved although the algorithms were only optimising the worst axis (mostly the lateral axis). All the algorithms produced similar improvements. Only the greatest improvement is converted into a percentage. The grey blocks show for which algorithm the greatest improvement was achieved. It was discovered that a *29.8%* reduction in the RMS and *27.4%* reduction in VDV is attainable within the given constraints for the worst axis (albeit not at the exact same suspension settings).

Table 10: Combined optimal suspension parameters for RMS exposure

Optimisation Algorithm	Nominal	MATLAB		ADAMS		
		DIRECT	fmincon	SQP	GRG	
Strut	1	0.6	0.6	0.6	0.6	
Cab Mount	1	1.18	1.2	1.2	1.2	
Tires	1	0.8	0.8	0.8	0.8	
Sandwich Block	1	0.99	0.8	1	1	
Seat	1	0.9	0.85	1.04	1.05	
Torsion Spring	1	1	1.1	1.1	1.1	
		RMS (m/s^2)				% Improvement
Vertical	0.137	0.082	0.079	0.080	0.080	42.3
Lateral	0.279	0.198	0.197	0.196	0.196	29.8
Longitudinal	0.117	0.069	0.077	0.069	0.069	41.3

Table 11: Combined optimal suspension parameters for VDV exposure

Optimisation Algorithm	Nominal	MATLAB		ADAMS		
		DIRECT	fmincon	SQP	GRG	
Strut	1	0.62	0.62	0.61	0.6	
Cab Mount	1	1.13	1.13	1.1	1.12	
Tires	1	0.81	0.82	0.8	0.81	
Sandwich Block	1	0.8	0.8	1	0.87	
Seat	1	0.9	0.6	0.6	0.6	
Torsion Spring	1	1	1.1	1.1	1.1	
		VDV (m/s$^{1.75}$)				% Improvement
Vertical	0.422	0.279	0.279	0.273	0.277	35.3
Lateral	0.800	0.584	0.582	0.581	0.583	27.4
Longitudinal	0.446	0.242	0.241	0.246	0.243	46.1

Each loading condition and each road input would have a different optimal solution as is seen from the optimal parameters obtained in the previous section. It does, however, appear as though the following adjustments (from Table 10) would give the largest improvement in RMS and VDV for all conditions:

- Front struts (spring and damper) should be softened by 40%
- Cab mounts should be stiffened by 20%
- Tires should be softened by 20%
- Sandwich blocks should remain as simulated
- Seat should remain as simulated
- Torsion springs should be stiffened by 10%

The adjustments to the front struts, cab mounts and tires are limited by the side constraints discussed in Chapter 5. This corresponds well with results published by Jiang (2001) who reported in his literature study that when optimizations were unconstrained, negative damping appears, showing that energy (active suspensions) are required for an optimal solution.
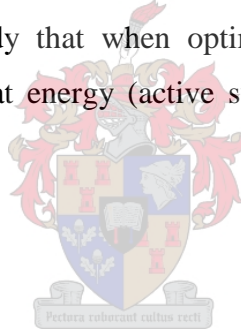
6.3 Verification

To verify the "optimal solution" the VDV and RMS exposures of the "optimal" truck were compared to the exposures of the original truck under different loading conditions and road surface inputs as described by Cebon (1999), ISO 8608 (1995) and Wong (1978). The trucks were simulated as travelling at a speed of 10m/s. The simulation results are recorded in Table 12 as a percentage improvement in exposure level. The "optimal" road represents the road surface that was used for the optimisation study. Positive entries indicate a reduction in exposure while negative entries indicate an increase in exposure level for the "optimal" setting. The bold entries indicate the worst-axis for the respective load condition and road surface of the original truck. The grey blocks indicate the worst-axis for the respective load condition and road surface of the optimised truck. The "worst axis" columns indicate the direct percentage improvement between initial and final worst axes.

From Table 12 it is seen that the optimised suspension does lead to higher vibration exposures in certain cases (indicated by negative entries). It was, however, found that all

the axes (and in particular the worst axes) were improved for all the road types when the vibration exposure levels of the loaded and unloaded conditions were considered together (combined model). For example; the optimised suspension increased lateral vibrations on the seat (Seat Top X) by 85.3% (RMS) when the truck was driven over a very poor road surface in the loaded condition, but reduced Seat Top X vibration exposure level by 90.7% (RMS) in the unloaded condition for the same road surface. The overall combined effect of the optimised suspension for the loaded and unloaded truck driving over the very poor road surface was to reduce the Seat Top X vibration exposure by 83.9% (RMS).

Generally, as the road surface deteriorates, the percentage improvements achieved by the "optimal" suspension also diminish (although the absolute improvement may increase or stay the same). It may also be noticed that the worst axis changes depending on load condition, road input and method of evaluation. The worst axis may also be different after the optimal parameters are applied to the original truck. The combined cycle of the original truck on a good road, for example, had the lateral direction as the worst axis. A larger improvement in the lateral direction than the vertical direction during the optimisation has lead to the vertical direction becoming the new worst axis for VDV measurements and the longitudinal direction becoming the new worst axis for RMS measurements.

Table 12: % Improvement with optimal parameters on different road surfaces

Model	Road	RMS				VDV			
		Seat Top Z	Seat Top Y	Seat Top X	Worst axis	Seat Top Z	Seat Top Y	Seat Top X	Worst axis
Unloaded	**Good**	39.0	-110.9	**86.2**	79.5	46.1	70.9	**76.8**	66.7
	Poor	56.6	64.5	**92.0**	88.2	49.5	67.4	**79.9**	71.1
	Very Poor	56.1	79.9	**90.7**	86.3	35.3	79.4	**70.8**	58.1
	Optimal	45.9	**16.4**	49.0	16.4	35.4	**31.0**	50.6	31.0
	Plowed Field	35.1	25.7	**83.6**	75.8	7.6	32.7	**41.2**	16.0
Loaded	**Good**	93.6	**99.9**	62.9	97.6	78.5	**99.7**	73.3	94.4
	Poor	**91.9**	80.4	86.2	89.6	**89.5**	89.9	79.1	89.5
	Very Poor	**-35.4**	16.5	-85.3	-82.4	**-19.1**	36.0	-26.9	-19.1
	Optimal	31.8	**33.9**	31.9	33.9	31.1	**29.3**	40.5	29.3
	Plowed Field	**-26.3**	57.7	-68.8	-62.2	**-14.3**	46.3	-20.3	-14.3
Combined	**Good**	89.1	**99.7**	77.7	97.2	68.0	**99.4**	76.2	91.4
	Poor	86.9	68.3	**89.3**	88.6	83.6	67.8	79.8	83.6
	Very Poor	47.5	72.9	**83.9**	83.2	34.7	79.3	**70.5**	57.8
	Optimal	36.7	**26.9**	44.7	26.9	33.6	**30.0**	50.2	30.0
	Plowed Field	31.0	41.0	**78.9**	73.7	7.5	32.8	**41.2**	16.0

Bold numbers indicate original suspension's worst-axis; Grey blocks indicate optimised suspension's worst-axis

To verify whether a softer seat suspension would not give better solutions, the experiments were repeated with the seat softened by 40% (as suggested by Table 11). It was discovered that for good road surfaces, i.e. where the end-stops are not engaged, the softer seat gave even lower exposure levels (in RMS and VDV), but when the road surface became rougher, the advantage shrank and, for the worst road surface (ploughed field), the exposure levels in all axis were reduced by a smaller amount than they could have been had the seat stiffness not been changed. The difference of improvement in worst axis exposure level between a softened seat and the current seat, with the other suspension systems set to optimal, was usually less than 2% for all loading conditions and road surfaces. It was thus decided to keep the seat as it is.
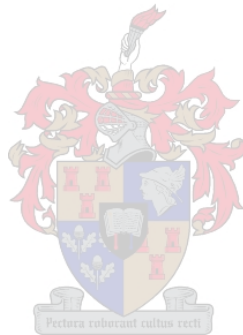
Chapter 7: Conclusions and Recommendations

The introduction of the EU-Directive that limits vibration exposure means that suspension systems on ADTs need to be optimised for improved vibration comfort. In order to optimise the suspension systems for comfort a reliable model of the truck is needed. A literature study of modelling techniques was completed to determine which assumptions may be made to simplify the model of such a truck. It was established that a variety of models have been tried over the years and that some simplified models did in fact give reliable results.

The three major components of a simulation model is the road input, the truck and the human driver. The road may be reconstructed from PSD measurements of similar road surfaces and introduced to the model through vertical actuators. The truck was simplified by ignoring the steering and drive-train and constraining some degrees of freedom. The human and seat was modelled with a lumped parameter model obtained from literature.

The suspension parameters were linearized over the entire range of motion and the linearization was validated by three MATLAB models of increasing complexity and degrees of freedom. The results from the MATLAB models were compared to those of a truck driving over irregular terrain and it was shown that after the linearization of the parameters the model still generates realistic results.

To model the truck even more accurately a 24 degrees of freedom model was developed in ADAMS/VIEW. The ADAMS/VIEW model was verified by comparing the results to a previously (and independently) developed 50 degree-of-freedom ADAMS/CAR model as well as measured results from a truck traversing a sinusoidal obstacle. The ADAMS/VIEW model correlated very well with the measured results when large displacements were present. The model's accuracy was slightly lower when the displacements were small. This is mainly due to the linearization which is better suited for large displacements.

The influence of each suspension system parameter was investigated to determine the relative importance of each parameter on the vibration exposure. The parameters that needed to be optimised were identified together with four different optimisation

algorithms. A surface response function of each exposure was constructed and used as the objective function in each of the optimisation algorithms.

An optimisation study was performed and the optimal suspension parameters identified. The parameters were then verified by comparing exposure levels from the original truck with the optimised truck as it traverses different road surfaces. It was discovered that the optimised parameters gave improvements for all road surfaces for the combined (loaded/unloaded) cycle.

The main conclusions that may be derived from this research are:

- **A simplified, reduced order simulation model of an ADT can be used for optimisation studies to reduce vibration exposure levels of the driver.**

One of the objectives of the project was to determine whether a simplified reduced order model could be used to optimise the suspension parameters. By making the correct assumptions the complexity of a model can be reduced significantly while still producing reliable results. The 24-DOF model that was developed in ADAMS/VIEW accurately simulates the vibration exposure levels on the driver. The model can be used to investigate the influence of the suspension parameters on the exposure levels and can be simulated with different load conditions and road surface inputs. It was shown that the model is more accurate at predicting the vibration exposure than the 50-DOF model developed in ADAMS/CAR for a particular input. The model is, however, not suited for handling studies as it does not include a drive train or steering mechanism, neither is it suitable for component fatigue studies.

- **The horizontal directions may have higher vibration levels than the vertical direction for specific load conditions and road inputs.**

Most suspension components are designed to only isolate the driver from vertical vibration. From Table 12 it is seen that more than 80% of the conditions originally investigated had one of the horizontal axes as the worst axis. Measurements taken on a truck at a construction site (reported in Appendix A) also indicated that the horizontal axis often contribute larger exposure levels than the vertical direction even after applying the appropriate weighting factors.

- **It is possible to reduce the vibration exposure levels of the driver by changing the parameters of the passive suspension systems.**

Donati (2001) concluded in his article that there are three main ways of reducing vibration exposure, namely to reduce the source (road improvement, driving style, etc.), to reduce the transmission by incorporating better suspension systems and by improving the ergonomics of the cab. It was shown in the previous chapter that the exposure levels of the driver may be reduced by as much as 99.9% (Loaded truck on good road in Table 12) by only changing the passive suspension systems' parameters. It was also shown that finding the optimal solution for the combined cycle gave improvements for the loaded and unloaded truck, but was not necessarily the optimal solution for either response. The improvements in vibration exposure levels were achieved without changing the operation, layout or physical dimensions of the current suspension systems.

- **The largest improvement was obtained by adjusting the stiffness of the front struts, tires and cab mounts.**

Of all the suspension system components, the front struts, tires and cab mounts proved to have the largest influence on the exposure levels of the driver. Investigating Table 5 and Figures 19 to 24 it is seen that the cab mounts have the largest influence on the longitudinal direction (causing the VDV exposure of the unloaded truck to change by as much as 165.5% if the parameter is varied from 20% stiffer to 20% softer), but also had significant influence on the vibration exposures in the other directions. The front struts had the largest influence on the vertical and longitudinal directions (changes of up to 31% being recorded for the VDV exposure of the longitudinal direction in the loaded truck as the parameter is varied). The tires make significant contributions to reducing the exposure levels in all the directions (26.4% change in longitudinal RMS of loaded truck recorded as parameter is varied) and is the only parameter that always caused a reduction in exposure (for all directions, loading conditions and evaluation measures) with a reduction in stiffness. About 95% of the improvements obtained by the optimisation study are as a result of these three parameters.

- **The sandwich blocks, walking beam torsion spring and seat had a small influence on the vibration exposure of the driver.**

On their own the sandwich blocks, walking beam torsion springs and seat influenced the exposure levels of the driver by very small amounts (usually by less than a percent) as they were varied within the constraint boundaries of the optimisation study. The seat gave a maximum improvement of 8% in the vertical direction of the unloaded truck, but only decreased the exposure by 2.5% for the combined cycle. Only about 5% of the improvements obtained by the optimisation study are attributed to these parameters.

Recommendations for future work:

- **The influence of the optimised parameters on the vehicle dynamics should be investigated.**

The model that was used for the optimisation study was not suited for handling studies and thus the influence of the parameters on the handling of the vehicle was not properly investigated. The softening of the front struts, tires and cab mounts will compromise the handling of the vehicle. A study of the influence of the optimal parameters on the dynamics of the vehicle is required to determine whether the roll stiffness of the steering axle (which according to Fu *et al*. (2002) and Cebon (1999) is usually much higher than required) is still within acceptable limits. The influence of softer tires on tire wear should also be investigated.
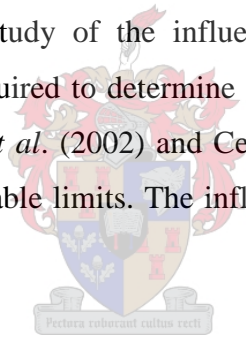
- **Suspension systems with isolating capacity in directions other than the vertical direction should be investigated.**

Sankar and Afonso (1993) (quoted in Prasad, 1995) studied the concept of a lateral seat suspension as a means of improving the ride comfort in off-road vehicles. A computer parametric study showed that a lateral seat suspension with a dynamic vibration absorber could improve the ride comfort by 75% while reducing relative displacements by as much as 7%. Reducing the vibration exposure of lateral and longitudinal vibrations is as important as reducing the vibration exposure in the vertical direction and should therefore be investigated.

- **The viability of semi-active or active suspensions should be investigated.**

Passive suspensions are limited in that they can only truly be optimised for one specific load condition and road input. Due to the fact that the suspension characteristics in semi-

active or active suspensions can be changed according to the terrain requirements, these types of suspension systems can improve ride quality over a wide spectrum of terrain. Jiang (2001) reported in his literature study that when optimizations were unconstrained, negative damping appears, showing that energy (active suspensions) are required for an optimal solution.

- **A study of the viability of other types of suspensions for ADTs (such as air suspensions) should be commissioned.**

It was shown in the literature study that the current suspension setup produces the highest dynamic forces of all the suspension types commonly used in heavy vehicles. The high dynamic forces not only lead to higher exposure levels, but also cause the roads to be damaged faster and may even increase the rate of tire wear. Air suspensions are reported to produce the smallest dynamic forces (Cebon and Cole, 1992). Through his research Hostens (2004) has showed that air-spring seat suspensions are better than mechanical-spring seats. The main reasons for this is that air dampers provide high damping at low frequencies (by throttling in the orifice), but low damping at high frequencies (due to choking in the orifice).

The exposure levels that the driver is exposed to are strongly dependent on the driving style (speed and line). An improvement in the suspension may only lead to more aggressive driving (not reducing speed when road becomes rough) and thus similar exposure levels. Maintaining the road surfaces (by regular scraping, for example), to reduce the inputs from the road, is a vital part in reducing the exposure levels of the driver.

It is the hope of the author that the research presented in this document may prove to be useful to the manufacturers and industry at large to reduce the vibration exposure levels of the drivers of ADTs.

References

ADAMS/Insight Version 2005, Help Files, MSC.Software Corporation, Santa Ana, CA, USA.

Ahmed, O.B. and Goupillon J.F., 1997, Predicting the ride vibration of an agricultural tractor, Journal of Terramechanics, Vol. 34, No 1, pp 1-11.

Brereton, P. and Nelson C., 2004, Progress with implementing the EU Physical Agents (Vibration) Directive in the United Kingdom, 39th United Kingdom Group Meeting on Human Response to Vibration, 15-17 September 2004, pp 293-300, Ludlow, England.

Cebon, D., 1999, Handbook of Vehicle-Road Interaction, Advances in Engineering 2, Swets & Zeitlinger, Lisse, the Netherlands.

Close, M.C., Frederick D.K., Newell J.C., 2002, Modeling and Analysis of Dynamic Systems, Third Edition, John Wiley \& Sons Inc, New York.

Cole, D.J. and Cebon, D., 1994, Predicting Vertical Dynamic Tire Forces of Heavy Trucks, Vehicle-Road Interaction, ASTM, STP 1225, B. T. Kulakowski, Ed., American Society for Testing and Materials, Philadelphia, pp 27-35.

Cole, D.J. and Cebon, D., 1992, Validation of an articulated vehicle simulation, Vehicle System Dynamics, Vol. 21, No 4, pp 197–223.

Darlington, P. and Tyler, R.G., 2004, Measurement uncertainty in human exposure to vibration, 39th United Kingdom Group Meeting on Human Responses to Vibration, 15-17 September 2004, pp 301-308, Ludlow, England.

Deprez, K., Hostens, I., Ramon, H., 2004, Modelling and design of a pneumatic suspension for seats and cabins of mobile agricultural machines, Proceedings of ISMA, 22 September 2004, pp 1185 – 1194.

El Madany, M.M., 1988, Active damping and load leveling for ride improvement, Computers & Structures Vol. 29, No. 1, pp. 89-97.

El Madany, M.M., 1987, An analytical investigation of isolation systems for cab ride, Computers & Structures Vol. 27, No. 5, pp. 679-688.

Esat, I., 1996, Optimisation of a double wishbone suspension system, Engineering Systems Design and Analysis, PD-Vol 81, Vol. 9, ASME, pp. 93-98.

EU-Directive, 2002, Directive 2002/44/EC of the European Parliament and of the council of 25 June 2002, Official Journal of the European Communities.

Fairley, T.E. and Griffin M.J., 1988, Prediction of the discomfort caused by simultaneous vertical and fore-and-aft whole-body vibration, Journal of Sound and Vibration, Vol. 124, No 1, pp 141-156.

Finkel, D.E., 2003, DIRECT Optimization Algorithm User Guide. Technical Report, CRSC, N.C. State University.

Donati, P., 2001, Survey of technical preventative measures to reduce whole-body vibration effects when designing mobile machinery, Journal of Sound and Vibration, (2002) Vol. 253, No 1, pp 169-183.

Fothergill, L.C. and Griffin, M.J., 1977, The use of an intensity matching technique to evaluate human response to whole-body vibration, Ergonomics, Vol. 20, No 3, pp 249-261, 263-276, 521-533.

Fu, T.T. and Cebon, D., 2002, Analysis of a truck suspension database, International Journal of Heavy Vehicle Systems, Vol. 9, No. 4, pp 281-297.

Gallais, C., 2004, Duration of whole-body vibration exposure: Evaluating and comparing the changes in comfort between two lateral oscillations at 1Hz and 4Hz, 39th United Kingdom Group Meeting on Human Responses to Vibration, 15-17 September 2004, pp 381-394, Ludlow, England.

Gill, P.E., Murray, W. and Wright, M.H., 1981, Practical Optimization, Academic Press, London.

Gillespie, T.D., 1992, Fundamentals of Vehicle Dynamics, Society of Automotive Engineers, Warrendale.

Gillespie, T.D. and Karamihas, S.M., 2000, Simplified models for truck dynamic response to road inputs, Heavy Vehicle Systems, International Journal of Vehicle Design, Vol. 7, No 1, pp 231-247.

Gipser, M., 1999, FTire, a new fast tire model for ride comfort simulations, International ADAMS' Users Conference, Berlin, Germany.

Gouw, G.J., Rakheja, S., Sankar, S., Afework, Y., 1990, Increased comfort and safety of drivers of off-highway vehicles using optimal seat suspension, SAE Trans 99, Sec 2, pg 541-548.

Griffin, M.J., 1990, Handbook of Human Vibration, Academic Press Harcourt Brace \& Company, London.

Grovè, T., 2003, Flexible & suspension component characterisation test requirements, TID NLC01.

Han, S.P., 1977, "A Globally Convergent Method for Nonlinear Programming," Vol. 22, Journal of Optimization Theory and Applications, pp. 297.

Heyns, P.S., Naudè. A.F., Bester, C.R., et al, 1992, Ondersoek na aspekte van die ontwerp van 'n houersmobiliseringseenheid ("Investigation on aspects of the design of a container carrier"), Report number LG192/023, Laboratory for advanced engineering, South Africa, pp. 1-64.

Hostens, I., 2004, Analysis of Seating during Low Frequency Vibration Exposure, PhD Thesis, Katholieke Universiteit Leuven.

Health and Safety Executive (HSE), *Whole Body Vibration Exposure Calculator*, Nov 2003, (http://www.hse.gov.uk/vibration/wbv.xls).

Huang, Y., 2004, Review of the nonlinear biodynamic responses of the seated human body during vertical whole-body vibration: The significant variable factors, 39th United Kingdom Group Meeting on Human Responses to Vibration, 15-17 September 2004, pp 161-172, Ludlow, England.

Inman, D.J., 2000, Engineering Vibration, Second Edition, Prentice Hall, Upper Saddle River, New Jersey.

Ibrahim, I.M., Crolla, D.A. and Barton, D.C., 1996, Effect of Frame Flexibility on the ride vibration of trucks, Computers \& Structures Vol. 58, No. 4, pp. 709-713.

International Organization for Standardization, 1981, Vibration and shock – Mechanical driving point impedance of the human body, ISO 5982.

International Organization for Standardization, 1987, Mechanical vibration and shock – Mechanical transmissibility of the human body in the z-direction, ISO 7962.

International Organization for Standardization, 1995, Mechanical vibration - Road surface profiles - Reporting of measured data, ISO 8608.

International Organization for Standardization, 1997, Mechanical vibration and shock - Evaluation of human Exposure to whole-boby vibration Part 1: General Requirements, ISO 2631-1.

Ji, T. and Wang, D., 2004, The natural frequency of a seated person in structural vibration, 39th United Kingdom Group Meeting on Human Responses to Vibration, 15-17 September 2004, pp 223-234, Ludlow, England.

Jiang, Z., Streit, D.A. and El-Gindy, M., 2001, Heavy vehicle ride comfort: Literature survey, Heavy vehicle Systems, International Journal of Vehicle Design, Vol. 8, No 3-4, pp 258-284.

Kising, A., and Gohlich, H., 1988, Dynamic characteristics of large tires, Agricultural Engineering Conference, Paris, 2-5 March 1988, Paper no. 88-357.

Kulakowski, B. T., 1994, Vehicle-Road Interaction, STP 1225, ASTM, Philadelphia.

Lee, H., Lee, G., Kim, T., 1997, A study of ride analysis of medium trucks with varying the characteristics of suspension design parameters, SAE Technical Paper 973230, SP 1308, Society of Automotive Engineers, Warrendale, U.S.A., pp 75-80.

Lee, T.H., Lee, K., 2000, Fuzzy multi-objective optimization of a train suspension using response surface model, 8th AIAA/USAF/NASA/ISSMC Symposium on Multidisciplinary Analysis and Design, 6-8 September 2000, Long Beach, California, pp 1-7.

Lines, J.A. and Murphy, K., 1991, The stiffness of agricultural tires, Journal of Terramechanics, Vol. 28, No 1, pp 49-64.

Mansfield, N.J., 2005, Human Response to Vibration, CRC Press, New York.

Mansfield, N.J., Holmlund, P., and Lundström, R., 2000, Comparison of subjective responses to vibration and shock with standard analysismethods and absorbed power, Journal of Sound and Vibration, Vol. 230, No 3, pp 477-491.

Margolis, D., 2001, Optimal Suspension Parameter Distributions and Roadway Profiles for Isolation of Heavy Trucks, Vehicle System Dynamics, Vol. 35, No. 1, pp. 1-18.

Motoyama, K., Yamanaka, T., Hoshino, H., 2000, A study of automobile suspension design using optimization technique, 8th AIAA/USAF/NASA/ISSMC Symposium on Multidisciplinary Analysis and Design, 6-8 September 2000, Long Beach, California, pp. 1-6.

MATLAB Optimization Toolbox Version 3.0.1, 2004, User's Guide, The MathWorks Inc, Natic, Massachusetts.

MSC.Software Enterprises, 2002, MSC.ADAMS Product Catalog, MSC. Software Corporation, 2 MacArthur Place, Santa Ana, California, www.mscsoftware.com.

Naude, A.F., 2001, Computer-Aided Simulation and Optimisation of Road Vehicle Suspension Systems, PhD Thesis, University of Pretoria.

Nawayseh, N., 2004, Forces on seat and backrest during the fore-and-aft whole-body vibration: Effect of foot support and vibration magnitude, 39th United Kingdom Group Meeting on Human Responses to Vibration, 15-17 September 2004, pp 197-210, Ludlow, England.

Newell, G.S. and Mansfield, N.J., 2004, Exploratory study of whole-body vibration 'artefacts' experienced in a Wheel Loader, Mini-Excavator, car and office worker's chair, 39th United Kingdom Group Meeting on Human Responses to Vibration, 15-17 September 2004, pp 337-346, Ludlow, England.

Powell, M.J.D., 1978, A Fast Algorithm for Nonlinearly Constrained Optimization Calculations, Numerical Analysis, ed. G.A. Watson, Lecture Notes in Mathematics 630.

Prasad, N., Tewari, V.K. and Yadav, R., 1995, Tractor ride vibration - a review, Journal of Terramechanics, Vol. 32. No. 4, pp. 205-219.

Rao, S.S., 1996, Engineering optimization, John Wiley \& Sons Inc, New York.

Rimell, A.N. and Mansfield, N.J., 2004, The influence of loading cycle on measured vibration levels in off-highway dump trucks, 39th United Kingdom Group Meeting on Human Responses to Vibration, 15-17 September 2004, pp 359-368, Ludlow, England.

Sankar, S. and Afonso, M., 1993, Design and Testing of lateral seat suspension for off-road vehicles, Journal of Terramechanics, Vol. 30, No 5, pp 371-393.

Siah, E.S., Papalambros, P. and Volakis, J.L., 2002, Parameter Optimization Using the Divided Rectangles Global Algorithm with Kriging Interpolation Surrogate Modeling, The University of Michigan, Ann Arbor, Michigan 48109-2122.

Toward, M.G.R., 2004, Apparent mass of the human body in the vertical direction: Effect of holding a steering wheel, 39th United Kingdom Group Meeting on Human Responses to Vibration, 15-17 September 2004, pp 211-222, Ludlow, England.

Vanderplaats, G.N., 2001, Numerical optimization techniques for engineering design, 3rd edition, Vanderplaats Research & Development, Inc. Colorado Springs.

van Niekerk, J.L., Heyns, P.S., Heyns, M., Hassall, J.R., 1998, The measurement of vibration characteristics of mining equipment and impact percussive machines and tools, Laboratory for Advanced Engineering, University of Pretoria, South Africa, November 1998, Prepared for SIMRAC, Project No. GEN 503.

van Tonder, F., 2003, Characterisation of components used on the - - Articulated Dump Truck, Business Enterprises at University of Pretoria, South Africa, Project No. MA004, Report No 762.

Verheul, C.H., Bastra, G., Jansen, S.T.H., 1994, Simulation and analysis of trucks using the modeling and simulation program BAMMS, Vehicle-Road Interaction, ASTM STP 1225, B.T. Kulakowski, Ed., American Society for Testing and Materials, Philadelphia, pp 7-26.

Vining, G.G., 1998, Statistical Methods for Engineers, Duxbury Press, University of Florida.

Wong, J.Y., 1978, Theory of Ground Vehicles, John Wiley & Sons, New York.

Wu, X., Rakheja, S. and Boileau, P.E, 1998, Study of human-seat interface pressure distribution under vertical vibration, International Journal of Industrial Ergonomics, Vol. 21, pp 443-449.

Zegelaar, P.W.A., 1998, The dynamic response of tyres to brake torque unevennesses, PhD Thesis, Delft University of Technology.

Zhou, J., 1998, Ride simulation of a nonlinear tractor-trailer combination using the improved statistical linearization technique, Heavy Vehicle Systems, Special Series, International Journal of Vehicle Design, Vol. 5, No. 2, pp 149-166.

Appendix A: Loading Cycle Measurements on ADT

An analysis of measured data for two off-highway articulated dump trucks working in different environments is presented in this appendix. The data shows the variation in vibration levels experienced by the operators for the different parts of their cycle (loading, travelling full, dumping and travelling empty) and also shows at which parts of the cycle the operator is most at risk from the effects of WBV.

A.1. Analysis

The measurements were taken using a rubber seat pad on the driver's seat; the seat pad (PCB mould) contained a tri-axial accelerometer. Measurements were taken with a Larson-Davis HVM 100 data logger set to record the weighted RMS average values at 30 second intervals. The data was weighted by the appropriate ISO 2631-1 filters and scaled by the multiplier as shown in Figures 16 and 17 (ISO, 1997).

Values for RMS and VDV were calculated (by the HVM 100) using Equations 4 and 5 and the A(8) value was calculated using Equation 7, as given by the HSE in their WBV exposure calculator (HSE, 2003).
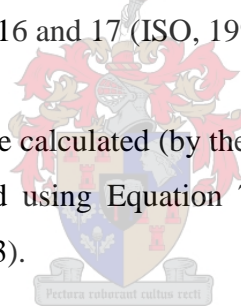
A.2. Loading cycle

The first set of measurements was taken at a dam construction site. The slipway of the dam wall was being excavated and ground transferred to the foundation. The second set of measurements was taken at a quarry. The typical loading cycle (for both scenarios) comprises the following phases:

- A: Driving empty, from dumping to loading areas
- B: Positioning truck for loading
- C: Loading, by an excavator
- D: Driving loaded, slowly over rough terrain in the loading area
- E: Driving loaded, on maintained dirt road to dumping site
- F: Unloading

The major roads are scraped more often and usually have a hard, smooth surface. The roads are periodically sprayed with water to prevent excessive dust on site. The trucks reach speeds of up to 50km/h on the good road sections (phase A and E). At the excavation- and dumping sites (phase B, D, F) the roads are more irregular, but often also softer than the major road sections. The drivers complete 40 to 75 cycles per day (depending on distance that needs to be travelled) during a 10 hour (12 hour for quarry) shift.

A.3. Measurements

The RMS and VDV values for the separate cycle elements of a **single cycle** of a truck at the construction site are given in Figure 26 and Figure 27 below.
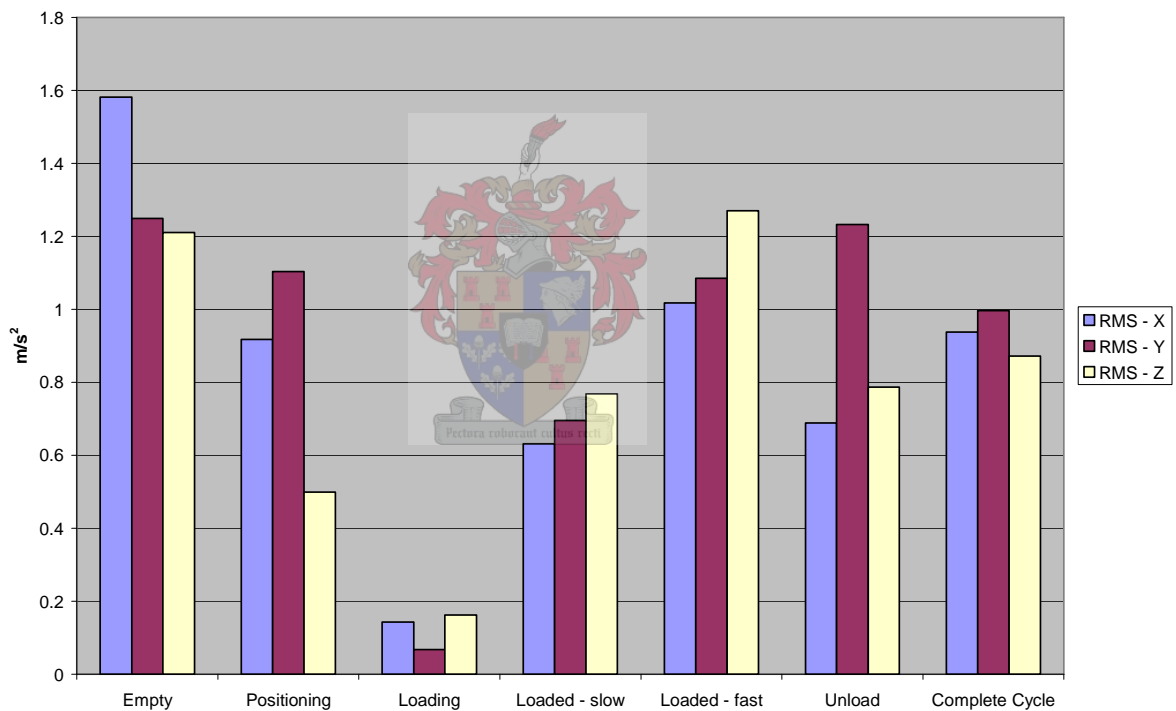

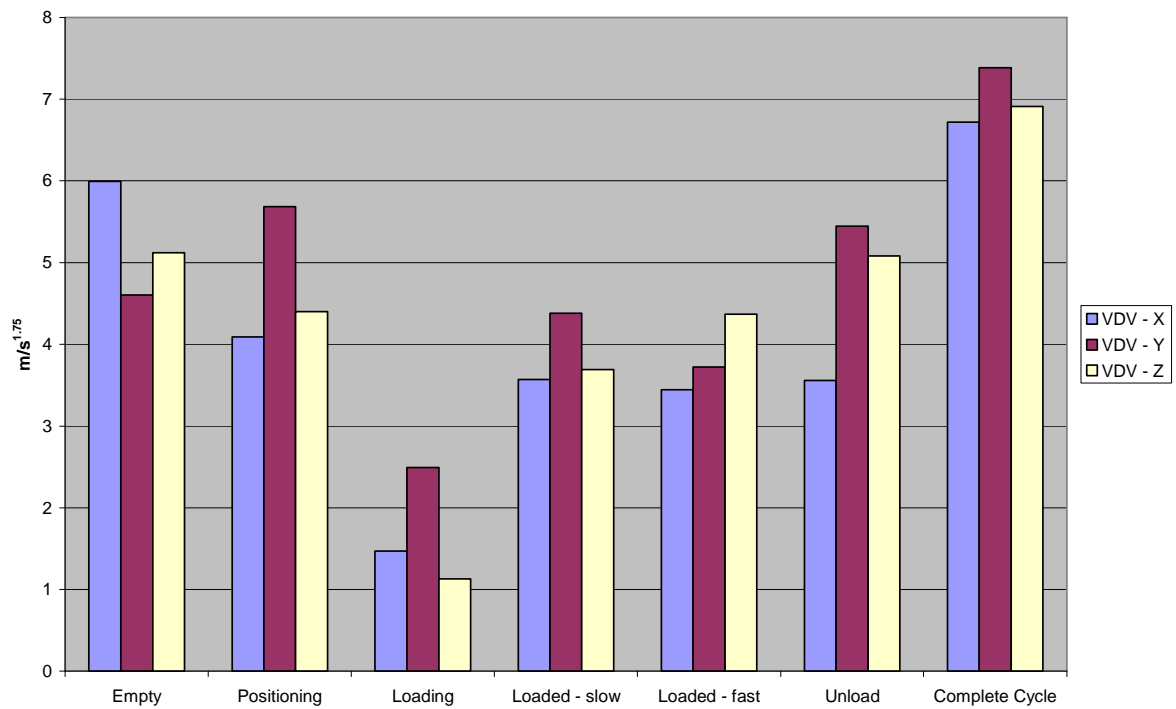**Figure 26: Averaged, weighted RMS values per cycle element – Construction Site**

Figure 27: Weighted VDV values per cycle element – Construction Site

From both figures it is evident that the WBV level is highest while the truck is empty. The hard suspension and relative low mass causes the truck to jump around while empty. The vibrations in all directions are fairly high, but this is mainly due to high driving speed. The x-direction is prominent, but this could be attributed to driving technique. The rear suspension, not carrying any load, is very stiff and consequently bounces more than the front suspension, causing a pivoting motion of the cab. This results in backslapping by the backrest, leading to the driver being unable to maintain a constant depression of the accelerator pedal. The truck jerks as a result, contributing to the high longitudinal vibration.

Positioning the truck for the load involves driving over very irregular terrain at low speed. This is seen in the VDV graph, since many peaks will cause the VDV to climb faster than the RMS. The truck is articulating sharply during this period (sometimes the cab is moved by the hydraulic steering mechanism while the truck is stationary to provide space for other trucks) and the transverse and longitudinal directions recorded high values. Rolling of the cab as the vehicle traverses large obstacles with almost no correlation between left and right tire inputs also contribute to the high transverse measurements.

The loading period consists of peaks followed by waiting periods and thus the VDV values climb much faster than the RMS values. The values obtained depend on how the load is placed as well as the size of the load. Some loaders "place" the load on the bin, while others "drop" the load on the bin. Some loaders load 10 tons at a time (which may contain giant boulders) while others load only 5 tons at a time. The y-direction may have a high value when the driver straightens out the truck during loading (the front chassis articulates behind the cab, thus when the hydraulic pistons steer the chassis, the cab moves sideways dragging the wheels slightly as it yaws) for a quicker exit.

Once loaded, the truck needs to traverse the rough terrain before joining the main road. This is usually done at low speed. Sometimes the terrain is fairly soft and will give way under the truck (such as at the slipway), but sometimes the terrain is very hard leading to high values in all directions (such as in the burrow pit). Vibrations in all directions are very similar.

When the loaded truck reaches the maintained road the driver starts to speed up. Here the transverse and longitudinal vibrations are less than the vertical direction, but the values are dependent on the severity of road irregularities.

Approaching the dumping site, the terrain starts to deteriorate again. The truck slows down and articulates a lot during this time causing lateral vibrations to increase. Unloading only takes a couple of seconds, but is dominated by lots of peaks as large rocks fall off the back. As the bin is lowered and impacts the rear chassis an impulse is recorded on the driver's seat in the vertical direction, hence the high VDV value in the vertical direction.

It is interesting to note that, for the complete cycle, the lateral direction has the highest exposure levels for RMS and VDV.

RMS and VDV values for the separate cycle elements of a **single cycle** of a truck at the quarry are given in Figure 28 and Figure 29 below.
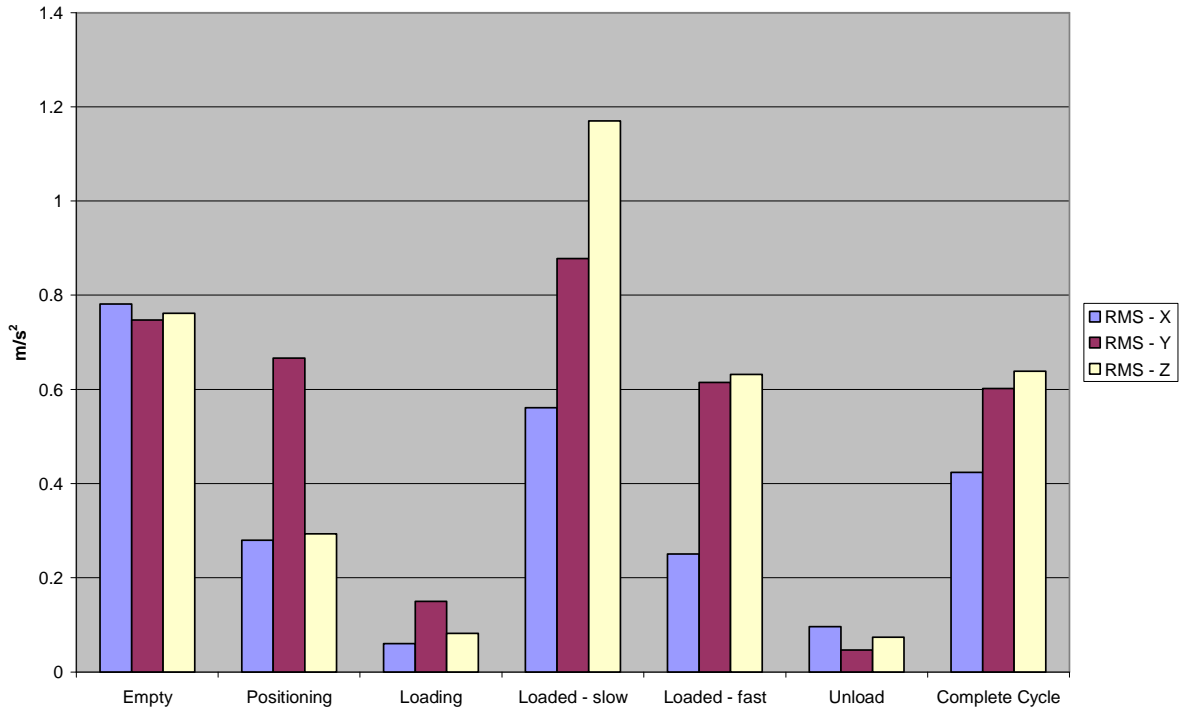
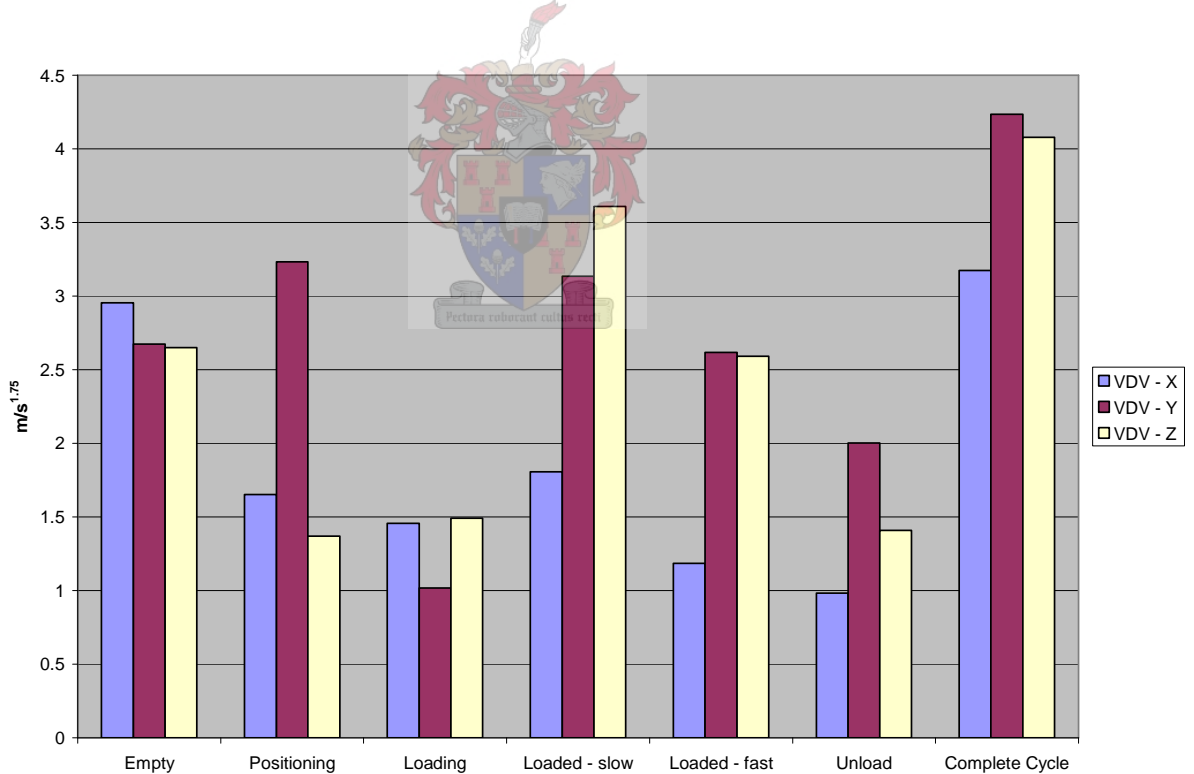**Figure 28: Average, weighted RMS values per cycle element - Quarry**

**Figure 29: Weighted VDV values per cycle element - Quarry**

The figures show that the WBV is highest when the truck is loaded and driving slowly near the loading spot. The vibration is the highest in the z-direction. The highest vibration in the x-direction is perceived while driving the empty truck from the dumping site to the loading site. The vibration in the y-direction is the highest during positioning.

74

Positioning the truck for the load involves driving over very irregular terrain at low speed. This is seen in the VDV graph, since many peaks will cause the VDV to climb faster than the RMS. Since the truck is articulating sharply during this period (there is little space to turn and position the truck next to the excavator), the transverse and longitudinal directions recorded high values.

The loading period consists of peaks followed by waiting periods and thus the VDV values climb much faster than the RMS values. After each cycle, the driver picks up a notepad from the dash board to make notes of the previous cycle and puts it back near the windscreen. During this manoeuvre, the driver is getting up from and falling back into the seat twice. The vibrations during loading are not only caused by the load dropping in the bin, but mainly by the driver himself (also observed by Newell, 2004).

Once loaded, the truck needs to traverse the rough terrain before joining the road down the hill. This is usually done at a low speed. In this area, the holes and bumps in the road are the most severe. Vibrations in all directions are very similar.

When the loaded truck reaches the maintained road the driver starts to speed up. During this part of the cycle, the vibrations are less and almost no shocks occur.
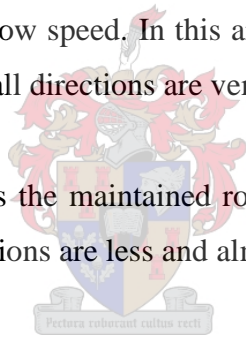
Approaching the dumping site, the terrain starts to deteriorate again. The truck slows down and articulates a lot during this time pushing the lateral vibrations up. The unloading is quite quick, but is dominated by lots of peaks as large rocks fall off the back. The bin itself causes vertical vibrations when lowered.

Over the complete cycle it is seen that while the vertical direction has the highest RMS vibration exposures level, it is the lateral direction that has the highest VDV vibration exposure level (just as at the construction site).

A.4. Comparison

From the figures given above it may be seen that the levels at the construction site is much higher than that at the quarry. This is mainly due to better road surfaces at the quarry, inducing smaller vibration inputs to the truck through the wheels. It is also seen that for

both scenarios the vibration exposure levels are high in all directions when the truck is empty and travelling at high speeds. It is also clearly seen that the vertical direction is not the worst axis for most of the cycle elements, as is so commonly assumed when designing suspensions. The lateral direction is the worst when there is poor correlation between the left and right wheel inputs (poor road surfaces) and the longitudinal axis is the worst axis when the truck is empty and travelling at high speed.

A.5. Exposure

The measurements above were representative of a single cycle. The drivers at the construction site work 10 hour shifts and aim to complete between 40 and 60 cycles depending on the distance travelled per cycle. At the time taken to complete one cycle, as recorded above, 40 cycles would be completed in 10 hours. The drivers at the quarry work 12 hour shifts and aim to complete up to 75 cycles depending on the distance travelled per cycle. With the cycle time that was accomplished during the measurements, there would be 73 cycles in the 12 hour working day.

Both drivers were approximately 1.75m tall and weighed 80kg - 90kg. It is evident from the figures above that the driving style has a large influence on the exposure levels. If the driver were to drive slower, or, not turn the cab while the truck is stationary, the exposure levels will be reduced.

Each cycle element of the comparison measurements takes 1 - 3 min, bringing a complete cycle to ±14 min. In Table 1 and 2 below the WBV exposure and calculations are recorded for an equivalent 8 hour day. Each recorded exposure represents a different element of the cycle as explained above. The "partial" values in the first two columns are the 8 hour equivalent values calculated from the measured values and time of exposure. The "Time to reach" columns indicate the time in hours and minutes (up to 24 hrs) it would take (at that vibration magnitude) to reach the EAV or ELV. The "Total exposure" columns are calculated from the "partial" values and thus represent the equivalent exposure for 8 hours. The 10- and 12 hour exposures are thus bunched into 8 hours, to get an 8-hour equivalent exposure.

It has been shown by the HSE that for durations of exposure less than 8 hours, the RMS is more lenient, while for exposures of more than 8 hours, the VDV is more lenient (provided there are not too many peaks) (HSE, 2004).

For the construction site, in a 10 hour day, the driver would spend only 100 minutes on each of the 6 cycle elements and thus, when calculating the time (for each element) to reach EAV, the RMS will be more lenient than the VDV (as each exposure is less than 8 hours) As a whole, however, the driver is exposed to more than 8 hours of vibration, thus the total VDV will be more lenient than the total RMS and we find that the RMS exceeds the ELV (1.42 m/s^2), while the VDV (20.8 m/s$^{1.75}$) does not. At the quarry, the exposure times are slightly longer, but the levels much lower. The daily exposure values that are calculated by the HSE calculator are 0.72 m/s^2 en 14.5 m/s$^{1.75}$.

A.6. Conclusions

At present the EU-Directive does not stipulate whether the VDV or RMS values should be used to determine whether the EAV or ELV have been exceeded. It can thus be concluded, if the VDV total is used that, although the EAV is exceeded, the drivers are not exceeding the ELV. The measurements, however, show that they are very close to the limit and action should be taken to reduce the exposure levels at both sites.

The exposure levels could be reduced in various ways, but one of the easiest ways would be to educate the drivers of the consequences of their driving styles. Changing the driving style slightly (such as not turning while stationary) would not influence production efficiency much, yet reduce the vibration exposure. It was noticed that the trucks often wait for the excavator to load other trucks before being loaded themselves. If the driver were to drive slower, the vibration exposure levels and the waiting time will be reduced.

It was seen that the highest exposure levels occur when the truck is empty (at the construction site) and when the truck is full (at the quarry) and the lowest levels occur when the truck is being loaded. Attention should be given to improving the suspension for ride during the hauling periods. The suspension seat should also be adjusted correctly for the driver to reduce the vibration exposure levels.

It has been shown that vibration along all three axes (x, y and z) should be considered and not only the vertical axis. The condition of the road plays a vital role in vibration exposure and care should be taken to keep the road smooth and hard at all times.

Rimell and Mansfield (2004) investigated the difference in vibration exposure levels between two ADTs operating in a quarry. The one ADT had a normal steel bin (hopper) while the other ADT had a rubber-lined bin (hopper). They discovered that, although the rubber lining did not contribute much to the attenuation of vibration exposure levels during the hauling periods, it attenuated the vibration exposure levels during the loading, unloading and positioning periods. Once the suspension systems are optimised for the hauling periods, a solution such as this may be introduced to improve ride comfort during the other phases as well.

Table 13: WBV exposure as calculated by HSE calculator for construction site

	Partial VDV m/s$^{1.75}$	Partial exposure m/s² $A(8)$	Time to reach EAV (VDV option) 9.1 m/s$^{1.75}$ VDV		Time to reach EAV ($A(8)$ option) 0.5 m/s² $A(8)$		Time to reach ELV ($A(8)$ option only) 1.15 m/s² $A(8)$		Total VDV m/s$^{1.75}$	Total exposure m/s² $A(8)$
			hours	minutes	hours	minutes	hours	minutes		
Empty	15.9	0.72	0	11	0	48	4	14	20.8	1.42
Positioning	15.1	0.50	0	13	1	39	8	42		
Loading	3.0	0.07	>24	0	>24	0	>24	0		
Loaded - slow	9.8	0.35	1	14	3	23	17	56		
Loaded - fast	11.6	0.89	0	38	0	32	2	47		
Unloading	14.5	0.56	0	16	1	19	6	58		

Table 14: WBV exposure as calculated by HSE calculator for quarry

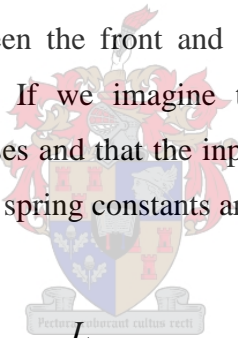|	Partial VDV m/s$^{1.75}$	Partial exposure m/s² $A(8)$	Time to reach EAV (VDV option) 9.1 m/s$^{1.75}$ VDV		Time to reach EAV ($A(8)$ option) 0.5 m/s² $A(8)$		Time to reach ELV ($A(8)$ option only) 1.15 m/s² $A(8)$		Total VDV m/s$^{1.75}$	Total exposure m/s² $A(8)$
			hours	minutes	hours	minutes	hours	minutes		
Empty	9.8	0.39	1	31	3	17	17	21	14.5	0.72
Positioning	10.7	0.33	1	3	4	31	23	51		
Loading	4.9	0.08	23	11	>24	0	>24	0		
Loaded - slow	11.9	0.44	0	40	2	35	13	40		
Loaded - fast	8.6	0.32	2	28	5	2	>24	0		
Unloading	6.6	0.05	7	9	>24	0	>24	0		

Appendix B: Theoretically Perfect Isolation

Theoretically it is possible to completely isolate the driver from any vibration exposure. Assume the truck could be represented by a 2D rigid body with 3 force inputs (one at each axle). It is possible for the body to be in force and moment equilibrium, however, because the system is statically indeterminate, it is not possible to solve for the forces explicitly, but only for 2 of the forces in terms of the third. If, F_f, is specified, then the condition for equilibrium is,

$$F_{r1} = \frac{L}{d_r} F_f \qquad (15)$$

and,

$$F_{r2} = (\frac{L}{d_r} - 1)F_f \qquad (16)$$

where L is the distance between the front and rear most force, and d_r is the distance between the two rear forces. If we imagine the forces to be due to springs with displacement inputs at their bases and that the input displacements are of equal amplitude and properly phased, then if the spring constants are distributed according to,

$$k_{r1} = (\frac{L}{d_r})k_f \qquad (17)$$

and,

$$k_{r2} = (\frac{L}{d_r} - 1)k_f \qquad (18)$$

the rigid body would be perfectly isolated from the input. This means that although the bases of the springs are all being driven, the body would be perfectly still.

The input phasing that would produce this occurrence is shown in Figure 30. If the roadway were distributed such that the steer axle and rear live axle were in phase while the front live axle was out of phase, and the springs were distributed as stated, then the rigid body would roll along the roadway and experience no accelerations at all. Interestingly, the

very road that results from the truck driving over it has exactly this distribution (Margolis, 2001).
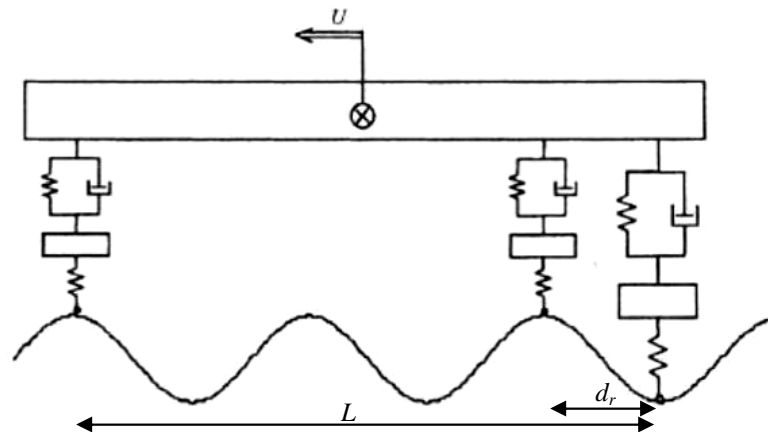

Figure 30: Roadway profile for isolation of beaming (Margolis, 2001)

For most trucks the quantity L/d_r, is about 4 and, $L/d_r - 1$, is 3. This means that the front live axle must be 4 times stiffer than the steer axle and the rear live axle must be 3 times stiffer.

It must be remembered that the prescribed suspension parameter distribution is only for rigid body isolation from the prescribed roadway. If such a roadway existed, and a truck sat upon this roadway with the required configuration, then the truck will always be in this configuration regardless of speed. Thus the rigid body isolation would take place for all forward speeds, which translates into all frequencies.

Appendix C: MATLAB Simulation Models:

The MATLAB simulation models were developed by first setting up the equations of motion by applying Newton II and then rewriting them in matrix form:

$$M\ddot{\overline{x}} + C\dot{\overline{x}} + K\overline{x} = F \qquad (19)$$

where:

$M = n$ x n diagonal mass-and-inertia-matrix

$C = n$ x n symmetrical damping-matrix

$K = n$ x n symmetrical stiffness-matrix

$F = $ n x 1 vector of forcing functions created by road

$\underline{x} = n$ x 1 vector of responses

$n = $ number of degrees of freedom

If the damping matrix, C, is not proportional, (that is $C \neq \alpha K + \beta M$, where α and β are constants) then the problem may be solved using the state space formulation with a numerical integration method (such as the Runga Kutta function ode45) in MATLAB. The equation of motion becomes:

$$\begin{bmatrix} \dot{\overline{x}} \\ \ddot{\overline{x}} \end{bmatrix} = \begin{bmatrix} 0 & I \\ -M^{-1}K & -M^{-1}C \end{bmatrix} \begin{bmatrix} \overline{x} \\ \dot{\overline{x}} \end{bmatrix} + \begin{bmatrix} \overline{0} \\ M^{-1}F \end{bmatrix} \qquad (20)$$

Solving the equation with ode45 in MATLAB will produce answers for velocity and displacements, but not acceleration. The acceleration may be approximated by using Euler's algorithm.

If the damping matrix, C, is proportional (that is $C = \alpha K + \beta M$, where α and β are constants) then the problem may be uncoupled into n single degree of freedom problems and thus could be solved using any method applicable to single degree of freedom systems. It must, however, be noted that vehicle suspension generally do not have proportional damping.

Assume

$$\bar{x} = U\bar{y} \tag{21}$$

$$C = \alpha M + \beta K \tag{22}$$

Then:

$$U^T M U \ddot{\bar{x}} + U^T C U \dot{\bar{x}} + U^T K U \bar{x} = U^T F \tag{23}$$

$$\hat{M}\ddot{\bar{y}} + \hat{C}\dot{\bar{y}} + \hat{K}\bar{y} = \hat{F} \tag{24}$$

where U is the matrix with the eigenvectors of the undamped system as columns and $\hat{M}$, $\hat{C}$ and $\hat{K}$ are uncoupled diagonal matrices. Solving each y is as easy as solving a single degree of freedom system for which the solution is known.

C.1. 2 Dimensional, 4-DOF Model:

The first MATLAB model is a simplification of the real truck. The truck was essentially divided into two parts, namely the chassis and the walking beams. Each part having 2 degrees of freedom (pitch and bounce). The tires and struts were added in series to model the front suspension and the tires and sandwich blocks were added in series to model the rear suspension. Figure 31 shows the graphical representation of what the first MATLAB model simulated.
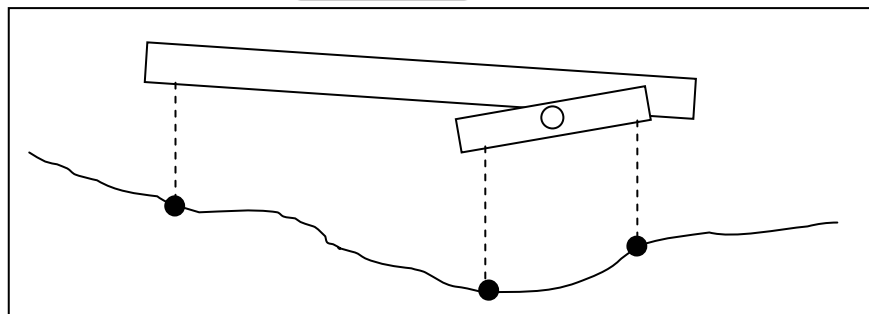

Figure 31: First 2D MATLAB model

C.2. 2 Dimensional, 7-DOF Model:

The first MATLAB model was upgraded to 7 degrees-of-freedom (shown in Figure 32). The main differences being that the cab and the bin were modelled as separate rigid bodies. The cab was allowed to pitch and bounce independently from the chassis, while the bin could only bounce and not pitch relative to the chassis.
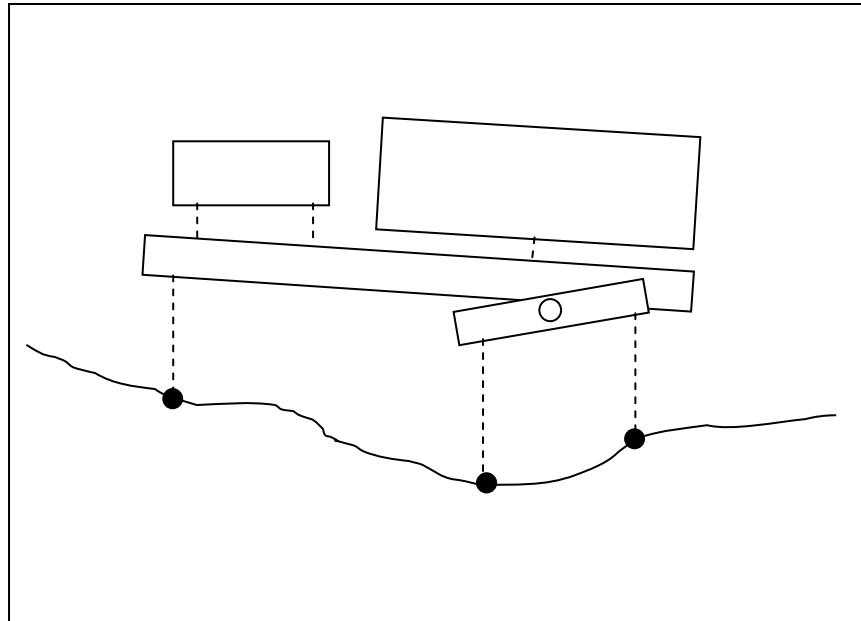
Figure 32: Second 2D MATLAB model

C.3.   3 Dimensional, 15-DOF Model:

A 3 dimensional model of the truck was created in MATLAB. The difference between a 2 dimensional and 3 dimensional model is the planes in which it can move. The 2 dimensional could not roll or displace in the lateral direction. The 3 dimensional model, however, is able to move and rotate about all three the major axes. The model developed in MATLAB was based on the 7-DOF model, but given more degrees of freedom by allowing roll motions of the chassis, cab and bin. A simplified seat model was also included in the model. The 15 degrees-of-freedom MATLAB model is shown in Figure 33.
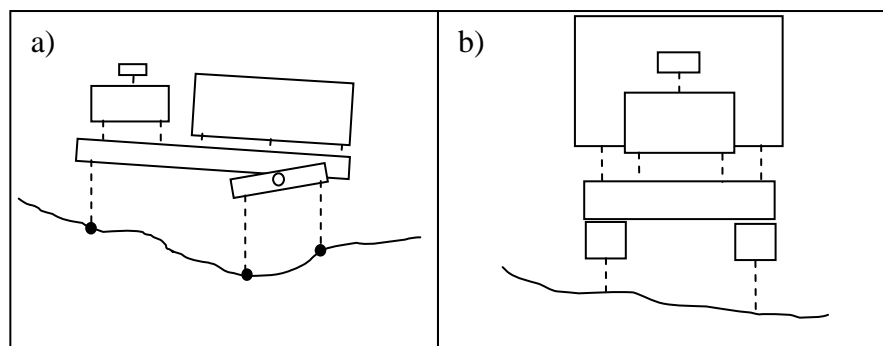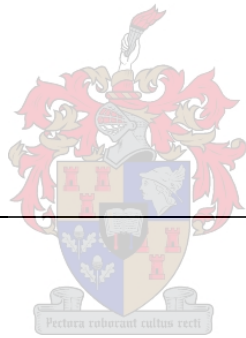

Figure 33: 3D MATLAB model - a) Side view, b) Front view

For clarity Table 3: Degrees-of-freedom of MATLAB models is repeated below.

Table 15: Degrees-of-freedom of MATLAB models

2 Dimensional 4 degree-of-freedom model	2 Dimensional 7 degree-of-freedom model	3 Dimensional 15 degree-of-freedom model
Vertical displacement: • Chassis • Walking beam Angular displacement about y-axis (pitch): • Chassis • Walking beam	Vertical displacement: • Chassis • Walking beam • Cabin • Bin Angular displacement about y-axis (pitch): • Chassis • Walking beam • Cabin	Vertical displacement: • Chassis • Two walking beams • Cabin • Bin • Seat Angular displacement about y-axis (pitch): • Chassis • Two walking beams • Cabin • Bin Angular displacement about x-axis (roll): • Front chassis • Rear chassis • Cabin • Bin

Appendix D: Beaming

From the literature review it was seen that certain vibrations may be generated by the bending vibration of the chassis, commonly known as beaming. Ibrahim *et al.* (1994) developed a model to investigate the effect of a flexible frame on ride vibration in large trucks. He concluded that frame flexibility may contribute significantly to vibration measurements, especially on the trailer. In his article Donald Margolis (2001) stated that the rigid body modes of a truck are most important at frequencies below 5Hz, while beaming occurs close to the wheel-hop frequency at about 10Hz.

The beaming frequency of the ADT's chassis may be determined by approximating the rear chassis as a beam that has a large inertia at the one end (representing the cabin) and a added inertia at specified points along its length (representing the bin). The beam is connected to a fixed plane (the road) via springs (representing the front and rear suspension components) at specified points along its length. The approximations are shown in Figure 34 below. The nodes are numbered 1 – 5. The "m" represents added inertia from bin and load; the "M" represents the added inertia of the cab and front chassis. The dashed vertical lines represents the spring-characteristics of the front and rear suspension. The dash-dotted line shows the first mode-shape of the transverse vibration at the frequency of interest.
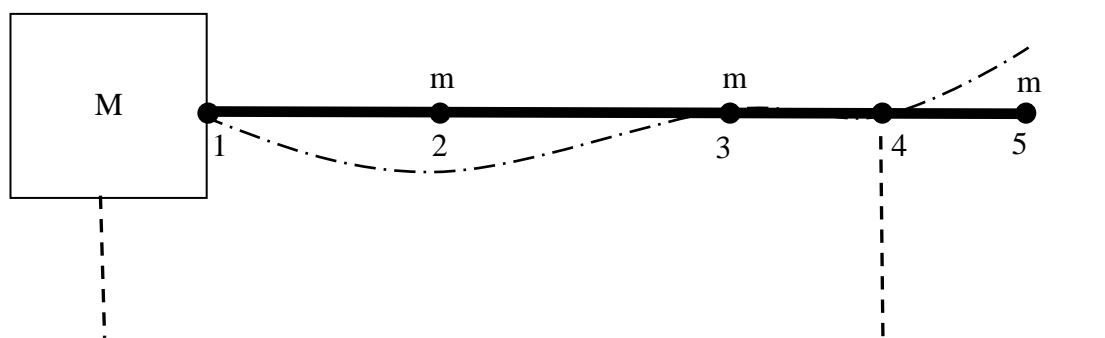

Figure 34: Chassis beaming simplification

Two techniques (Finite Elements and Bernoulli as described in sections 6.5 and 8.3 of Inman, 2001) were used to determine the natural frequency of the transverse vibration of the chassis. Both techniques gave a beaming mode at about 11.8Hz for the loaded truck

and a beaming mode at 22Hz for the unloaded truck. This correlates quite well with the 10Hz predicted by Margolis (2001).

Studying Figure 34, it may be seen that beaming is difficult to control from the suspension locations, as the shock absorbers do little to extract energy from the beaming mode. The primary suspension can, however, be used to control the rigid body modes. If beaming is excited, it should be dealt with through cab isolation techniques.

The beaming of the chassis was not considered in the optimisation study. The beaming mode of interest does not contribute significantly to vertical vibrations at the cabin (see Figure 34) and is at too high a frequency to contribute significantly to the horizontal vibrations (see W_d filter in Figure 17), especially for the unloaded condition.